

Composition and function of the pyrenoids  
of algal chloroplasts

R. Michael L. McKay

Department of Biology  
McGill University, Montreal  
August 1991

A Thesis submitted to the Faculty of Graduate  
Studies and Research in partial fulfillment  
of the requirements of the degree of  
Doctor of Philosophy

© R. Michael L. McKay 1991

To Mom, Dad and Aynsley

## Abstract

Immunocytochemical analyses have demonstrated that the Calvin cycle enzyme ribulose 1,5-bisphosphate carboxylase/oxygenase (Rubisco) is predominantly localized in the pyrenoid region of chloroplasts of evolutionarily diverse algae. That Rubisco remains pyrenoid-localized at photosynthetically-saturating irradiance in the green alga *Chlorella pyrenoidosa* indicates a catalytic, rather than storage function for pyrenoid-localized Rubisco. This is further supported by the immunolocalization of Rubisco activase to the pyrenoids of two species of green algae. The exclusion of phosphoribulokinase from the pyrenoids of a red and a green alga indicates that pyrenoids do not possess the full complement of Calvin cycle enzymes.

Thylakoid lamellae traverse the pyrenoids of many algae. The absence of light-harvesting phycoerythrin and of photosystem (PS) II activity, but not PSI activity, from the intrapyrenoid thylakoids of the red alga *Porphyridium cruentum* indicates a structural and functional heterogeneity between these lamellae and those located in the chloroplast stroma. In contrast, the intrapyrenoid thylakoids of cryptomonads, algae whose chloroplast is thought to have evolved from red algae, possess both PSI and PSII protein complexes. These results are discussed with reference to Rubisco being mainly pyrenoid-localized in these algae.

## Résumé

Des études immunocytochimiques ont démontré que l'enzyme ribulose 1,5-biphosphate carboxylase/oxygénase (Rubisco), impliquée dans le cycle de Calvin, est localisée de façon prédominante dans la région pyrénolde des chloroplastes de plusieurs algues phylogénétiquement différentes. Le fait que l'enzyme Rubisco demeure localisée dans la région pyrénolde lors d'une illumination photosynthétiquement saturante chez l'algue *Chlorella pyrenoidosa* indique que la fonction de cette enzyme serait catalytique plutôt que d'accumulation.

L'immunolocalisation de la Rubisco activase dans les pyrénolides de deux espèces d'algues vertes suggère également un rôle catalytique pour cette enzyme. L'exclusion de la phosphoribulokinase des pyrénolides chez une algue verte et une algue rouge indique que toutes les enzymes impliquées de le cycle de Calvin ne se retrouvent pas dans les pyrénolides.

Les lamelles thylakoides traversent les pyrénolides de plusieurs algues. L'absence de phycoerythrin récoltant la lumière et d'activité du photosystème (PS) II, mais pas d'activité PS I, des thylakoides intrapyrénolides de l'algue rouge *Porphyridium cruentum* indique que ces lamelles sont fonctionnellement et structurellement différentes de celles situées dans le stroma chloroplastique. Cependant, les thylakoides intrapyrénolides des cryptomonades qui sembleraient être un assemblage d'algues

phylogénétiquement proches de l'algue rouge possèdent les deux complexes protéiques PSI et PSII. Ces résultats seront discutés en tenant compte de la localisation de l'enzyme Rubisco dans ces algues.

## Table of Contents

Abstract	111
Re-sume	1V
Acknowledgements	X11
Preface	X1V
Contributions to Original Knowledge	XV111
List of Figures	XX
List of Tables	XXV111
List of Abbreviations	XXX
Chapter I	
Pyrenoids and their involvement in the compartmentalization of the Calvin cycle and other metabolic processes	1
1.0. Introduction	2
2.0 Immunocytochemical Techniques	4
2.1 Immunofluorescence	4
2.2. Immunoenzymatic technique	6
2.3. Immunogold electron microscopy	7
3.0. Ribulose 1,5-Bisphosphate Carboxylase/Oxygenase and Pyrenoids	9
4.0. Other Calvin Cycle Enzymes	20
4.1 Phosphoribulokinase	20
5.0 Carbonic Anhydrase	21
6.0. The Nitrate Reductase Conundrum	23
7.0. DNA and Pyrenoids	26
8.0. The Avena Stromacentre: A Vestigial Pyrenoid	27

Chapter II	Immunocytochemical localization of ribulose	29
	1,5-bisphosphate carboxylase/oxygenase in	
	light-limited and light-saturated cells of	
	<i>Chlorella pyrenoidosa</i>	
	Summary	30
1 0.	Introduction	31
2 0	Materials and Methods	33
2 1.	Cell culture	33
2 2	Photosynthetic oxygen evolution	33
2.3.	Fixation and embedding	34
2 4.	Immunolabelling	34
2.5	Quantitative evaluation	35
3 0	Results	35
4.0	Discussion	42
	Acknowledgements	44
	Notes Added	45
Chapter III	Rubisco activase is present in the pyrenoid	46
	of green algae	
	Summary	47
1.0	Introduction	48
2.0.	Materials and Methods	50
2.1.	Plant material	50
2.2.	Immunoelectron microscopy	51
2 3	Quantitative evaluation	53
2.4.	Antiserum specificity	53
3.0.	Results	54

	3 1	Western immunoblotting	54
	3 2	Immunoelectron microscopy	56
	4 0	Discussion	60
		Acknowledgements	64
Chapter IV		Immunocytochemical localization of phosphoribulokinase in microalgae	65
		Summary	66
	1 0.	Introduction	67
	2 0.	Materials and Methods	68
	2.1	Cell culture	68
	2.2.	Characterization of antisera	68
	2.3	Immunoelectron microscopy	70
	3 0	Results	71
	3.1	Immunoblotting	71
	3.2.	Immunoelectron microscopy	74
	4.0.	Discussion	76
	4 1.	Characterization of antisera	76
	4.2.	Subcellular distribution of phosphoribulokinase	79
		Acknowledgements	83
Chapter V		Effect of dissolved inorganic carbon on mode of carbon transport, expression of carboxysomes and localization of Rubisco in cells of the cyanobacterium <i>Synechococcus</i> UTEX 625	84
		Preface	85
		Summary	88
	1.0.	Introduction	89

2 0	Materials and Methods	91
2 1	Organism and growth conditions	91
2 2	Immunoelectron microscopy	93
2 3.	Quantitative evaluation	94
2 4	Protein extraction and immunoblotting	94
2 5.	Transport of inorganic carbon	95
3 0	Results	96
3.1.	Antisera specificity	96
3 2	Subcellular location of Rubisco	96
3 3	Morphological expression of carboxysomes	98
3.4	Transport of inorganic carbon	104
4.0	Discussion	104
4 1.	Subcellular location of Rubisco	104
4 2	Is extra-carboxysomal label genuine?	109
4 3	Morphological expression of carboxysomes	111
4 4	Carboxysome positioning photosynthetic implications?	113
	Acknowledgements	117
Chapter VI	Intrapyreoid thylakoids a paradox?	118
1 0.	Introduction	119
1.1	Light-harvesting and photosystem complexes	121
1 2.	Polyphenol oxidase	124
Chapter VII	Phycocerythrin is absent from the pyrenoid of <i>Porphyridium cruentum</i> photosynthetic implications	126
	Summary	127

1 0	Introduction	128
2 0	Materials and Methods	130
2 1	Plant material	130
2 2	Immunoelectron microscopy	131
2 3	Quantitative evaluation	132
2 4	Cytochemical detection of PS activity	132
3 0	Results	133
3 1	Immunoelectron microscopy	133
3 2	Cytochemical detection of PSI	138
3.3	Cytochemical detection of PSII	140
4 0.	Discussion	140
4.1	Absence of PE and PSII activity in the pyrenoid	140
4 2	Photosystem I activity in the pyrenoid	143
4 3	Rubisco and pyrenoids	144
	Acknowledgements	145
	Notes Added	145
Chapter VIII	Immunocytochemical characterization of the intrapyrenoid thylakoids of cryptomonads	148
	Summary	149
1 0	Introduction	150
2.0.	Materials and Methods	151
2 1.	Algal culture	151
2 2.	Immunoelectron microscopy	152
2 3	Protein extraction and immunoblotting	154
3 0.	Results and Discussion	156
3.1	Antisera specificity	156

3 2	Immunoelectron microscopy	159
	Acknowledgements	166
	Concluding Remarks	167
	Literature Cited	174
	Appendix 1	215
	Appendix 2	217
	Appendix 3	220
	Appendix 4	222

## Acknowledgements

I wish to express thanks to all those who "aided and abetted" me during my tenure as a student at McGill. To those I have worked with in the lab: Martha Ludwig, Elisabeth Mangeney, Genevieve Bricheux, Christiane Lichtle and Andrew Pyszniak, I extend my appreciation for your patience in teaching and for your friendship. I extend my thanks to Dr. Greg Brown and Dr. Ron Poole, both members of my supervisory committee for the past five years. Their advice was always appreciated, as was their willingness to accomodate scheduling of meetings, etc. I would also like to thank Dr. Mel Goldstein whom I assisted in the laboratory section of Introductory Phycology. He took an interest in my research and provided enlightening discussions on various aspects of phycology.

Special thanks are extended to Dr. George Espie and Dr. Kevin Vaughn, both for their interest in my work and for the friendships that have developed during the past two years. The experience gained working in their laboratories has been invaluable. My month-long "sabbatical" in Kevin's lab in Stoneville will always be remembered. I reserve very special thanks for my supervisor, Dr. Sarah P. Gibbs. Sally took a chance by accepting me as a student and for that I will always be grateful. The environment of the lab, I believe, was ideal for my development. I was constantly encouraged but never pushed.

I would also like to thank those who provided technical assistance with various aspects of this project. Guy L'Heureux and Robert Lamarche always provided top quality work in the photography center. Kathy Hewitt, our EM technician maintained the microscopes and dark room

facilities in good working order. Bruce Goodchild provided access to, and assistance with electrophoresis and blotting equipment. Dr. Marc Lussier a fait la traduction du resume.

I must also express my gratitude to those who provided antisera used in this work. These people are acknowledged individually in the text of the thesis. Obviously, without their gracious provision of these reagents, this work would not have been possible. Thanks are also extended to Dr. Charlie Smith for providing access to the MOP digital analyzer which was used throughout the course of this study.

To fellow members of our departmental ice hockey team, "The Asthmatics" and to my friends at the Montreal Thistle Curling Club, I thank you for offering the more than occasional diversion from thesis research. Several of these people, notably Drs. Peter Cserjesi, Antony Cooper and Howard Bussey as well as Mike Devouge and Simon John also assisted in my research. They were always willing to lend equipment and provided sound advice on electrophoretic and immunoblotting procedures.

I reserve my deepest gratitude for my family and my wife Aynsley. They constantly offered encouragement and maintained their enthusiasm even at times when mine may have been waning. Aynsley deserves special praise; during the past five years she has had to live with not only my successes (and accompanying "big head" undoubtedly) but also my failures.

Finally, I would like to thank the Natural Sciences and Engineering Research Council of Canada for financial support through a postgraduate scholarship during the past two years of my doctoral studies.

## Preface

In accordance with guidelines put forth by the Faculty of Graduate Studies and Research at McGill University, the following statement is reproduced:

The candidate has the option, subject to approval of their Department, of including as part of the thesis the text, or duplicated published text, of an original paper or papers. Manuscript-style theses must still conform to all other requirements explained in the Guidelines Concerning Thesis Preparation. Additional material (procedural and design data as well as descriptions of equipment) must be provided in sufficient detail (eg. in appendices) to allow clear and precise judgement to be made of the importance and originality of the research reported. The thesis should be more than a mere collection of manuscripts published or to be published. It must include a general abstract, a full introduction and literature review and a final overall conclusion. Connecting texts which provide logical bridges between different manuscripts are usually desirable in the interest of cohesion. It is acceptable for these to include, as chapters, authentic copies of papers already published, provided these are duplicated clearly and bound as an integral part of the thesis. In such instances, connecting texts are mandatory and supplementary explanatory material is always necessary. Photographs or other materials which do not duplicate well must be included in their original form. While the inclusion of manuscripts co-authored by the candidate and others is acceptable, the candidate is required to make an explicit statement in the thesis of who contributed to such work and to what extent, and supervisors must attest to the accuracy of the claims at the Ph.D. Oral Defense. Since the task of the Examiners is made more difficult in these cases, it is in the candidate's interest to make the responsibilities of authors perfectly clear.

This thesis consists of an abstract (in English and French), two general chapters in which pertinent literature is reviewed, six chapters describing experimental results which are written in manuscript form, general concluding remarks and attached appendices. Chapter I consists of a general introduction and an overview of the literature pertaining to pyrenoids and their involvement in the compartmentalization of the

Calvin cycle and other metabolic processes. Chapter VI is a brief review of literature dealing with the thylakoid lamellae that traverse the pyrenoid regions of pyrenoid-containing organisms. These two chapters have been published as part of a single review paper contributed as part of the proceedings of the Second International Symposium on Inorganic Carbon Utilization by Aquatic Photosynthetic Organisms, Kingston, Ont., August 5-9, 1990. The complete reference of this paper is:

McKay, R.M.L., and Gibbs, S.P. 1991. Composition and function of pyrenoids: cytochemical and immunocytochemical approaches. *Can. J. Bot.* **69**:1040-1052

Chapter II has been published in the journal *Protoplasma*. The complete reference of this paper is:

McKay, R.M.L., and Gibbs, S.P. 1989. Immunocytochemical localization of ribulose 1,5-bisphosphate carboxylase/oxygenase in light-limited and light-saturated cells of *Chlorella pyrenoidosa*. *Protoplasma* **149**:31-37

A brief "Notes Added" section has been appended to this chapter for the purpose of introducing relevant literature that appeared subsequent to the publication of this manuscript.

Chapter III has also been published in the journal *Protoplasma*. The complete reference of this paper is:

McKay, R.M.L., Gibbs, S.P., and Vaughn, K.C. 1991. Rubisco activase is present in the pyrenoid of green algae. *Protoplasma* **162**:38-45

The experimental results presented in this chapter are solely the work of the Candidate and were obtained while the Candidate was visiting the laboratory of Dr. K.C. Vaughn at the U.S. Department of Agriculture, Stoneville, MS, during April/May, 1990. Preparation of the manuscript comprising this chapter was the result of a collaborative endeavour.

undertaken with Dr. Vaughn and Dr S.P. Gibbs.

Chapter IV has recently (August 1991) been accepted for publication in the journal *Botanica Acta*. The reference for this paper

is

McKay, R.M.L , and Gibbs, S.P. 1991. Immunocytochemical localization of phosphoribulokinase in microalgae. *Bot. Acta* In press

Chapter V will shortly be submitted to the journal *Archives of Microbiology* for consideration for publication. Experimental results reported in this chapter were the result of a collaborative effort between the Candidate and Dr. G.S. Espie (Erindale College, University of Toronto) The Candidate was responsible for the experimental work described in sections 2.2., 2.3., and 2.4. Preparation of the manuscript comprising this chapter was the result of a collaborative endeavour undertaken with Dr. Espie and Dr. Gibbs. A preface has been added in the interest of connecting this chapter to those preceding it.

Chapter VII has been published in the journal *Planta*. The complete reference of this paper is:

McKay, R M.L., and Gibbs, S.P. 1990. Phycoerythrin is absent from the pyrenoid of *Porphyridium cruentum*: photosynthetic implications *Planta* **180**:249-256.

As with Chapter II, a brief "Notes Added" section has been appended to this chapter for the purpose of introducing relevant literature appearing subsequent to publication of this manuscript.

Chapter VIII has been submitted (July 1991) to *Journal of Phycology* for consideration for publication. The experimental results presented in this chapter are solely the work of the Candidate. Preparation of the manuscript comprising this chapter was the result of

a collaborative endeavour undertaken with Dr. Gibbs and Dr. C. Lichtle, who was a French visiting scientist resident in our lab during the latter part of 1989.

Except where noted, all of the experimental results presented are solely the work of the Candidate. Antisera and other special reagents supplied for this research are acknowledged in each chapter. Except where noted, preparation of manuscripts comprising the various chapters were collaborative endeavours undertaken with Dr. S.P. Gibbs. Because the chapters were prepared as individual manuscripts, an unavoidable degree of redundancy is present. For this same reason, references to our own work was unavoidable; however, these references have been augmented with references to the appropriate chapters as they appear in this thesis. Finally, all of the literature cited in each chapter has been combined and appears immediately preceding the appendices.

## Contributions to Original Knowledge

1. Demonstration that pyrenoids of diverse species of algae contain Rubisco. Also, the first demonstration that pyrenoids of rhodophyte (red algae), cryptophyte (cryptomonad algae) and bacillariophyte (diatoms) algae contain Rubisco.
2. Provided evidence for a catalytic, rather than storage role for pyrenoid-localized Rubisco. This evidence was obtained from:
  - i) Investigation of the effect of growth irradiance on the subcellular distribution of Rubisco in a green alga. Rubisco remained pyrenoid-localized even under light-saturating conditions for photosynthesis.
  - ii) Immunolocalization of Rubisco activase to the pyrenoids of two species of green algae.
3. First demonstration of the subcellular location of Rubisco activase in  $C_3$ -type higher plants and green algae.
4. Demonstrated by immunocytochemistry that pyrenoids do not possess the full complement of Calvin cycle enzymes; phosphoribulokinase was predominantly localized in the chloroplast stroma in a red and a green alga.

- 5 Demonstrated that inclusions of chloroplast stroma are sometimes found in the pyrenoid of *Chlamydomonas reinhardtii* and possibly other green algae whose pyrenoids appear to be demarcated by starch
6. Demonstration that Rubisco remains predominantly carboxysome-localized in the cyanobacterium *Synechococcus* UTEX 625 grown over a wide range of DIC levels.
7. Immunocytochemical demonstration that phosphoribulokinase is restricted to the thylakoid-containing cell periphery in *Synechococcus*. The association with photosynthetic membranes was not made clear in a previous investigation (Hawthornthwaite et al. 1985).
- 8 Extended the cytochemical assay for the detection of PSII activity at the electron microscope level to use with algae (*Porphyridium cruentum*).
9. Provided the first demonstration of a functional heterogeneity between the thylakoids of the pyrenoid and those of the chloroplast stroma; intrapyrenoid thylakoids of *P. cruentum* were observed to be lacking PSII activity.
10. Immunocytochemical demonstration that the intrapyrenoid thylakoids of cryptomonads possess PSII-associated light-harvesting complexes.

## List of Figures

### Chapter II

- Fig. 1. Immunolocalization of Rubisco LS in log phase cell of *Chlorella pyrenoidosa* cultured under low light ( $25 \mu\text{mol} \cdot \text{m}^{-2} \cdot \text{s}^{-1}$ ) 37
- Fig. 2. Immunolocalization of Rubisco LS in log phase cell of *C. pyrenoidosa* cultured under  $75 \mu\text{mol} \cdot \text{m}^{-2} \cdot \text{s}^{-1}$  37
- Fig. 3. Irradiance effect on photosynthesis in *Chlorella*. 38
- Fig. 4. Immunolocalization of Rubisco LS in log phase cell of *C. pyrenoidosa* cultured under light-saturating conditions. 39

### Chapter III

- Fig. 1. *Chlamydomonas reinhardtii* soluble protein extract immunoblotted with anti-Rubisco activase 55
- Fig. 2. Immunolocalization of Rubisco activase in mesophyll cell of *Vicia faba*. 57

Fig. 3	Immunolocalization of Rubisco activase and Rubisco LS in <i>C. reinhardtii</i>	58
Fig. 4	Immunolocalization of Rubisco activase and Rubisco LS in <i>Coleochaete scutata</i>	58

#### Chapter IV

Fig 1.	Immunoblot analysis of <i>Chlamydomonas reinhardtii</i> and <i>Porphyridium cruentum</i> soluble protein extracts incubated with anti-PRK and anti-Rubisco LS	73
Fig 2.	Immunolocalization of PRK in <i>P. cruentum</i>	75
Fig. 3.	Immunolocalization of Rubisco LS in <i>P. cruentum</i>	75
Fig. 4.	Immunolocalization of PRK in <i>C. reinhardtii</i>	75
Fig. 5	Immunolocalization of Rubisco LS in <i>C. reinhardtii</i> .	75
Fig. 6.	Immunolocalization of PRK in <i>C. reinhardtii</i> with emphasis on thylakoid-like tubules	77
Fig.7.	Stromal inclusion in pyrenoid of <i>C. reinhardtii</i>	

immunolabelled by anti-PRK. 77

Fig 8 Stromal inclusions in pyrenoid of *C reinhardtii* are not labelled by anti-Rubisco LS. 77

## Chapter V

Fig 1. Immunoblot analysis of *Synechococcus* UTEX 625 soluble protein extract incubated with anti-Rubisco LS. 97

Fig. 2. Immunolocalization of Rubisco LS in air-grown *Synechococcus* harvested at low ( $3.4 \mu\text{g chl } a \cdot \text{ml}^{-1}$ ) cell density. 99

Fig. 3. Immunolocalization of Rubisco LS in *Synechococcus* harvested at high ( $20 \mu\text{g chl } a \cdot \text{ml}^{-1}$ ) cell density. 99

Fig 4. Immunolocalization of Rubisco LS in *Synechococcus* harvested from cultures bubbled with air at a high rate ( $540 \text{ ml} \cdot \text{min}^{-1}$ ). 100

Fig. 5. Immunolocalization of Rubisco LS in *Synechococcus* grown under 5%  $\text{CO}_2$ . 100

Fig. 6	Immunolocalization of Rubisco LS in <i>Synechococcus</i> grown under 5% CO <sub>2</sub>	100
Fig. 7	Standing-culture cells of <i>Synechococcus</i> cut in cross-section and immunolabelled by anti-Rubisco LS	101
Fig. 8	Standing-culture cell of <i>Synechococcus</i> cut in longitudinal-section and immunolabelled by anti-Rubisco LS	101
Fig. 9	<i>Synechococcus</i> bubbled with 30 $\mu$ l CO <sub>2</sub> l <sup>-1</sup> Cross-sections have been labelled by anti- Rubisco LS	101
Fig. 10	<i>Synechococcus</i> bubbled with 30 $\mu$ l CO <sub>2</sub> l <sup>-1</sup> Longitudinal-section immunolabelled by anti-Rubisco LS	101
Fig. 11	Immunolocalization of PRK in air-grown cell of <i>Synechococcus</i>	101
Fig. 12	Control section incubated in non-immune serum.	101

## Chapter VII

- Fig. 1      Immunolocalization of phycoerythrin in log  
phase cell of *Porphyridium cruentum*      135
- Fig. 2      Immunolocalization of Rubisco LS in log  
phase cell of *P. cruentum*.      136
- Fig. 3a      Cytochemical detection of PSI activity  
in *P. cruentum* by photooxidation of DAB      139
- Fig. 3b      Control cell incubated with DAB in the dark.      139
- Fig. 4a.      Cytochemical detection of PSII activity  
in *P. cruentum* by photoreduction of DS-NBT.      141
- Fig. 4b.      Control cell incubated with DS-NBT in  
presence of PSII inhibitor atrazine.      141

## Chapter VIII

- Fig. 1      Immunoblot analysis. *Chroomonas* sp. and  
*Hemiselmis brunnescens* soluble proteins  
incubated with anti-PE 545, anti-Rubisco LS  
and anti-PSI.      158

Fig. 2	Immunolocalization of phycoerythrin in Epon- embedded <i>Chroomonas</i> sp	161
Fig. 3	Immunolocalization of phycoerythrin in Epon- embedded <i>H. brunnescens</i>	161
Fig. 4.	Immunolocalization of the 19 kDa apoprotein of the chl <i>a/c</i> <sub>2</sub> LHC in Lowicryl-embedded <i>H</i> <i>brunnescens</i> .	161
Fig. 5.	Immunolocalization of PSI polypeptides in Lowicryl-embedded <i>H brunnescens</i> .	161
Fig. 6.	Immunolocalization of Rubisco LS in Epon- embedded <i>Chroomonas</i> sp	161
Fig. 7.	Immunolocalization of Rubisco LS in Epon- embedded <i>H. brunnescens</i>	161

#### Appendix 1

Fig. 1.	Immunolocalization of Rubisco LS in <i>Pisum</i> <i>sativa</i>
Fig. 2.	Immunolocalization of Rubisco LS in the non-

pyrenoid-containing alga *Ochromonas danica*.

#### Appendix 2

- Fig. 1. *Chlorella pyrenoidosa*. Control section incubated with non-immune serum.
- Fig. 2. *Chlamydomonas reinhardtii*. Control section incubated with pre-immune serum.
- Fig. 3. *Phaeodactylum tricornutum*. Control section incubated with PBS.
- Fig. 4. *Porphyridium cruentum* Control section incubated with non-immune serum.
- Fig. 5. *Hemiselmis brunnescens*. Control section incubated with pre-immune serum.

#### Appendix 3

- Fig. 1. Effect of The PSII inhibitor atrazine on photosynthetic O<sub>2</sub>-evolution in *Porphyridium cruentum*.

I  
Appendix 4

- Fig. 1. Immunolocalization of apoproteins of the chl *a/c* LHC in Epon-embedded cells of *Phaeodactylum tricornutum*.
- Fig. 2. Immunolocalization of PSI in L.R White-embedded cell of *P. tricornutum*.
- Fig. 3. Immunolocalization of Rubisco LS in L R White-embedded cell of *P. tricornutum*.

## List of Tables

### Chapter II

- Table 1. Density of labelling over various cell compartments of *Chlorella pyrenoidosa* cultured at different light intensities. 40

### Chapter III

- Table 1. Immunocytochemical investigations of Rubisco localization in pyrenoid-containing species. 49

### Chapter IV

- Table 1. Antisera employed in the present investigation. 69

### Chapter V

- Table 1. Mode of carbon transport, morphological expression of carboxysomes, and Rubisco labelling density as dependent on culture growth parameters. 93

Chapter VII

Table 1.	Density of labelling over various cell compartments of <i>Porphyridium cruentum</i>	137
----------	---	-----

Chapter VIII

Table 1.	Antisera employed in the present investigation	153
----------	--	-----

## List of Abbreviations

BSA	bovine serum albumin
C <sub>i</sub>	inorganic carbon
CA	carbonic anhydrase
chl	chlorophyll
DAB	3,3'-diaminobenzidine·4HCl
DCMU	3-(3,4-dichlorophyl)-1,1-dimethyl urea
DIC	dissolved inorganic carbon
DOPA	dihydroxyphenylalanine
DS-NBT	distyryl nitroblue tetrazolium
GAPDH	NAD(P) <sup>+</sup> glyceraldehyde-3-phosphate dehydrogenase
IgG	immunoglobulin G
kDa	kilodalton
LHC	light-harvesting complex
NR	nitrate reductase
PBS	phosphate-buffered saline
PC	phycocyanin
PE	phycoerythrin
PEPC	phosphoenol pyruvate carboxylase
PPO	polyphenol oxidase
PRK	phosphoribulokinase
PS	photosystem
Pipes	1,4-piperazinediethanesulfonic acid
O.D.	optical density
RuBP	ribulose 1,5-bisphosphate

Rubisco	ribulose 1,5-bisphosphate carboxylase/oxygenase
Rubisco LS	large subunit of Rubisco
Rubisco SS	small subunit of Rubisco
SDS	sodium dodecyl sulfate
TBS	tris-buffered saline

## CHAPTER I

Pyrenoids and their involvement in the  
compartmentalization of the Calvin  
cycle and other metabolic processes

## 1.0. Introduction

The pyrenoid is a distinguishing characteristic of many algal species, appearing in electron micrographs as an electron-dense inclusion body located in the chloroplast. In addition to algae, pyrenoids have also been observed in several species of hornworts (Anthocerotae)<sup>1</sup>. Although pyrenoid morphology has been investigated extensively (for reviews, see Griffith 1970; Dodge 1973), pyrenoid function remains unclear. Some investigators have considered the pyrenoid a protein storage region. Holdsworth (1971) speculated that ribulose 1, 5-bisphosphate carboxylase/oxygenase (Rubisco) and possibly other enzymes of the photosynthetic carbon reduction cycle may be stored in the pyrenoid, ready to provide recently divided cells with a source of these enzymes. Alternatively, it has been proposed that the pyrenoid serves as a general storage area whose nitrogen reserves can be mobilized when needed (Fischer and Klein 1988). The persistence of these views, however, reflects a general shortage of biochemical and physiological data concerning pyrenoids. Unlike cell organelles, pyrenoids are generally not membrane-bound, and thus do not easily lend themselves to isolation using standard cell-fractionation techniques. Most investigators report that unfixed pyrenoids will solubilize rapidly during purification procedures. Some investigators have availed

<sup>1</sup> A pyrenoid-like region has been described in the quillwort, *Isoetes*. Immunolabelling results, however, indicate that this region is not preferentially labelled by anti-Rubisco (K. Vaughn, pers. comm.) and thus is not a true pyrenoid.

themselves of species containing pyrenoids demarcated by a starch sheath (Holdsworth 1971; Rosowski and Hoshaw 1971, Salisbury and Floyd 1978) The starch shell affords some protection during the isolation procedure and allows for a moderate yield of intact pyrenoids. This practice, however, is limited to certain green algal species and therefore cannot provide information about the pyrenoid in diverse groups of algae. Higher yields of purified pyrenoids have been obtained by fixing algae with  $HgCl_2$  prior to cell disruption (Kerby and Evans 1978, 1981; Satoh et al 1984, 1985; Kuchitsu et al. 1988a). This treatment serves to stabilize pyrenoid protein and the technique has been useful in obtaining pyrenoid fractions which have been used for polypeptide composition analyses. This, however, is done at the expense of measuring enzyme activities. Recently, some success has been reported in maintaining pyrenoid integrity during isolation by using buffers of high ionic strength (Kuchitsu et al 1988a; Okabe and Okada 1988). Employing this procedure, Okabe and Okada (1988) were able to investigate the polypeptide composition of isolated pyrenoids and measure Rubisco activity.

As an alternative, microscopical methods employing cytochemistry and immunocytochemistry can be applied to the study of pyrenoids. These techniques offer in situ biochemical information with the additional advantage that only small quantities of tissue are required. Upon considering the inherent disadvantages associated with pyrenoid isolation employing conventional cell-fractionation methodologies, it is clear that cytochemical and immunocytochemical techniques represent a valuable tool for the elucidation of pyrenoid composition and function.

This report reviews the advances made using microscopical cytochemistry and immunocytochemistry towards clarifying a functional role for pyrenoids.

## 2.0. Immunocytochemical Techniques

Immunocytochemistry involves the use of antibodies as specific reagents for the in situ detection of intracellular macromolecules. Various immunocytochemical techniques have been employed in the study of pyrenoid composition and function and these will be outlined briefly in this section. Specific techniques of microscopical cytochemistry will not be reviewed in this section. Instead, they are introduced where relevant in other sections of this report.

### 2.1. Immunofluorescence

Immunofluorescence microscopy has been employed in several investigations of pyrenoid protein composition (Vladimirova et al. 1982, Kiss et al. 1986; Kajikawa et al. 1988). This technique involves the detection of antibodies which have been labelled with specific fluorochromes such as fluorescein and rhodamine. In the application of immunofluorescence microscopy, most investigators employ an indirect labelling technique where tissue incubation with unlabelled primary antiserum is followed by reaction with a specific fluorochrome-labelled secondary antibody. Unlike primary antiserum, fluorochrome-labelled secondary antibodies are readily available from commercial sources

Moreover, use of a secondary antibody provides amplification of the reaction signal thereby making immunofluorescence microscopy a sensitive detection technique. However, limitations of this technique, particularly in its application to plant and algal cells, need to be addressed. Antiserum penetration into plant and algal cells poses a technical problem mainly due to the complex nature of their cell walls. This, however, can be overcome by the appropriate selection of an experimental organism. Vladimirova et al. (1982) reported greatest success in effecting antisera penetration into the cell when using a mutant of *Chlamydomonas reinhardtii* lacking a cell wall. Likewise, both Kiss et al. (1986) and Kajikawa et al. (1988) reported successful antiserum entry by employing intact, isolated chloroplast preparations in place of whole cells. Moreover, these investigators briefly fixed the chloroplasts with methanol, a reagent thought to aid in membrane permeabilization (Knox 1982).

Cell and tissue autofluorescence also presents a concern for immunofluorescence investigations when plant and algal cells are used. Autofluorescence of phenolic compounds, cell wall components and chlorophyll occur with wavelengths of light normally employed to excite the routinely used fluorescent marker fluorescein. In addition, the fixative glutaraldehyde is known to autofluoresce. Use of an alternative fluorochrome such as rhodamine, treatment of the tissue with Evans blue, a reagent which reduces autofluorescence, and omission of glutaraldehyde from the fixation protocol are all approaches that have been employed to circumvent the problem of autofluorescence. As an alternative, Vladimirova et al. (1982) reduced chlorophyll

autofluorescence by fixing their cells in 96% ethanol, thereby effectively bleaching them

A third limitation of this technique is in its resolving capabilities. The technique can be performed only at the resolution provided by the light microscope. In addition, the amounts of fluorescence over a particular cell compartment are readily described only in a qualitative manner, thus, making it difficult to assess intracellular protein levels. Furthermore, marker-specific fluorescence fades with time (e.g. Kajikawa et al 1988), thereby making comparisons between different cell preparations difficult. Nevertheless, investigations employing immunofluorescence microscopy have provided valuable information regarding pyrenoid composition and function

## 2.2. *Immunoenzymatic technique*

To our knowledge, the immunoenzymatic technique has been employed in only one investigation of pyrenoid protein composition (Kajikawa et al 1988). In this technique, detection of the primary antiserum is generally made through an enzyme-linked secondary or tertiary antibody or antibody-binding compound following tissue incubation in a specific substrate solution. Often, the linked enzyme is horseradish peroxidase and a reaction product is formed by its action on a substrate solution containing  $H_2O_2$  and either 3, 3'-diaminobenzidine or 4-chloronaphthol. Similar to the immunofluorescence technique, limited access into the cell by antiserum could present a limitation to this method. In their investigation, however, Kajikawa et al. (1988) used isolated chloroplasts of the green alga *Bryopsis maxima* just as they had done for

their immunofluorescence analysis. A further limitation of this technique particularly applicable to plant and algal cells is the presence of endogenous peroxidase in these organisms. Its presence is capable of generating confusing results and must be taken into consideration when analyzing data.

One advantage that this technique holds over immunofluorescence is that it can be used at both the light and electron microscope levels as the enzymatic reaction generates an electron-dense product. However, one is still confronted with the difficulty of attempting to describe the immunoreaction in anything except qualitative terms.

### 2.3 Immunogold electron microscopy

Despite the availability and successful applications of the aforementioned techniques, at present, immuno-electron microscopy represents the method of choice in most immunocytochemical investigations. This technique combines a level of fine-structural resolution afforded only by the electron microscope with a precise localization of intracellular macromolecules. Detection of primary antiserum is facilitated by a secondary antibody or an IgG-binding protein to which an electron-opaque marker is adsorbed. Although the iron-containing protein, ferritin, has been employed with some success, the marker of choice is usually colloidal gold. Unlike ferritin, gold particles exhibit little non-specific binding and display less tendency to aggregate. Moreover, the wide range of particle sizes available and the uniformity of individual colloidal gold preparations readily facilitate data acquisition and analysis. *Staphylococcus* protein A is

widely employed as the IgG-binding protein to which colloidal gold particles are adsorbed. In contrast to individual species-specific secondary antibodies, protein A recognizes IgG molecules from a variety of sources and thereby presents itself as a broad-spectrum reagent. Recently, Bendayan (1987) has suggested that *Staphylococcus* protein G might provide a better tool for high-resolution immunocytochemistry since its IgG-binding properties are superior to those of protein A.

Most immunogold investigations are performed on ultrathin sections of resin-embedded tissue and in this manner, the problem of poor antiserum penetration imposed by cell walls and intact membranes is alleviated. However, using the post-embedding immunogold technique, one is confronted by a problem not normally associated with whole cell immunofluorescence and immunoenzymatic methods. Examination of material using the transmission electron microscope requires that the tissue be processed; yet, harsh conventional processing can destroy antigenicity. Therefore, a compromise is often necessary between tissue preparation for microscopical observation and retention of antigenicity. For a more comprehensive discussion of methods of tissue preparation for immunoelectron microscopy, the reader is referred to several recent reviews (Roth 1982; Herman 1988; Beesley 1989).

Thus, through the use of fixation and embedding protocols amended specifically for immuno-electron microscopy, many antigens can be successfully localized with high resolution at the intracellular level. It is clear then, that this technique is a powerful tool for the microscopist and will continue to be used to garner valuable information concerning pyrenoid composition and function.

### 3.0. Ribulose 1,5-Bisphosphate Carboxylase/Oxygenase and Pyrenoids

In photosynthetic organisms, Rubisco catalyses the initial reactions of the opposing pathways of photosynthetic carbon reduction and photorespiratory carbon oxidation. That is, Rubisco is able to catalyze the fixation of both CO<sub>2</sub> and molecular O<sub>2</sub> to substrate ribulose 1,5-bisphosphate (RuBP). The efficiency with which it catalyzes either reaction is determined by both the concentrations of CO<sub>2</sub> and O<sub>2</sub> at the site of catalysis and the substrate specificity factor for a particular Rubisco enzyme. In order to understand further the involvement of Rubisco in these two pathways, some knowledge of its intracellular localization is important. Numerous immunocytochemical studies of higher plants have shown that Rubisco is an enzyme of the chloroplast stroma (e.g. Vaughn 1987a; Rother et al. 1988; see also Appendix 1). In C<sub>3</sub> plants, there is no evidence to support a differential intercellular distribution of the enzyme; Rother et al. (1988) observed labelling by anti-Rubisco in all cell types of spinach leaves. C<sub>4</sub> plants, however, possess a Kranz anatomy in which structurally differentiated mesophyll and bundle sheath cells exist in mature leaf tissue. Moreover, immunofluorescence studies using C<sub>4</sub> plants have shown that phosphoenolpyruvate carboxylase (PEPC) is largely concentrated in the cytoplasm of mesophyll cells whereas Rubisco appears to be restricted to the chloroplasts of bundle sheath cells (e.g. Perrot-Rechenmann and Gadal 1986). It appears that in C<sub>4</sub> plants, inorganic carbon is initially fixed by PEPC in the cytoplasm of mesophyll cells with the resulting C<sub>4</sub> acids being transported to bundle sheath cells where they

are decarboxylated. This results in a local concentration of CO<sub>2</sub> at the site of Rubisco catalysis, thereby promoting the carboxylation of RuBP. Furthermore, a spatial separation exists between photosynthetic O<sub>2</sub> evolution and CO<sub>2</sub> fixation by Rubisco in NADP-malic acid-type C<sub>4</sub> plants since the agranal chloroplasts of their bundle sheath cells possess no photosystem II activity (Downton et al. 1970). Absence of photosynthetic O<sub>2</sub> evolution further serves to maintain a high CO<sub>2</sub>/O<sub>2</sub> ratio in bundle sheath cells. Consequently, C<sub>4</sub> species possess low CO<sub>2</sub> compensation points and exhibit little photorespiration.

Many species of cyanobacteria and algae cultured under limiting dissolved inorganic carbon levels, also possess an inorganic carbon concentrating mechanism where carbon species are concentrated intracellularly to levels higher than in the surrounding medium (see Aizawa and Miyachi 1986, for review). Therefore, it would be of interest to know whether a specific intracellular localization of Rubisco in these organisms contributes to the function of the concentrating mechanism as is the case for C<sub>4</sub> plants. Among those algae and hornworts that do not contain pyrenoids, immunogold studies have shown that, similar to higher plants, Rubisco is distributed throughout the chloroplast stroma (Lacoste-Royal and Gibbs 1985, Ekman et al. 1989; Vaughn et al. 1990; see also Appendix 1). In contrast, biochemical and immunocytochemical investigations indicate that in pyrenoid-containing organisms, a substantial portion of Rubisco is localized in the pyrenoid. Many of the immunocytochemical investigations of Rubisco distribution among pyrenoid-containing algae and hornworts have been survey-like in nature and indicate that pyrenoids from diverse species

of algae all contain Rubisco. Employing antiserum raised against the large subunit of Rubisco purified from tobacco, McKay and Gibbs (1990; see also Chapter VII) observed Rubisco to be highly localized over the pyrenoid of the red alga *Porphyridium cruentum*. In contrast, immunogold label over the chloroplast stroma was present at only low levels. This result has since been confirmed by Mustardy et al. (1990) and Cunningham et al. (1991). Using antiserum raised against the large subunit of Rubisco purified from the chromophyte alga *Olisthodiscus luteus*, similar observations have been made for two species of cryptomonad algae. Gold particles were observed highly concentrated over the pyrenoids of both *Chroomonas* sp. and *Hemiselmis brunnescens* (McKay et al. 1991b; see also Chapter VIII). Moreover, using the same antibody, we report a pyrenoid localization for Rubisco in the diatom *Phaeodactylum tricorutum* (see Appendix 4). Recently, a similar observation has also been made for the diatom *Cylindrotheca fusiformis* (F.G. Plumley, pers. comm.) It should be noted that detection of Rubisco in chlorophyll *c*-containing algae such as cryptomonads and diatoms is more readily facilitated by use of antiserum raised against chromophyte Rubisco, even though the large subunit of the Rubisco enzyme is considered to be evolutionarily well-conserved. When higher plant Rubisco antiserum is used for immunolabelling studies with these algae, we consistently observe only low levels of cross-reactivity (R.M. McKay and S.P. Gibbs, unpublished data). In support of this, recent investigations have indicated, that, although Rubisco enzymes from diverse sources share similarity in terms of physical properties, the enzyme subunits from chromophyte algae possess few antigenic determinants in common with those from green algae

and higher plants (Plumley et al. 1986; Newman et al. 1989). In addition, Newman et al. (1989) have extended this observation to the Rubisco enzyme purified from the red macrophyte *Griffithsia pacifica*. This might then explain our failure to observe labelling over sections of *Porphyridium cruentum* when using antiserum raised against the small subunit of tobacco Rubisco (McKay and Gibbs 1990; see also Chapter VII). Likewise, poor antiserum recognition might account for the low levels of Rubisco labelling observed over the pyrenoid of the endosymbiotic dinoflagellate *Symbiodinium kawagutii* (Blank and Trench 1988). These investigators employed antisera prepared against purified tobacco Rubisco holoenzyme in addition to the SDS-dissociated subunits of this enzyme. Although their quantitative analysis of labelling densities over various cell compartments indicates significant immunolabelling of the pyrenoid and chloroplast stroma, labelling densities were very low.

Additional investigations of Rubisco distribution among pyrenoid-containing organisms also indicate Rubisco to be pyrenoid-localized in *Euglena*, green algae and various hornwort species. Osafune et al. (1989) have clearly demonstrated by immunogold cytochemistry and three-dimensional computer reconstruction of immunolabelled serial sections that Rubisco is predominantly localized in the pyrenoids of *Euglena gracilis*. Likewise, in green algae, Vladimirova et al. (1982) reported an intense fluorescence over the pyrenoids of both *Chlamydomonas reinhardtii* and *Dunaliella salina* following application of indirect immunofluorescence using antiserum raised against *Chlorella* Rubisco. However, they also reported a lower, but genuine signal over the remainder of the chloroplast. Using the immunogold technique, several

reports from our laboratory have subsequently confirmed a pyrenoid localization for Rubisco in *Chlamydomonas* (Lacoste-Royal and Gibbs 1985; 1987; McKay and Gibbs 1991b; see also Chapter IV; McKay et al. 1991a; see also Chapter III). Kajikawa et al. (1988) employing immunoenzymatic and immunofluorescence methods have similarly reported Rubisco to be mainly pyrenoid-localized in isolated, intact chloroplasts of the green alga *Bryopsis maxima*. Furthermore, their use of monoclonal antibodies directed against the large subunit of Rubisco purified from this alga ensured a high specificity of localization. Employing the immunogold technique, Nisius and Ruppel (1987) observed the pyrenoid of *Chlorella vulgaris* to be heavily labelled by Rubisco antiserum. The high amount of background labelling in their published micrograph, however, makes it difficult to comment on a possible association of at least a portion of the Rubisco with the stroma. More recently, McKay et al. (1991a) reported the pyrenoid of *Coleochaete scutata* to be heavily labelled following reaction with antiserum to the holoenzyme of Rubisco purified from tobacco. Likewise, the pyrenoids of hornworts also contain Rubisco. Vaughn et al. (1990) examined twelve pyrenoid-containing species and in each, they observed Rubisco to be restricted to the pyrenoid regions. Immunolabel over the chloroplast stroma was at the level of background.

Other investigations have taken a more experimental approach and have combined physiological and developmental studies with the immunocytochemical localization of Rubisco. Kiss et al. (1986) reported on the morphological expression of pyrenoids as a function of nutrition in *Euglena gracilis*. They observed pyrenoids to be present in cells

cultured under continuous light in a medium lacking organic carbon sources (incomplete medium) whereas cells grown photoheterotrophically in a complete medium did not possess pyrenoids until the organic carbon supply appeared to have been exhausted. Moreover, they demonstrated by indirect immunofluorescence microscopy that Rubisco was predominantly restricted to the pyrenoid under conditions where this structure was morphologically expressed. In contrast, Rubisco in cells cultured photoheterotrophically was demonstrated to be dispersed throughout the chloroplast. Similar results have been reported recently by Osafune et al. (1990b). These investigators observed that dark-grown cells of *Euglena* did not possess pyrenoids when cultured without agitation in a medium containing organic carbon. However, when cells were transferred to an "inorganic" medium (containing ammonium salts but lacking organic carbon) and maintained in the dark and aerated with 1.5% CO<sub>2</sub>, they developed "propyrenoids" in a process concomitant with the oxidative degradation of a wax ester that had previously accumulated in these cells. Moreover, immunogold cytochemistry indicated Rubisco to be highly localized over the propyrenoids. It appears then, that for *Euglena*, de novo pyrenoid formation can be a light-independent process and may be initiated once organic carbon is depleted from the medium.

The association between Rubisco and pyrenoids in *Euglena* has further been investigated as a function of the cell cycle (Osafune et al. 1990c). These investigators observed pyrenoid dispersion to occur immediately prior to chloroplast division in synchronously-cultured cells of *E. gracilis*. Using immunogold cytochemistry, they clearly demonstrated Rubisco to be distributed throughout the chloroplast stroma

in cells undergoing division. Furthermore, their data indicate that Rubisco becomes concentrated in certain regions of the chloroplast of recently divided cells prior to the beginning of the light period and in this way, it appears that pyrenoids are again formed. In a study of a similar nature, Lacoste-Royal and Gibbs (1987) investigated Rubisco distribution in the green alga *Chlamydomonas reinhardtii* at several stages of culture growth. In their report, they expressed labelling densities on a total volume basis in order to account for the difference in total cell volume between the chloroplast stroma and the pyrenoid, a difference that is not always obvious when observing a single section through a cell. Their data indicate that for light-harvested, synchronously-dividing cells, Rubisco is mainly localized to the pyrenoid; however, they also observed between 30-40% of Rubisco to be distributed throughout the chloroplast stroma. Moreover, cells exposed to an extended dark period or cells harvested at the late stationary phase of culture growth displayed proportionately less Rubisco in the chloroplast stroma. They interpreted these observations as an indication that the pyrenoid might represent a storage organelle.

In another study, McKay and Gibbs (1989; see also Chapter II), employing the immunogold technique, demonstrated that Rubisco was restricted to the pyrenoid in cells of the green alga *Chlorella pyrenoidosa* cultured at both photosynthetically limiting and saturating photon fluence rates. We speculated that at light-saturating irradiance, much of the cell's Rubisco would be catalytically competent and functional in order to account for the high photosynthetic rates observed. That Rubisco remained localized to the pyrenoid under

conditions of maximum photosynthesis indicated that pyrenoid Rubisco is functional in vivo. In support of this, Osafune et al. (1990c) report that when photosynthetic CO<sub>2</sub>-fixation in *Euglena* is measured at high light intensities, the rates observed would require the cells complement of Rubisco to be active. Furthermore, they confirmed that pyrenoids were present in the cells used for their measurements.

Although immunocytochemical studies indicate that Rubisco is predominantly localized in the pyrenoid among pyrenoid-containing organisms, the frequent observation that a portion of label is associated with the chloroplast stroma has led investigators to question the physiological role of pyrenoid Rubisco. Because Rubisco is generally regarded as being a stromal enzyme, speculation that the pyrenoid is a protein storage body is not uncommon. Moreover, several concerns regarding immunocytochemical methodology in its specific application to the study of Rubisco distribution in pyrenoid-containing organisms have further fueled speculation regarding the physiological role of pyrenoid-localized Rubisco, and thus, need be addressed. The first regards the possibility that Rubisco is present at moderate concentrations in the stroma yet the immunocytochemical technique employed has failed to detect it, perhaps due to a more favourable preservation of antigenicity of pyrenoid-localized Rubisco compared to stromal Rubisco during tissue processing. We feel, however, that this is not so. In support of our view, immunolocalizations of Rubisco in higher plants and non-pyrenoid-containing algae and hornworts demonstrate gold labelling over the chloroplast stroma to be relatively dense. In their investigation of Rubisco distribution in the red

macroalga *Gracilaria secundata*, Ekman et al. (1989) report anti-Rubisco labelling over the chloroplast stroma at a density of 54 gold particles  $\cdot \mu\text{m}^{-2}$ . Likewise, a similar density of labelling was reported over chloroplasts of the non-pyrenoid-containing hornworts *Anthoceros fusiformis* and *Megaceros flagellaris* (Vaughn et al. 1990). These values are 10 to 20 times higher than the stromal labelling densities reported from studies involving pyrenoid-containing algae (e.g. Lacoste-Royal and Gibbs 1987; McKay and Gibbs 1989; see also Chapter II). Furthermore, the investigation by Vaughn and colleagues surveyed both pyrenoid- and non-pyrenoid-containing hornworts, all of which were fixed, embedded and immunolabelled using the same protocols. The visual impression provided upon comparing the different types of hornworts in their report is very convincing and strongly indicates that tissue processing does not preferentially destroy the antigenicity of stromal Rubisco and that immunocytochemical techniques will readily detect stromal Rubisco if present in sufficient quantities necessary for photosynthetic function.

Speculation regarding the role of pyrenoid-localized Rubisco also exists due to an inherent limitation of the immunocytochemical technique; that being the inability of antisera to distinguish between active and inactive enzyme forms. In order to be catalytically competent, Rubisco must exist in an activated state, this being accomplished by the ordered addition of an activator  $\text{CO}_2$  molecule and  $\text{Mg}^{++}$  to the large subunit of the enzyme (Miziorko and Lorimer 1983). Although immunocytochemical investigations indicate Rubisco to be predominantly pyrenoid-localized, these investigations do not provide an assessment of Rubisco activation state. Thus, using antiserum generated

against Rubisco, it cannot be demonstrated conclusively that pyrenoid-localized Rubisco is catalytically functional. Recently, a soluble protein of chloroplasts of higher plants, Rubisco activase, has been implicated as being responsible for catalyzing the activation and maintaining the activated state of Rubisco *in vivo* (Salvucci et al. 1985; Portis et al. 1986; Salvucci et al. 1986). These investigations indicate that the existence of Rubisco activase enables Rubisco to achieve a high level of activation at concentrations of CO<sub>2</sub> normally encountered in the chloroplast stroma of leaves of higher plants. Furthermore, it is thought that Rubisco activase is able to promote the activation of Rubisco in the presence of various sugar-phosphate compounds, such as RuBP, which prevent Rubisco activation *in vitro* by tightly binding to the inactive form of the enzyme (Jordan and Chollet 1983). Employing mouse polyclonal antiserum raised against a mixture of the 41 and 45 kDa polypeptides of spinach Rubisco activase, a single activase polypeptide has been detected in protein extracts from the green alga *Chlamydomonas reinhardtii* (Roesler and Ogren 1990a, McKay et al. 1991; see also Chapter III). In addition, Roesler and Ogren (1990a) report that purified spinach Rubisco activase polypeptides are capable of promoting the activation of *Chlamydomonas* Rubisco in the presence of physiological concentrations of RuBP. Using the same antibody preparation, it was recently demonstrated by immunogold cytochemistry that Rubisco activase is predominantly localized to the pyrenoids of two species of green algae (*C. reinhardtii* and *Coleochaete scutata*) (McKay et al. 1991a; see also Chapter III) and several hornwort species (K. Vaughn, pers. comm.). In all of these species, gold particles were

mainly restricted to the pyrenoid whereas stromal labelling was present at only low levels. Thus, it appears that for pyrenoid-containing green algae and hornworts, Rubisco and Rubisco activase co-localize. Moreover, it would seem that, given its proposed role in the regulation of Rubisco activation in vivo, the immunolocalization of Rubisco activase should indicate the location of functional Rubisco in the chloroplast. It is proposed therefore, that at least in green algae and hornworts, pyrenoid Rubisco is functional.

In this context, several recent observations are noteworthy. The Rubisco binding protein (a member of the chaperonin family) has been detected in a pyrenoid preparation from *Chlamydomonas* (K. Kuchitsu, pers. comm.) Employing antiserum directed against the binding protein from pea, a stained band of ~66 kDa was detected by immunoblotting of SDS-treated *C. reinhardtii* pyrenoid proteins. That the Rubisco binding protein is present in the pyrenoid does not in itself indicate a catalytic role for pyrenoid-localized Rubisco; however, its presence there adds another level of complexity to the structure.

Also of significance is the detection of ubiquitin in the pyrenoid of *C. reinhardtii* (Wettern et al. 1990). Employing immunogold electron microscopy, these investigators found ubiquitin most concentrated over the pyrenoid, with substantial amounts also found elsewhere in the chloroplast, and in the cytoplasm and nucleus. It is likely that pyrenoid-localized ubiquitin has a role in the turnover of Rubisco protein; it has been demonstrated that Rubisco in chloroplasts of higher plants can be targeted for degradation by the ubiquitin-conjugating system (Veierskov and Ferguson 1991).

## 4.0. Other Calvin Cycle Enzymes

### 4.1. Phosphoribulokinase

The available immunocytochemical evidence indicates a functional role for pyrenoid-localized Rubisco. Of additional interest, however, is the fact that analyses of pyrenoid polypeptide composition indicate that proteins other than Rubisco are also present in pyrenoids. Holdsworth (1971) showed that 90% of the total pyrenoid protein of the green alga *Eremosphaera viridis* could be accounted for by the large and small subunits of Rubisco. Not surprisingly then, he also demonstrated the pyrenoid to possess a high specific activity of this enzyme. However, in addition to Rubisco activity, he measured low amounts of activity for the Calvin cycle enzymes phosphoribulokinase (PRK) and phosphoriboisomerase. The possibility that pyrenoids possess the full complement of Calvin cycle enzymes is a novel concept and has prompted further investigation of this matter. Satoh et al. (1984) identified as a minor component of their pyrenoid preparation from the green alga *Bryopsis maxima*, a 42 kDa protein, which, in a subsequent report, they initially speculated might be a subunit of PRK based on its molecular size (Satoh et al. 1985). In addressing this, they purified PRK from *B. maxima* and compared its peptide map with that of the 42 kDa pyrenoid protein. The maps, however, were very dissimilar thereby indicating that this particular pyrenoid polypeptide was not PRK. In support of this, a recent immunoblot analysis of *Chlamydomonas* pyrenoid proteins provided no evidence for the presence of PRK in pyrenoids of this alga (Kuchitsu et al. 1991).

The subcellular distribution of PRK in pyrenoid-containing algae has also been investigated by immunoelectron microscopy. Results from our laboratory obtained using antiserum raised against PRK purified from the cyanobacterium *Chlorogloeopsis fritschii* indicate that PRK is excluded from the pyrenoid of the red alga *Porphyridium cruentum* (McKay and Gibbs 1991b; see also Chapter IV). Moreover, employing antibodies raised against PRK prepared from the green alga *Chlamydomonas reinhardtii*, we have found PRK to be excluded from the pyrenoid of this alga as well (McKay and Gibbs 1991b; see also Chapter IV). Interestingly, we have observed what we believe to be numerous PRK-containing stromal inclusions associated with the pyrenoid of *Chlamydomonas*. It is postulated that these pyrenoid inclusions provide a means for more efficient interaction between pyrenoid and stroma when the pyrenoid appears, at least in micrographs, to be completely demarcated by starch.

### 5.0. Carbonic Anhydrase

Rubisco requires  $\text{CO}_2$  as a substrate in the process of photosynthetic carbon reduction. In photosynthesizing chloroplasts, however, the pH of the stroma is ~8 (Heber and Heldt 1981), thus much of the inorganic carbon accumulated intracellularly exists as  $\text{HCO}_3^-$ . The uncatalyzed dehydration of  $\text{HCO}_3^-$  occurs rather slowly and the rate at which  $\text{CO}_2$  is produced in this manner cannot account for rates of photosynthesis observed in air-grown cells. Carbonic anhydrase (CA) is the enzyme responsible for catalyzing the interconversion between  $\text{CO}_2$  and  $\text{HCO}_3^-$ . It

is anticipated that the presence of some CA in the pyrenoid would more readily facilitate supply of CO<sub>2</sub> to Rubisco localized in this region. Attempts at localizing CA in pyrenoid-containing organisms, however, have generated conflicting results. Yagawa et al (1987) employed immunogold electron microscopy to determine the subcellular location of a CA isozyme in the red alga *Porphyridium cruentum*. Gold particles clearly marked both the cytoplasm and the chloroplast stroma but were mainly excluded from the pyrenoid. Similar results have been obtained for several species of pyrenoid-containing hornworts (K. Vaughn, pers. comm.). Employing antiserum directed against a CA isozyme from spinach chloroplasts, specific labelling over the chloroplast, but not the pyrenoid, was observed. In contrast, Kuchitsu et al. (1991) have recently presented cytochemical evidence for a pyrenoid localization of CA. Sulfonamides are specific inhibitors of CA activity. Employing the fluorescent sulfonamide, dansylamide, these investigators demonstrated pyrenoid staining in the green alga *C. reinhardtii*. Moreover, unlike immunocytochemical analyses, identification of CA through sulfonamide binding provides a broad spectrum assay since all isozymes of CA, at least to some degree, should be reactive.

Our own attempts at localizing CA in pyrenoid-containing algae have met with very limited success. Attempts using cytochemical assays such as dansylamide fluorescence or the Hansson cobalt-phosphate method (Ridderstråle 1982; Lonnerholm 1984) have failed to yield positive results. Although we have enjoyed a modicum of success employing immunogold methodology, the results have not been insightful. Immunolocalization of the 37 kDa periplasmic CA of *C. reinhardtii* was

where expected (data not shown). The only substantial intracellular labelling occurred over what we believe to be the Golgi; not surprising since this protein is glycosylated. Hopes that *C. reinhardtii* periplasmic CA would cross-react with intracellular CA isozymes were not realized. Rather, it is now apparent that the chloroplastic and cytosolic CA isozymes of this alga are quite different from the periplasmic form (Husic et al. 1989).

#### **6.0. The Nitrate Reductase Conundrum**

The initial step of nitrate assimilation by photosynthetic organisms is catalyzed by the enzyme nitrate reductase (NR). While it is well established that the next enzyme in the nitrate assimilatory pathway, nitrite reductase, is predominantly chloroplast localized, the intracellular compartmentation of NR has been the subject of much contention. Earlier biochemical evidence suggested that in leaves of higher plants, NR is a cytoplasmic enzyme (e.g. Dalling et al. 1972). Similarly, histochemical (Vaughn and Duke 1981) and immunogold (Vaughn and Campbell 1988) investigations support a cytoplasmic localization for this enzyme. In contrast, Kamachi et al. (1987), employing immunoelectron microscopy, reported that NR was associated exclusively with the chloroplast in spinach leaves. These authors argue that a chloroplast localization for NR would enhance the efficiency of nitrate assimilation since translocation of nitrite from the cytoplasm into the chloroplast would not be required. Moreover, a close coupling between

nitrate and nitrite assimilation might be advantageous since nitrite is toxic when present at high levels (as reported in Solomonson and Barber 1990).

The intracellular localization of NR in algae has been investigated by a variety of techniques. Employing immunogold cytochemistry, Lopez-Ruiz et al. (1985a, 1985b) have shown that NR is localized predominantly in the pyrenoid in green algae cultured on nitrate. In their investigations, they used antiserum prepared against NR purified from the green alga *Monoraphidium braunii* in order to localize this enzyme on ultrathin cryosections of *Monoraphidium*, *Chlamydomonas reinhardtii*, *Chlorella fusca*, *Dunaliella salina* and *Scenedesmus obliquus*. In each alga, the pyrenoid was heavily labelled by the antiserum. In addition, a lower level of label was evident over the remainder of the chloroplast whereas other cellular compartments were mainly unlabelled. Similarly, Michaels et al. (1986) have demonstrated a pyrenoid localization for NR in resin-embedded cells of *Chlorella vulgaris*. However, in addition, these authors observed a portion of the label to be localized over the cell periphery. Recently, Okabe and Okada (1990) reported NADH-NR activity associated with the pyrenoid of the green alga *Brvois maxima*. Specific activity of the enzyme in the pyrenoid fraction was 80 times greater than that measured in the crude extract of chloroplasts.

In contrast to evidence that indicates a pyrenoid localization for NR in algae, a recent biochemical investigation suggests that NR is not associated with the chloroplast in the green alga *C. reinhardtii* (Fischer and Klein 1988). These investigators isolated intact chloroplasts from *Chlamydomonas* and measured specific activities for a

number of nitrogen-assimilating enzymes. Their data indicate that in *Chlamydomonas*, NR activity is associated with the cytoplasm; no extractable activity was found associated with the chloroplast fraction. Fischer and Klein (1988) attempt to reconcile their observations with those obtained through immunocytochemical analyses by suggesting that pyrenoid-localized NR is not active in vivo and possibly represents a protein store that can be mobilized when needed. The recent observation that a polyclonal antibody raised against corn leaf NR selected a clone containing chloroplast NAD(P)<sup>+</sup>:glyceraldehyde-3-phosphate dehydrogenase (GAPDH) cDNA (Gowri and Campbell 1989) has further prompted a re-examination of immunocytochemical results concerning the localization of NR. Although these authors report that NR and GAPDH do not share significant amino acid sequence identity, they explain that in order for the antiserum to select for this particular cDNA clone, it would appear that the two proteins must possess common epitope(s). That this particular antiserum recognized GAPDH is of significance for the elucidation of pyrenoid function since GAPDH catalyses an early reaction of the photosynthetic carbon reduction cycle. As already noted, Rubisco, which catalyses the initial reaction of this cycle, is predominantly localized to, and appears to be functional in the pyrenoid. Thus, if the NR antisera used in previous immunocytochemical investigations were also able to recognize GAPDH, the observed labelling results might actually indicate the presence of GAPDH instead of NR in the pyrenoid. In their immunolabelling studies, Lopez-Ruiz et al. (1985a; 1985b) tested for antiserum specificity; however, in doing this, they used a partially purified NR fraction instead of a crude protein

extract. That GAPDH was excluded from the fraction they tested is possible. Therefore, the observation that NR may share common epitopes with enzymes such as GAPDH might explain the conflicting results obtained through immunocytochemistry for the intracellular localization of NR in higher plants and algae. In any event, the possibility that GAPDH is localized to the pyrenoid must be further investigated.

Recently, Lopez-Ruiz and colleagues (1991) reported on the subcellular location of nitrite reductase in green algae. Their results confirm that this enzyme is located mainly in the chloroplast; however, they found between 20-35% of nitrite reductase to be pyrenoid-localized. This, they suggest, when taken together with their previous findings for NR, infers a direct coupling between  $\text{NO}_3^-$  and  $\text{NO}_2^-$  assimilation in these algae.

#### **7.0. DNA and Pyrenoids**

The distribution of DNA nucleoids in the chloroplasts of algae has been studied both at the level of the light microscope using the DNA-specific fluorochrome 4',6-diamidino-2-phenylindole (DAPI) (e.g. Coleman 1985) and at the electron microscope level using immunogold methodology (Hansmann et al. 1986). From these studies, it is evident that DNA is excluded from algal pyrenoids. Recently, however, Miyamura and Hori (1991) reported that DNA is present in the pyrenoids of some chlorophyte and xanthophyte siphonous algae. Employing DAPI fluorescence, these investigators observed a strong signal emanating from the pyrenoids of

two species of *Caulerpa* and from the xanthophyte *Pseudodichotomosiphon* (= *Vaucheria*) *constrictus*. Moreover, the staining appeared to be specific since treatment with DNase resulted in a loss of fluorescence. The significance of this staining with respect to pyrenoid function is not clear.

#### **8.0. The *Avena* stromacentre: a vestigial pyrenoid?**

The stromacentre is a conspicuous region in the plastids of several species of the higher plant genus *Avena*. Gunning et al. (1968) speculated that on the basis of subunit negative staining, the stromacentre might be comprised of Rubisco. This suggestion later prompted the interpretation that the stromacentre may represent a "pyrenoid relic" (Nisius and Ruppel 1987). Addressing their interpretation, Nisius and Ruppel (1987) purified a 63 kDa stromacentre element from *Avena sativa* and employing antiserum raised against it, probed tissue sections of both *Avena* and *Chlorella vulgaris*. The antiserum specifically labelled the stromacentre of *Avena* whereas the pyrenoid of *Chlorella* remained unlabelled. In contrast, the *Avena* stromacentre displayed no reaction when tissue sections were immunolabelled with antiserum prepared against the large subunit of Rubisco. Instead, Rubisco was distributed throughout the remainder of the chloroplast stroma whereas in *Chlorella*, it was predominantly localized to the pyrenoid. These results, along with proteolytic peptide cleavage patterns and immunoblotting indicated that the

stromacentre was not comprised of Rubisco (Nisius and Ruppel 1987).  
Recently, Nisius (1988) has demonstrated that the 63 kDa Avena  
stromacentre protein is a subunit of a  $\beta$ -glucosidase involved in  
converting oat leaf saponins (avenacosides) into a fungicidal compound.

## CHAPTER II

Immunocytochemical localization of ribulose 1,  
5-bisphosphate carboxylase/oxygenase in  
light-limited and light-saturated cells  
of *Chlorella pyrenoidosa*

## Summary

The localization of ribulose 1,5-bisphosphate carboxylase/oxygenase (Rubisco) in cells of *Chlorella pyrenoidosa* grown at varying light intensities was determined by immunoelectron microscopy. Log phase cells grown at photon flux densities of 25 and 75  $\mu\text{mol m}^{-2} \text{s}^{-1}$  (light-limiting) and 540  $\mu\text{mol} \cdot \text{m}^{-2} \text{s}^{-1}$  (light-saturating) were fixed in 3% glutaraldehyde and embedded in Lowicryl K4M. Sections were labelled with antiserum to each subunit of Rubisco followed by protein A-gold. At each light fluence rate, the pyrenoid was heavily labelled by each antibody whereas chloroplast stromal labelling was not above background levels. The apparent absence of stromal Rubisco at each light level, and hence the lack of enzyme redistribution from pyrenoid to stroma following an increase in light fluence rate, indicates that pyrenoid Rubisco is functional in vivo.

## 1.0. Introduction

Chloroplast pyrenoids are a distinguishing characteristic of many algal species and of some hornworts (Anthocerotae). Proteinaceous in composition (Rosowski and Hoshaw 1971), their function has remained obscure. However, being a chloroplast inclusion, it is plausible that the pyrenoid may be implicated in some aspect of cell photosynthesis. Analysis of the protein isolated from the pyrenoid of the green alga *Eremosphaera viridis* indicated that 90% of the total protein could be accounted for by two components having molecular weights similar to those of the large and small subunits of the bifunctional photosynthetic enzyme ribulose 1,5-bisphosphate carboxylase/oxygenase (Rubisco, EC 4.1.1.39) (Holdsworth 1971). Similar observations have since been extended to the pyrenoids of two additional green algal species, *Bryopsis maxima* (Sato et al. 1984; Okabe and Okada 1988) and *Chlamydomonas reinhardtii* (Kuchitsu et al. 1988a), a prasinophycean alga, *Micromonas squamata* (Salisbury and Floyd 1978), and a brown alga, *Pilayella littoralis* (Kerby and Evans 1981).

Rubisco, however, is generally regarded as being a stromal enzyme and its localization there has been confirmed by immunoelectron microscopy among non-pyrenoid-containing algae (Lacoste-Royal and Gibbs 1985) and higher plants (Caers et al. 1987; Shojima et al. 1987; Vaughn 1987a). Several immunocytochemical studies have similarly shown that at least a portion of the Rubisco in pyrenoid-containing algae is also located in the stroma. Vladimirova et al. (1982) reported an intense fluorescence over the pyrenoid regions of both *C. reinhardtii* and

*Dunaliella salina* following application of indirect immunofluorescence using antibodies raised against *Chlorella* Rubisco. However, they also reported a lower but genuine signal over the rest of the chloroplast. Kiss et al. (1986) have similarly shown by immunofluorescence that Rubisco may be present in both the stroma and pyrenoid of isolated chloroplasts of *Euglena gracilis*. Kajikawa et al. (1988) have recently extended similar observations to *Brvopsis maxima*. In a quantitative investigation employing immunoelectron microscopy, Lacoste-Royal and Gibbs (1987) estimated that 30-40% of the total enzyme was present in the chloroplast stroma of *C. reinhardtii*, with the remainder being concentrated in the pyrenoid.

The observation that chloroplast Rubisco may be partitioned between the pyrenoid and stroma leads one to question the role of pyrenoid Rubisco. Does the pyrenoid function merely as a storage depot for non-catalytically active Rubisco, or does it provide a site for active catalysis? Lacoste-Royal and Gibbs (1987) suggest that the pyrenoid may be a storage body. They observed a greater proportion of label over the pyrenoid in stationary phase cells than in log phase cells of *C. reinhardtii*. However, Rubisco isolated from pyrenoids is able to carboxylate ribulose 1,5-bisphosphate (RuBP) in vitro (Holdsworth 1971; Salisbury and Floyd 1978; Kerby and Evans 1981, Okabe and Okada 1988).

In this study we examine the effect of varying photon flux density on the distribution of Rubisco within the chloroplast of the green alga *Chlorella pyrenoidosa*. A net redistribution of the enzyme from the pyrenoid to the stroma as photon flux density is increased would provide

evidence for the pyrenoid acting in a storage capacity, whereas a lack of enzyme redistribution would suggest that pyrenoid Rubisco can be functionally active in vivo. We demonstrate by protein A-gold immunoelectron microscopy that a net redistribution of Rubisco between pyrenoid and stroma does not occur upon increasing photon flux density in *Chlorella pyrenoidosa*.

## 2.0. Materials and Methods

### 2.1. Cell culture

*Chlorella pyrenoidosa* Chick (UTEX 251) was grown in batch culture in a modified Allen's medium (Yokota and Calvin 1986). Light was provided by cool white fluorescent bulbs at photon flux densities of either 25, 75 or 540  $\mu\text{mol m}^{-2}\cdot\text{s}^{-1}$  in a 14 h light, 10 h dark cycle. Culture temperature was maintained at 25°C. Log phase cells grown at each light fluence rate were harvested for transmission electron microscopy at h 5 or h 12 of the light period. Cell shading while in culture was minimized by: a) continuous culture agitation by use of a rotary shaker, and b) maintaining a low culture volume of 100 ml in a 250 ml Erlenmeyer flask.

### 2.2. Photosynthetic oxygen evolution

The photosynthetic rate of *C. pyrenoidosa* was measured as oxygen evolution in a temperature-controlled Clark-type oxygen electrode (Rank Brothers, Bottisham, Cambridge, UK), calibrated as described by Delieu

and Walker (1972). Aliquots of cells in N<sub>2</sub>-purged culture medium were placed in the oxygen electrode and allowed to photosynthesize for several minutes until the rate of oxygen evolution declined. Photosynthesis was then reinitiated by addition of NaHCO<sub>3</sub>. Illumination was provided by a Kodak Autofocus carousel projector (850H) employing a metal halide lamp and intensity was varied by use of neutral density filters.

### *2.3. Fixation and embedding*

Cells were fixed in either pellet form or in situ. Cell pellets were fixed in 3% glutaraldehyde in 0.1 M sodium phosphate buffer, pH 7.4, for 2 h at 4°C. Pellets were washed with cold buffer and the cells dehydrated through a graded ethanol series and embedded in Lowicryl K4M (J.B. EM Services, Montreal) at -18°C as described previously (Lacoste-Royal and Gibbs 1985). Cells fixed in situ were fixed at the experimental photon flux density in culture medium at 25°C. Glutaraldehyde buffered with 0.1 M sodium phosphate, pH 7.4, was added to provide a final glutaraldehyde concentration of 3%. Cells were fixed for 3 h, centrifuged to obtain a pellet and treated as above for dehydration and embedding.

### *2.4. Immunolabelling*

Antibodies raised in rabbits against the large (LS) and small (SS) subunits of tobacco Rubisco were kindly provided by Jacqueline Fleck (IBMC-CNRS, Strasbourg, France). Colloidal gold was prepared according to the method of Frens (1973) and coupled to protein A (Pharmacia,

Dorval, P.Q ) (Roth et al. 1978). Pale gold-coloured sections were cut with a diamond knife and mounted on formvar-coated nickel grids.

Immunolabelling was performed by placing the grids section-side down on drops of the following solutions phosphate-buffered saline (PBS), 15 min; 1% ovalbumin, 15 min; antibody (anti-LS or anti-SS) diluted 1:1000, 30 min, PBS rinse, protein A-gold diluted 1:10, 30 min; PBS rinse; de-ionized water rinse All dilutions were made in PBS.

Sections were post-stained with 2% aqueous uranyl acetate and viewed in a Philips EM 410 at an operating voltage of 80 kV.

In control experiments, the antibody was replaced with rabbit non-immune IgG, or with PBS alone prior to protein A-gold incubation.

### 2.5 Quantitative evaluation

The density of labelling over each cell compartment was obtained by determining the number of gold particles per square micrometre of compartment sectioned. Area determinations were made using a Zeiss MOP-3 digital analyser

### 3.0. Results

The partitioning of Rubisco between the pyrenoid and stromal regions of the chloroplast of *Chlorella pyrenoidosa* was determined for cells cultured at a variety of photon flux densities by protein A-gold immunocytochemistry Figure 1 shows a section through a log phase cell cultured at a light fluence rate of  $25 \mu\text{mol} \cdot \text{m}^{-2} \cdot \text{s}^{-1}$  which has been

labelled with anti-Rubisco LS. Gold particles are highly concentrated over the pyrenoid, whereas only a few particles are present over the thylakoid-containing stromal regions of the chloroplast. Cells cultured at  $75 \mu\text{mol} \cdot \text{m}^{-2} \text{s}^{-1}$  exhibit a similar distribution of gold particles in sections labelled with anti-Rubisco LS (Fig. 2). The pyrenoid is heavily labelled whereas the remainder of the chloroplast is unlabelled. Only background labelling is present over the cell's nucleus or cytoplasm.

For our strain of *Chlorella*, cultures grown at either of these light fluence rates are light-limited with respect to photosynthesis, a factor which may influence Rubisco distribution. In order to determine the light fluence rate which is light-saturating for photosynthesis, measurements of photosynthetic oxygen evolution were performed on cells cultured at  $75 \mu\text{mol} \cdot \text{m}^{-2} \cdot \text{s}^{-1}$  (Fig. 3). These measurements indicate that in our strain of *C. pyrenoidosa*, photosynthesis is light-saturated at photon flux densities of greater than  $400 \mu\text{mol} \cdot \text{m}^{-2} \cdot \text{s}^{-1}$ . Employing this data, cells were cultured at  $540 \mu\text{mol} \cdot \text{m}^{-2} \cdot \text{s}^{-1}$  and fixed for immunoelectron microscopy while in the log phase of growth. Further photosynthetic oxygen evolution measurements on cells cultured at this light level confirmed that these cells exhibited a light-saturated rate of photosynthesis (data not shown). Cell sections labelled with anti-Rubisco LS (Fig. 4) display the same pattern of enzyme distribution as cells cultured under light-limiting conditions (Figs 1 and 2). Gold label is highly concentrated over the pyrenoid, whereas the remainder of the chloroplast exhibits only a few dispersed gold particles.

Table 1 gives the density of labelling over different cell and

Fig. 1. Log phase cell of *Chlorella pyrenoidosa* cultured under low light ( $25 \mu\text{mol} \cdot \text{m}^{-2} \cdot \text{s}^{-1}$ ). Anti-Rubisco LS is concentrated over the pyrenoid (py) whereas few gold particles are evident over the remainder of the chloroplast (c). Bar =  $0.5 \mu\text{m}$ .

Fig. 2. Log phase cell of *C. pyrenoidosa* cultured at a light fluence rate of  $75 \mu\text{mol} \cdot \text{m}^{-2} \cdot \text{s}^{-1}$ . Anti-Rubisco LS is localized to the pyrenoid whereas the level of labelling over the chloroplast stroma is lower than background nuclear (n) labelling. Bar =  $0.5 \mu\text{m}$ .



1



2

**Fig. 3.** Photosynthetic rate as a function of irradiance for log phase *Chlorella* cells cultured at  $75 \mu\text{mol}\cdot\text{m}^{-2}\cdot\text{s}^{-1}$ . Values represent the average of two measurements.

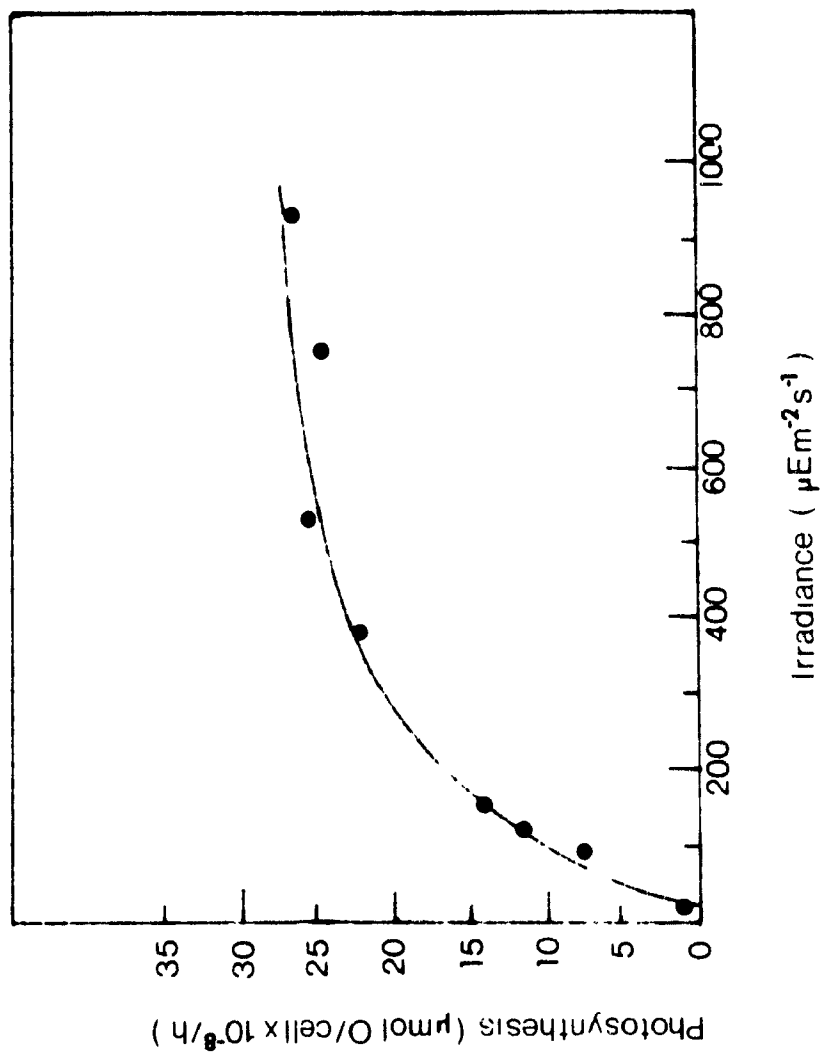


**Fig. 4.** Log phase cell of *C. pyrenoidosa* cultured under light-saturating conditions for photosynthesis ( $540 \mu\text{mol m}^{-2} \text{s}^{-1}$ ). Anti-Rubisco LS is concentrated in the pyrenoid (*py*) whereas immunolabelling of the chloroplast (*c*) stroma is below that of both nucleus (*n*) and cytoplasm. Bar =  $0.5 \mu\text{m}$ .



**Table 1.** Density of labelling over various cell compartments of *Chlorella pyrenoidosa* cultured at different light intensities.

	Chloroplast		Cytoplasm	Vacuole	Nucleus <sup>a</sup>	n <sup>b</sup>	
	Pyrenoid	Starch shell					Stromal region
gold particles $\mu\text{m}^{-2} \pm \text{SE}$							
25 $\mu\text{mol m}^{-2} \text{s}^{-1}$							
Anti-LSU	506.0±20.3	0.4±0.1	3.2±0.4	5.8±0.6	1.4±0.2	7.8±1.2 <sub>(10)</sub>	25
Anti-SSU	461.8±35.6	1.1±0.3	6.8±0.5	5.5±0.5	2.2±0.3	6.0±1.2 <sub>(7)</sub>	18
75 $\mu\text{mol m}^{-2} \text{s}^{-1}$							
Anti-LSU	375.1±26.1	0.3±0.1	1.3±0.2	1.4±0.2	0.3±0.1	2.1±0.3 <sub>(11)</sub>	26
Anti-SSU	305.9±16.9	0.7±0.2	2.3±0.3	1.6±0.3	0.4±0.1	2.1±0.4 <sub>(6)</sub>	23
540 $\mu\text{mol m}^{-2} \text{s}^{-1}$							
Anti-LSU	354.8±52.3	0.7±0.3	2.7±0.6	3.0±0.7	0.6±0.3	6.2±1.6 <sub>(7)</sub>	17
Anti-SSU	208.2±17.1	1.0±0.4	3.5±0.4	2.5±0.2	0.4±0.1	3.3±0.8 <sub>(8)</sub>	20
Controls <sup>c</sup>							
Nonimmune IgG	1.0±0.3	0.2±0.1	0.8±0.2	1.3±0.3	0.2±0.1	2.8±0.7 <sub>(8)</sub>	16
PBS	1.0±0.3	0.3±0.2	0.7±0.1	1.4±0.3	0.4±0.2	-----	13

<sup>a</sup> Number of nuclei analyzed

<sup>b</sup> Number of cell sections analyzed

<sup>c</sup> Controls reported for cells cultured at 75  $\mu\text{mol} \cdot \text{m}^{-2} \text{s}^{-1}$

plastid compartments for *Chlorella* grown at each light fluence rate and labelled by antibodies against both the large and small subunit of Rubisco. Anti-Rubisco SS gave the same labelling pattern as anti-Rubisco LS. At each photon flux density, the pyrenoid was heavily labelled by antibodies to each subunit of Rubisco, whereas the stromal region contained levels of labelling similar to the cytoplasm or nucleus. Stromal labelling by anti-Rubisco LS was consistently below background levels (cytoplasmic and nuclear labelling). Stromal labelling by anti-Rubisco SS was slightly above background (nuclear labelling) at each photon flux density; however, statistical analyses (one tailed paired *t* tests) indicate that the differences are not significant. Although the density of labelling by each subunit over the pyrenoid appears to decrease when the light fluence rate is increased, these figures cannot be directly compared, since different protein A-gold solutions were used in each experiment. One can directly compare only those labelling densities over the various cellular compartments by antibody to a single subunit within a single light level.

To ensure that temporal delays caused by cell harvesting (centrifugation, buffer rinses) prior to fixation did not affect intracellular Rubisco distribution, cells were also fixed in situ in culture medium at each experimental photon flux density. Labelling densities by antibody to each subunit of Rubisco over the various cellular compartments (not shown) provided results similar to those obtained in Table 1. We suggest, then, that short delays prior to cell fixation, caused by the harvesting methods employed in this investigation, did not contribute to the observed enzyme partitioning.

Control experiments were performed by replacing antibody with either non-immune rabbit IgG or with PBS alone, followed by protein A-gold (Table 1, see also Appendix 2). For each control, labelling densities were very low and similar values were obtained for pyrenoid, stroma and the cell's cytoplasm. In addition, the specificity of anti-Rubisco LS used in this study to commercially prepared samples of Rubisco holoenzyme has been previously reported (Mangoney and Gibbs 1987).

#### 4.0. Discussion

In higher plants, an increase in light fluence rate is usually characterized by an increase in Rubisco activation state (i.e., the proportion of the enzyme in the active form) and is paralleled by a coordinate increase in photosynthetic rate (Perchorowicz et al 1981; Salvucci et al 1986, Salvucci and Anderson 1987). The relationship between in vivo Rubisco activation state and light fluence rate has not been determined for green algae; however, the enzyme seems to be modulated by light in a manner similar to that observed for higher plants (Tavlor et al 1986). In our present investigation, cells of *Chlorella pyrenoidosa* were cultured under various light fluence rates, including both light-limiting and light-saturating conditions for photosynthesis. One might speculate that if Rubisco is catalytically functional only in the stroma and not in the pyrenoid, transfer of cells to a higher photon flux density would result in an increase in the

activation state of the enzyme already located in the stroma. In addition, a substantial and maintained increase in light fluence rate would likely necessitate a net efflux of pyrenoid stored Rubisco to the stroma followed by increased rates of synthesis of Rubisco subunits. However, a net redistribution of pyrenoid Rubisco to the chloroplast stroma was not observed following increases in photosynthetic photon flux density. In fact, stromal levels of Rubisco were not significantly above background at any light fluence rate tested. Instead, Rubisco was highly concentrated in the pyrenoid at each light level. The observed pattern of enzyme distribution suggests that Rubisco localized in the pyrenoid is capable of catalytic activity.

The possibility that Rubisco is present in the stroma at moderate concentrations and we have failed to detect it by the immunolabelling method employed is unlikely. Other studies from this laboratory using similar fixation, embedding and immunolabelling protocols have successfully demonstrated the presence of Rubisco in the chloroplast stroma of the non-pyrenoid-containing alga *Ochromonas danica* (Lacoste-Royal and Gibbs 1985; see also Appendix 1) and in both the stroma and pyrenoid of the plastids of log phase cells of *Chlamydomonas reinhardtii* (Lacoste-Royal and Gibbs 1987). The absence of a significant level of labelling of the stroma of *Chlorella* chloroplasts by anti-LS and anti-SS indicates that the concentration of Rubisco there is low and that most of the plastid's Rubisco is localized in the pyrenoid.

The results of this study make it difficult to dismiss algal pyrenoids simply as storage bodies. Why Rubisco is segregated within the chloroplast is not clear. Such an arrangement would necessitate

routing of substrate RuBP from the stroma into the pyrenoid while product 3-phosphoglycerate would subsequently require direction back into the stroma. For these events to occur, it is possible that localization of Rubisco in the pyrenoid rather than in the stroma might confer some advantage. One hypothesis is that the algal pyrenoid provides a microenvironment for Rubisco where the efficiency with which the carboxylation reaction may proceed is enhanced. That this is attained through a carbonic anhydrase regulated concentration of CO<sub>2</sub> at the pyrenoid is one possibility. It is well known that in many species of algae, cells grown in air levels of CO<sub>2</sub> have high levels of carbonic anhydrase whereas in cells grown in high CO<sub>2</sub>, the synthesis of this enzyme is repressed (Aizawa and Miyachi 1986). It was recently shown by immunoelectron microscopy that an isozyme of carbonic anhydrase is localized throughout the chloroplast stroma in the red alga *Porphyridium cruentum* (Yagawa et al 1987). However, it was not clear from their micrographs whether the small amount of label present over the pyrenoid was specific. Carbonic anhydrase activity is located intracellularly in *Chlorella pyrenoidosa* (Aizawa and Miyachi 1986). Its specific intracellular location, however, is not known. It is anticipated that having a portion of carbonic anhydrase activity located in the pyrenoid would ensure a supply of CO<sub>2</sub> to Rubisco.

#### **Acknowledgements**

We gratefully thank Dr. Jacqueline Fleck for providing us with the

antibodies used in this study. We also thank Dr. C. E. Smith for use of the Zeiss MOP-3 digital analyser. This research was supported by the Natural Sciences and Engineering Research Council of Canada (grant no. A-2921).

#### Notes Added

Two reports published subsequent to this manuscript support our findings. Employing the protein A-gold method, Osafune et al. (1990c) showed Rubisco to be predominantly pyrenoid-localized in non-dividing cells of *Euglena gracilis*. Furthermore, upon measuring rates of photosynthetic CO<sub>2</sub>-fixation for cells grown under light of high intensity, they report that Rubisco is fully activated. Moreover, they confirmed that pyrenoids were present in the cells used for their measurements.

More recently, Cunningham et al. (1991) determined the subcellular distribution of Rubisco in cells of the red alga *Porphyridium cruentum* grown at photosynthetically limiting ( $6 \mu\text{mol}\cdot\text{m}^{-2}\cdot\text{s}^{-1}$ ) and saturating ( $280 \mu\text{mol}\cdot\text{m}^{-2}\cdot\text{s}^{-1}$ ) light fluence rates. Their results provided no evidence for a redistribution of Rubisco between pyrenoid and stroma when cells were grown under saturating light. Regardless of growth irradiance, Rubisco remained predominantly pyrenoid localized.

### CHAPTER III

Rubisco activase is present in the pyrenoid  
of green algae

## Summary

Rubisco activase catalyzes the activation and maintains the activated state of the photosynthetic enzyme ribulose 1,5-bisphosphate carboxylase/oxygenase (Rubisco, EC 4.1.1.39). We employed antisera prepared against the Rubisco holoenzyme purified from tobacco and Rubisco activase isolated from spinach to determine the localization of these proteins in leaves of C<sub>3</sub>-type higher plants and green algae. In leaves of *Vicia faba*, both Rubisco activase and Rubisco are distributed throughout the chloroplast stroma. In contrast, Rubisco activase and Rubisco are predominantly localized to the pyrenoid in the green algae *Chlamydomonas reinhardtii* and *Coleochaete scutata*. The co-immunolocalization of Rubisco activase and Rubisco to the pyrenoid in these two green algal species indicates that pyrenoid-localized Rubisco is catalytically competent. We conclude that the pyrenoid functions as a unique metabolic compartment of the chloroplast in which the reactions of the photosynthetic carbon reduction pathway are initiated.

## 1.0. Introduction

Ribulose 1,5-bisphosphate carboxylase/oxygenase (Rubisco, EC 4.1.1.39) catalyzes the carboxylation of ribulose 1,5-bisphosphate (RuBP) in the initial reaction of the photosynthetic carbon reduction pathway. In higher plants, immunocytochemical investigations have shown that Rubisco is localized in the chloroplast stroma (e.g. Vaughn 1987a; Rother et al. 1988). The chloroplasts of a number of algal and hornwort species, however, are characterized by the presence of proteinaceous inclusion bodies known as pyrenoids. Moreover, immunocytochemical analyses have shown that in pyrenoid-containing algae and hornworts, Rubisco is predominantly localized in this region (Table 1). Many of these reports, however, indicate that a portion of the Rubisco in pyrenoid-containing organisms is also located in the stroma. In non-pyrenoid-containing algae and hornworts, Rubisco is distributed throughout the chloroplast stroma (Lacoste-Roval and Gibbs 1985, Elman et al. 1989, Vaughn et al. 1990). Because Rubisco is commonly regarded as being a stromal enzyme, the observation that Rubisco may be partitioned between the pyrenoid and stroma has led to speculation that the pyrenoid may be a storage region containing inactive Rubisco. Moreover, due to the inability of Rubisco antiserum to differentiate between active and inactive forms of the enzyme, we have been unable to assess the activity state of pyrenoid-localized Rubisco.

Recently, a soluble chloroplast protein, Rubisco activase, has been implicated as being responsible for catalyzing the activation and

Table 1. Immunocytochemical investigations of Rubisco localization in pyrenoid-containing species

Class	Species	Technique <sup>a</sup>	Reference
Rhodophyceae	<u>Porphyridium cruentum</u>	G	McKay and Gibbs (1990;1991b <sup>b</sup> )
		G	Mustardy et al. (1990)
		G	Cunningham et al. (1991 <sup>c</sup> )
Cryptophyceae	<u>Hemiselmis brunnescens</u> <u>Chroomonas</u> sp.	G	McKay et al. (1991b <sup>b</sup> )
		G	McKay and Gibbs (1991a)
		G	McKay et al. (1991b <sup>c</sup> )
Bacillariophyceae	<u>Phaeodactylum tricornutum</u>	G	McKay and Gibbs (1991a)
Dinophyceae	<u>Symbiodinium kawaagutii</u>	G	Blank and Trench (1988)
Euglenophyceae	<u>Euglena gracilis</u>	F	Kiss et al. (1986)
		G	Osafune et al. (1989;1990)
Chlorophyceae	<u>Bryopsis maxima</u> <u>Chlamydomonas reinhardtii</u>	E,F	Kajikawa et al. (1988)
		F	Vladimirova et al. (1982)
	G	Lacoste-Royal and Gibbs (1985, 1987)	
	C	this report	
	G	McKay and Gibbs (1991b <sup>d</sup> )	
	G	McKay and Gibbs (1989)	
	G	Nisius and Ruppel (1987)	
	G	this report	
	G	this report	
	F	Vladimirova et al. (1982)	
Anthocerotae	various species	G	Vaughn et al. (1990)

<sup>a</sup> E, immunoenzymatic; F, immunofluorescence; G, immunogold

<sup>b</sup> references added after manuscript had gone to press

maintaining the activated state of Rubisco (Salvucci et al. 1985). The mechanism by which activase catalyzes activation of Rubisco is not well understood, however, it likely involves ATP hydrolysis (Streusand and Portis 1987) and protein-protein interactions in order to promote enzyme carbamylation (Werneke et al. 1988a). In the present investigation, we have employed antiserum prepared against a mixture of the 41 and 45 kDa polypeptides of spinach Rubisco activase in order to determine the localization of activase in leaves of C<sub>3</sub>-type higher plants and green algae. Since Rubisco activase catalyzes the activation of Rubisco in vivo, its immunolocalization should indicate the location of functional Rubisco in the chloroplast.

## 2.0. Materials and Methods

### 2.1 Plant Material

Seeds of *Vicia faba* L. (cv. Longpod) were sown in potting mix (3:1:1, peat:perlite:vermiculite) and watered daily. Plants were maintained in a controlled environment chamber (continuous light, 250  $\mu\text{mol photons} \cdot \text{m}^{-2} \cdot \text{s}^{-1}$ , 20°C). *Chlamydomonas reinhardtii* Dangeard was obtained from the Culture Collection of Algae at the University of Texas at Austin (UTEX 90) and grown in batch culture in a modified Bold's minimal medium. Cultures were maintained at 25°C and were continuously agitated by use of a rotary shaker. Light was provided by cool-white fluorescent lamps at a photon fluence rate of 40  $\mu\text{mol} \cdot \text{m}^{-2} \cdot \text{s}^{-1}$  in 12 h light - 12 h dark cycles. *Coleochaete scutata* de Brebisson was obtained from Carolina

Biological Supply Co (Burlington, N C , USA) and was used for experimental work immediately upon receipt

## 2.2 Immunoelectron Microscopy

Plants of *Vicia faba* were harvested 2 months after planting and small pieces (1 mm<sup>2</sup>) of fully expanded terminal leaflets were cut into ice-cold fixative (3% glutaraldehyde in 0.05 M 1.4-piperazinediethanesulfonic acid (Pipes), pH 7.4). The leaf pieces were fixed for 2 hours, following which they were washed with buffer and dehydrated through a graded ethanol series to 100% ethanol. Leaf tissue was embedded in Lowicryl K4M resin (Polysciences, Warrington, PA, USA) and tissue blocks were polymerized under ultraviolet light at 4°C for 24 h in a commercially obtained light box (Ladd Industries Inc., Burlington, VT, USA).

Logarithmic phase cells of *Chlamydomonas reinhardtii* were harvested at h 4 of the light period. All pellets were fixed at 4°C for 90 min in a solution containing 1% glutaraldehyde in 0.05 M Pipes, pH 7.4. The pellets were washed with cold buffer and the cells dehydrated through a graded ethanol series and embedded in Lowicryl K4M (J. B. EM Services) as described in Lacoste-Royal and Gibbs (1985).

Small pieces (1 mm<sup>2</sup>) of *Coleochaete scutata* thallus were cut directly into cold 3% glutaraldehyde in 0.05 M Pipes buffer, pH 7.4, and fixed in the same solution at 4°C for 2 hours. The specimens were washed in cold 0.1 M sodium cacodylate buffer, pH 7.2, and then post-fixed in 2% OsO<sub>4</sub> in 0.1 M cacodylate, pH 7.2, for 2 hours at 4°C. The specimens were washed in de-ionized water and then dehydrated through a

graded ethanol series to 100% ethanol, following which, they were embedded in LR white soft grade resin (Fullam Inc., Latham, NY, USA)

Pale gold-coloured sections of the tissue were cut with a diamond knife and collected on formvar-coated nickel grids. For immunolabelling, grids were placed section-side down on drops of the following solutions: 1% bovine serum albumin (BSA) in phosphate-buffered saline (PBS), 30 min; antiserum, 1 h; 1% BSA in PBS, 4 drops during 10 min; colloidal gold reagent diluted 1:25, 20 min; PBS, 4 drops during 10 min; de-ionized water rinse. In addition, immunolabelling of sections of *Chlamydomonas* and *Coleochaete* was preceded by incubation on a drop of 12% sodium *m*-periodate for 10 or 30 min followed by a de-ionized water rinse in order to restore antigenicity. Mouse antiserum against a preparation containing both the 41 and 45 kDa polypeptides of spinach Rubisco activase was kindly provided by J.M. Werneke and W.L. Ogren (United States Department of Agriculture, Agricultural Research Service, Urbana, IL, USA) and was used at dilutions of 1:80 to 1:160. The preparation of this antiserum has been described previously (Salvucci et al. 1987). Rabbit antiserum against tobacco Rubisco was obtained commercially (Cappel Laboratories, Cochranville, PA, USA) and was employed at a dilution of 1:400. Goat anti-mouse-gold (15 nm particles, EY Laboratories, San Mateo, CA, USA) was used to detect anti-activase whereas protein A-gold (15 nm particles; EY Laboratories) was employed to detect anti-Rubisco on tissue sections. Antisera and colloidal gold reagents were diluted in 1% BSA in PBS. Immunolabelled sections were post-stained for 4 min with 2% aqueous uranyl acetate and for 1 min with lead citrate (Reynolds 1963) prior to observing in either

a Philips EM 410 or Zeiss EM 10CR electron microscope at an operating voltage of 60 kv

In control experiments, the antiserum was replaced by PBS or by non-immune serum prior to colloidal gold reagent incubation. In addition, one other Rubisco activase antiserum (prepared against spinach activase and kindly provided by M.F. Salvucci, USDA-ARS, Lexington, KY, USA) was employed and results obtained using this antibody were similar to those provided by the initial anti-spinach Rubisco activase (data not shown)

### 2.3. Quantitative Evaluation

The density of labelling over various cell compartments was obtained by determining the number of gold particles per square micrometre of compartment sectioned. Area determinations were made using a Zeiss (New York, NY, USA) MOP-3 digital analyzer

### 2.4. Antiserum Specificity

A *Chlamydomonas* crude protein extract was obtained by sonicating (Sonifier Cell Disruptor, Model W140D, Heat Systems Ultrasonics Inc., Plainview, NY, USA) freshly harvested cells resuspended in ice-cold extraction buffer (100 mM Tris-HCl, pH 7.8, 10 mM MgCl<sub>2</sub>, 10 mM dithiothreitol, 1 mM phenylmethanesulfonyl fluoride). The protein extract was clarified by centrifugation, following which, proteins from the soluble fraction were separated essentially as described by Laemmli (1970) on 12.5% sodium dodecyl sulfate-containing polyacrylamide gels. Separated polypeptides were transferred electrophoretically to

nitrocellulose filters (0.45  $\mu$ M Bio-Rad Laboratories Ltd., Mississauga, Ont., Canada) at room temperature for 2 h at 60 V in 25 mM Tris, 192 mM glycine and 20% methanol. Filters containing transferred polypeptides were blocked with 2% BSA in tris-buffered saline (TBS; 50 mM Tris-HCl, pH 7.4, 150 mM NaCl) at 4°C overnight and were then incubated at room temperature in the following solutions: anti-Rubisco activase diluted 1:500, 30 min; PBS containing 0.05% Tween 20 (PBST), 3 x 10 min; goat anti-mouse IgG-horseradish peroxidase (heavy and light chains, BIO/CAN Scientific Inc., Toronto, Ont., Canada) diluted 1:1000, 30 min; PBST, 3 x 10 min; TBS, 10 min. Immunoreactive bands were visualized by incubating blots in a solution containing the chromogen 4-chloro-1-naphthol (Sigma Chemical Co., St. Louis, MO, USA). Primary and secondary antisera were diluted in PBST containing 1% BSA.

Protein concentration was determined with the Bio-Rad protein assay kit using BSA as a standard and following the manufacturer's instructions.

### 3.0. Results

#### 3.1. Western Immunoblotting

Antiserum prepared against a mixture of spinach Rubisco activase 41 and 45 kDa polypeptides was used to probe a Western blot of a soluble protein extract from *Chlamydomonas reinhardtii* (Fig. 1). The antibody mixture cross-reacts with only a single polypeptide of about 42 to 43 kDa; an observation in accord with recent findings by Roesler and Ogren

**Fig. 1.** Immunoblot of *Chlamydomonas reinhardtii* soluble protein extract (5  $\mu$ g total protein). Transferred polypeptides were probed with anti-Rubisco activase as described in the Materials and Methods. Positions of molecular mass standards (in kDa) are shown. The antiserum cross-reacted with only a single polypeptide band of ~42-43 kDa.

66.2 -

42.7 -

31.0 -

(1990a) In addition, Salvucci et al (1987) have demonstrated that the antiserum recognizes two polypeptides in the range of 41 to 47 kDa from pea leaves. Specificity of the anti-Rubisco used in this study has also been demonstrated previously (Vaughn 1987, Vaughn et al 1990). These studies have shown that this antibody preparation specifically recognizes the large subunit of Rubisco.

### 3.2 Immunoelectron Microscopy

The intracellular localization of Rubisco activase differs between  $C_3$  type higher plants and green algae. We have employed antibodies to spinach Rubisco activase to probe tissue sections of leaves of two higher plants (*Vicia faba* and pea) and two green algal species (*Chlamydomonas reinhardtii* and *Coleochaete scutata*). In all cases, the enzyme is restricted to the chloroplast. In *Vicia* (Fig. 2) and pea (data not shown), Rubisco activase is largely restricted to the chloroplast stroma. Immunogold label over thylakoid grana stacks and cellular organelles is present at only low levels (Fig. 2). This pattern of immunolabelling by activase antiserum is identical to the observed intracellular localization of Rubisco in  $C_3$  plants (e.g. Vaughn 1987a; Rother et al. 1988).

Figures 3 and 4 show the immunolocalization of Rubisco activase and Rubisco in both *Chlamydomonas* and *Coleochaete*. In both algae, immunolabelling by Rubisco activase antiserum is confined mainly to the pyrenoid (Fig. 3a, 4a). For *Chlamydomonas*, a cross-section through an entire cell is provided from which it is evident that label over the chloroplast stroma and other cellular compartments is present only at

**Fig. 2.** Section through mesophyll cell of leaf of *Vicia faba* labelled by anti-Rubisco activase. Gold particles are distributed throughout the stromal region of a chloroplast (c). The cytoplasm and a peroxisome (pe) are mainly unlabelled Bar = 0.5  $\mu$ m.

6



8

**Figs. 3a,b.** Immunolocalization of Rubisco activase and Rubisco in logarithmic phase cells of *Chlamydomonas reinhardtii*. Bars = 0.5  $\mu\text{m}$ . **a.** Anti-Rubisco activase is concentrated over the pyrenoid (py) whereas the remainder of the chloroplast is only lightly labelled. Few gold particles are evident over other cell compartments. nucleus (n). **b.** Similarly, anti-Rubisco is localized to the pyrenoid. Again, the remainder of the cell is relatively unlabelled.

**Figs. 4a,b.** Immunolocalization of Rubisco activase and Rubisco in *Coleochaete scutata*. Bars = 0.5  $\mu\text{m}$ . **a.** Anti-Rubisco activase is localized to the pyrenoid (py). The remainder of the chloroplast (c) contains only a few scattered gold particles. **b.** The pyrenoid is heavily labelled by anti-Rubisco whereas the remainder of the chloroplast is unlabelled.



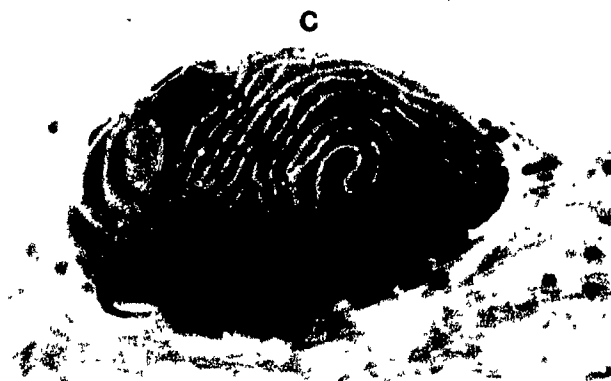
3a .



b



4a



b

low levels (Fig. 3a). This observation is supported by results of a quantitative analysis of the density of labelling by anti-Rubisco activase over different cell and plastid compartments in *Chlamydomonas*. Labelling density over the pyrenoid matrix ( $47.1 \pm 2.7$  particles  $\mu\text{m}^{-2}$ ) is much higher than that over the chloroplast stroma ( $1.8 \pm 0.2$  particles  $\cdot \mu\text{m}^{-2}$ ). Stromal labelling, however, is significantly higher than both cytoplasmic labelling ( $1.0 \pm 0.2$  particles  $\cdot \mu\text{m}^{-2}$ ; one-tailed *t*-test,  $P < 0.01$ ,  $n=23$ ) and nuclear labelling ( $0.7 \pm 0.2$  particles  $\cdot \mu\text{m}^{-2}$  one-tailed *t*-test,  $P < 0.005$ ).

Rubisco also appears to be confined to the pyrenoid in both *Chlamydomonas* and *Coleochaete* (Fig. 3b, 4b). In both green algae, the pyrenoid is heavily labelled by antiserum to the Rubisco holoenzyme whereas other cellular compartments remain largely unlabelled. A pyrenoid localization of Rubisco in green algae has been reported previously (e.g. Lacoste-Royal and Gibbs 1987; McKay and Gibbs 1989). Thus, as occurs with the two higher plant species surveyed, Rubisco activase co-localizes with Rubisco in green algae also.

Control experiments were performed by replacing the antiserum with PBS or with non-immune serum, followed by either goat anti-mouse-gold (control for anti-activase) or protein A-gold (control for anti-rubisco). For each control, labelling densities were low ( $< 1$  gold particle  $\cdot \mu\text{m}^{-1}$ ) over each cellular compartment analyzed (see Appendix 2).

#### 4.0. Discussion

Rubisco activase has been detected in all higher plant species thus far surveyed (Salvucci et al. 1987). In addition, immunoblots have demonstrated its presence in the green alga *Chlamydomonas reinhardtii* (Salvucci et al. 1987; Roesler and Ogren 1990a). In most higher plants, activase is comprised of two immunologically related polypeptides in the range of 40-47 kDa which appear to be derived from the same single-copy, nuclear-encoded gene (Werneke et al. 1988b). Initial studies indicated that activase was synthesized in the cytoplasm as a single precursor polypeptide which was subsequently processed into mature activase polypeptides following transport into the chloroplast (Werneke et al. 1988b). Recent findings, however, indicate that at least in spinach and *Arabidopsis*, Rubisco activase polypeptides are generated by way of a conserved, alternative mRNA splicing mechanism (Werneke et al. 1989) which does not appear to exhibit developmental (Zielinski et al. 1989) or tissue-specific regulation (Werneke et al. 1989).

The exact nature of native Rubisco activase remains unclear. The two higher plant activase polypeptides can be partially resolved under native conditions using ion-exchange chromatography (Werneke et al. 1988a). This suggests that the functional holoenzyme is not necessarily heterogenous in composition. Moreover, analyses of individual activase polypeptides cloned and expressed in *Escherichia coli* indicate that the presence of both polypeptides is not requisite for Rubisco activase activity (Werneke et al. 1988a; also as reported in Portis 1990). This observation is further supported by the fact that *Chlamydomonas* contains

only one activase polypeptide species (Roesler and Ogren 1990a). The 41 kDa *Chlamydomonas* Rubisco activase polypeptide is immunologically related to the spinach Rubisco activase polypeptides and exhibits between 60-65% identity at the amino acid level with activase from both spinach and *Arabidopsis* (Roesler and Ogren 1990a). Furthermore, in contrast to the higher plant gene, *Chlamydomonas* Rubisco activase cDNA sequence analysis does not provide evidence for an alternative mRNA splicing mechanism (Roesler and Ogren 1990a), thus supporting the observation of a single activase polypeptide species in this alga.

In the present investigation, we observed a co-localization of Rubisco and Rubisco activase in green algae and in leaves of C<sub>3</sub>-type higher plants. In both *Vicia* (Fig. 2) and pea, activase is confined to the chloroplast stroma; an observation coinciding with a stromal location of Rubisco, as has been reported previously (e.g. Vaughn 1987a; Rother et al. 1988). In green algae, Rubisco is predominantly localized to the pyrenoid (e.g. Lacoste-Royal and Gibbs 1987, McKay and Gibbs 1989). We confirm this observation with both *Chlamydomonas* (Fig. 3) and *Coleochaete* (Fig. 3) and, in addition, we report the pyrenoid localization of Rubisco activase in these two species. Moreover, Vaughn et al. (1990) have recently shown a pyrenoid localization of Rubisco among several pyrenoid-containing hornworts and further studies from his lab indicate that activase is also predominantly localized to the pyrenoids of these hornwort species (K. Vaughn, unpublished data). The observed co-localization of Rubisco and Rubisco activase in the present study was not unexpected. Interactions between the two proteins have been proposed in order to reconcile inconsistencies with previous ideas

on Rubisco activation. Foremost among these is the observation that spontaneous in vitro Rubisco activation can be accomplished only in the presence of supraphysiological concentrations of  $\text{CO}_2$  ( $K_{\text{activation}} = 25\text{-}30 \mu\text{M}$ ) and  $\text{Mg}^{++}$  (Mizioro and Lorimer 1983). The physiological concentration of  $\text{CO}_2$  in the  $\text{C}_3$  plant chloroplast, however, approaches only  $10\text{-}12 \mu\text{M}$ , yet, Rubisco extracted from leaves exposed to photosynthetic saturating light intensities is reported to be highly activated (Perchorowicz et al. 1981). Portis et al (1986), however, reported that the addition of partially purified spinach Rubisco activase to a reconstituted illuminated chloroplast system led to activation of Rubisco with a  $K_{\text{activation}}$  of about  $4 \mu\text{M} \text{CO}_2$ . Thus it seems that activase enables Rubisco to achieve a high degree of enzyme activation in  $\text{C}_3$  plants in vivo. Why, however, would activase be required for in vivo Rubisco activation in green algae? It appears that its existence there might be superfluous in view of evidence that *Chlamydomonas* (Badger et al. 1978) and other chlorophytes (Aizawa and Miyachi 1986) possess an effective inorganic carbon ( $\text{C}_i$ ) concentrating mechanism where  $\text{C}_i$  species are concentrated intracellularly to levels higher than in the surrounding medium. The high concentration of intrachloroplastic  $\text{CO}_2$  which would result from the operation of this mechanism should be sufficient to ensure the spontaneous activation of Rubisco. The presence of Rubisco activase, however, might be anticipated if a major function of the enzyme was to catalyze the activation of Rubisco when it is complexed to inhibitors. RuBP, in addition to acting as a substrate for activated Rubisco, is a potent inhibitor of the higher plant inactive enzyme form, preventing addition

of the activator  $\text{CO}_2$  and  $\text{Mg}^{++}$  (Jordan and Chollet 1983). The effectiveness with which RuBP inhibits Rubisco activation among algae and photosynthetic prokaryotes, however, varies. Among the algae, Rubisco isolated from both the red alga *Griffithsia pacifica* and the chromophyte *Olisthodiscus luteus* is rather insensitive to inhibition by RuBP (Newman et al. 1989). Conversely, Jordan and Ogren (1983) report that RuBP strongly inhibits Rubisco activation in *Euglena gracilis* and *Chlamydomonas reinhardtii*. It is not known whether RuBP is an inhibitor of Rubisco in *Coleochaete*, however, given its position on the "bryophyten" line of evolution towards higher plants (Graham 1985), it is reasonable to assume that it does. RuBP is present in millimolar concentrations in the chlorophyte *Chlorella pyrenoidosa* (Yokota and Calvin 1986). Thus, it appears that in green algae, Rubisco activase might prevent Rubisco deactivation by catalyzing the activation of the tight binding Rubisco-RuBP complex or other potential Rubisco-sugar phosphate complexes. In support of this, Roesler and Ogren (1990a) have recently reported that purified spinach activase can promote the activation of *Chlamydomonas* Rubisco in the presence of physiological concentrations of RuBP.

The observed pyrenoid localization of Rubisco activase in green algae in the present investigation lends further support to the idea that the pyrenoid is an important metabolic compartment of the cell and not simply a protein storage region. Previous immunolabelling results from this lab (McKay and Gibbs 1989) strongly indicated that pyrenoid Rubisco was functional in vivo. However, due to limitations of the technique of immunocytochemistry, the study was not able to provide a

direct assessment of Rubisco activation state. As a result, we were unable to ascertain directly whether or not the pyrenoid represented the site of initial CO<sub>2</sub> fixation. The immunolocalization of Rubisco activase now provides a more direct method to elucidate the function of pyrenoid-localized Rubisco. Since Rubisco activation is catalyzed and regulated by activase in vivo (Salvucci 1989; Portis 1990) the presence of activase in the pyrenoid indicates that pyrenoid Rubisco is functionally active.

#### **Acknowledgements**

We thank Drs. W.L. Ogren, J.M. Werneke and M.E. Salvucci for providing us with the antibodies used in this study. We also thank Dr. G. Bell for providing the culture of *Chlamydomonas reinhardtii* and Ms. L. Libous-Bailey who supplied technical assistance. Dr. K. Roesler provided helpful discussions. A portion of this study was undertaken using the facilities of the McGill University Phytotron. This research was supported in part by the Natural Sciences and Engineering Research Council of Canada (grant No. A-2921 to S.P. Gibbs). In addition, R.M.L. McKay acknowledges support through a NSERC postgraduate scholarship. Mention of trademark, vendor, or proprietary product does not constitute a guarantee or warranty of this product by the U.S. Department of Agriculture and does not imply its approval to the exclusion of other products or vendors that may also be suitable.

**CHAPTER IV**

Immunocytochemical localization of phosphoribulokinase  
in microalgae

## Summary

Employing immunogold electron microscopy, the subcellular location of the Calvin cycle enzyme phosphoribulokinase (PRK) was determined for two diverse species of microalgae. In both the red alga *Porphyridium cruentum* and the green alga *Chlamydomonas reinhardtii*, PRK was distributed throughout the thylakoid-containing chloroplast stroma. In contrast, the next enzyme in the pathway, ribulose 1,5-bisphosphate carboxylase/oxygenase, was predominantly pyrenoid-localized in both species. In *Porphyridium*, the chloroplast stroma abuts the pyrenoid but in *Chlamydomonas* and other green algae, the pyrenoid appears encased in a starch sheath. Unique inclusions found in the pyrenoid of *Chlamydomonas* were immunolabelled by anti-PRK and thus identified as regions of chloroplast stroma. It is postulated that such PRK-containing stromal inclusions in the pyrenoids of *Chlamydomonas* and perhaps other green algae provide a means for exchange of Calvin cycle metabolites between pyrenoid and stroma.

## 1.0. Introduction

The enzyme phosphoribulokinase (PRK; E C 2 / 1 19) is recognized as an important regulatory protein in the process of carbon fixation. Unique to the Calvin cycle, PRK catalyzes the ATP-dependent phosphorylation of ribulose 5-phosphate, thereby regenerating ribulose 1,5-bisphosphate (RuBP), the CO<sub>2</sub> acceptor molecule and substrate for ribulose 1,5-bisphosphate carboxylase/oxygenase (Rubisco; E C 4 1 1 39). The enzyme has been isolated from a variety of sources including oxygen-evolving photosynthetic organisms and numerous anaerobic photosynthetic and chemolithoautotrophic bacteria (Tabita 1988).

In some prokaryotes, there exists a subcellular partitioning of Calvin cycle enzymes. In these organisms, Rubisco is predominantly localized in discrete inclusion bodies called carboxysomes, whereas PRK and other enzymes of the pathway are located elsewhere in the cell (Codd 1988; Shively et al. 1988; Tabita 1988). What, if any benefit results from such an arrangement is, at present, not known.

A similar partitioning of Calvin cycle enzymes may exist in some eukaryotic organisms. In pyrenoid-containing algae and hornworts, it is well documented that Rubisco is predominantly localized to the pyrenoid region of the chloroplast (McKay and Gibbs 1991a; see also Chapter 1). The subcellular distribution of other Calvin cycle enzymes in these organisms, however, has not been investigated. In this report, we have used the technique of immunoelectron microscopy to investigate the intracellular localization of PRK in a red and a green alga.

## 2.0. Materials and Methods

### 2.1 Cell Culture

*Porphyridium cruentum* (Agardh) Nageli (UTEX 161) was grown in an artificial seawater medium as described in McKay and Gibbs (1990, see also Chapter VII). *Chlamydomonas reinhardtii* Dangeard (UTEX 90) was grown in a modified Bold's minimal medium. Its culture conditions are described in McKay et al. (1991a; see also Chapter III).

### 2.2 Characterization of Antisera

The antisera employed in this study are described in Table 1. They were characterized by immunoblotting. Briefly, freshly harvested cells of *P. cruentum* and *C. reinhardtii* were resuspended in cold extraction buffer (100 mM Tris-HCl, pH 7.8, 10 mM MgCl<sub>2</sub>, 5 mM dithiothreitol) containing phenylmethylsulfonyl fluoride and sonicated (Sonifier Cell Disruptor, Model W140D, Heat Systems Ultrasonics Inc., Plainview, NY, USA) to provide crude protein extracts. The extracts were clarified by centrifugation at 14,000 X g for 15 min, following which, proteins from the soluble fraction were separated essentially as described by Laemmli (1970) on 12.5% sodium dodecyl sulfate (SDS)-containing polyacrylamide gels. Separated polypeptides were electroblotted to nitrocellulose at 60 V for 4 h in cold transfer buffer (25 mM Tris, 192 mM glycine, 20% (v/v) methanol) and then blocked with 1% (w/v) bovine serum albumin (BSA) in Tris-buffered saline (TBS) overnight at 4°C. Immunoreactive polypeptides were detected by incubating the blots in primary antiserum followed by incubation in either goat anti-mouse IgG-horseradish

Table 1. Antisera employed in the present investigation.

Antibody	Host	Source of Antigen	Dilution		Reference
			Immunoblots	Immunocytochemistry	
anti-PRK	rabbit	<u>Chlorogloeopsis fritschii</u>	1:1000	1:500	Marsden et al. 1984
anti-PRK	mouse	<u>Chlamydomonas reinhardtii</u>	1:750	1:100	Roesler and Ogren 1991b
anti-Rubisco LS	rabbit	<u>Nicotiana sylvestris</u>	1:1000	1:1000	Lett et al 1980

peroxidase (BIO/CAN Scientific Inc., Toronto, Ont., Canada) or goat anti-rabbit IgG-horseradish peroxidase (Bio-Rad Laboratories Ltd., Mississauga, Ont., Canada). Visualization of immunoreactive polypeptides was performed by incubating blots in a solution containing the chromogen 4-chloro-1-naphthol (Sigma Chemical Co., St. Louis, MO, USA).

Protein concentration was determined using the Bio-Rad protein assay kit with BSA as a standard and following the manufacturer's instructions.

### 2.3 Immunoelectron Microscopy

Logarithmic-phase cells of *P. cruentum* and *C. reinhardtii* were harvested at hours 3 and 4 of their respective light periods. Cells of *P. cruentum* were fixed at 4°C for 1 h in a solution containing 4% (v/v) paraformaldehyde and 0.8% (v/v) glutaraldehyde in phosphate-buffered saline (PBS), pH 7.4. Cells of *C. reinhardtii* were fixed at 4°C for 90 min in a solution containing 1% (v/v) glutaraldehyde in 50 mM 1,4-piperazinediethanesulfonic acid (Pipes), pH 7.4. Following fixation, cell pellets were washed in cold buffer and the cells dehydrated through a graded ethanol series and embedded in Lowicryl K4M (J.B. EM Services, Montreal, P.Q., Canada) as described in Lacoste-Royal and Gibbs (1985). Pale gold-coloured sections were cut with a diamond knife and mounted on formvar-coated nickel grids. For immunolabelling, grids were placed section-side down on drops of the following solutions: PBS, 10 min; 1% BSA in PBS, 30 min; antiserum, 30 min or 2 h; 1% BSA in PBS, 4 X 3 min; colloidal gold reagent diluted 1:25, 25 min; PBS, 4 X 3 min; de-ionized

water rinse. In addition, immunolabelling of *Chlamydomonas* by anti-PRK was preceded by incubation of the section on a drop of 1% (w/v) sodium *m*-periodate for 7 min followed by rinsing with de-ionized water. This was performed in order to eliminate non-specific binding of the antibody to starch grains. Goat anti-mouse-gold (15 nm; InterMedico, Markham, Ont., Canada) and protein A-gold (15 nm; InterMedico) were the colloidal gold reagents used. Antisera and gold reagents were diluted in 1% BSA in PBS. Sections were post-stained with 2% (w/v) aqueous uranyl acetate and lead citrate (Reynolds, 1963) prior to observing in a Philips EM 410 at an operating voltage of 80 kV.

In control experiments, the antiserum was replaced by PBS prior to incubation in the colloidal gold reagent. Cell sections incubated in this manner were largely free of gold label (data not shown).

The density of gold labelling over pyrenoid, stromal (including stromal starch, but not pyrenoid starch), nuclear, and cytoplasmic (including mitochondria and vacuoles) compartments of *C. reinhardtii* was determined essentially as described by Vaughn (1987a).

### 3.0. Results

#### 3.1. Immunoblotting

Immunoblotting results indicate that the antisera used in the present study are immunologically related to specific polypeptides in crude protein extracts of both *P. cruentum* and *C. reinhardtii*. Antiserum raised against PRK isolated from the cyanobacterium *Chlorogloeopsis*

*tritschii* reacted with a low mass polypeptide of ~16 kDa from the *P. cruentum* extract (Fig. 1a, Lane 3). The immunoreactive polypeptide migrated to a position immediately below that of the  $\beta$  subunit of phycoerythrin, which was evident as a pink-coloured band transferred from the gel to nitrocellulose. The identity of two minor staining bands of high mass is unknown. It is possible they may represent high mass aggregates of PRK subunits. The staining, however, is not likely the result of non-specific binding by the secondary antibody; similar bands were not observed when this same extract of *Porphyridium* was incubated with anti-Rubisco LS followed by the identical secondary antibody (Fig. 1c, Lane 2). No immunoreactive polypeptides were observed in the *Chlamydomonas* extract probed with anti-PRK from *Chlorogloeopsis* (Fig. 1a, Lane 2).

Conversely, antiserum raised against *Chlamydomonas reinhardtii* PRK recognized a specific polypeptide in the *Chlamydomonas*, but not in the *Porphyridium* protein extract. The antiserum cross-reacted with a polypeptide of ~40 kDa from *C. reinhardtii* (Fig. 1b, Lane 1) whereas no reaction was observed in the lane containing the *P. cruentum* extract (Fig. 1b, Lane 2).

A specific polypeptide from each extract cross-reacted with antiserum raised against the SDS-dissociated large subunit (LS) of tobacco Rubisco (Fig. 1c). The stained polypeptides co-migrated and each possessed an apparent mass of ~52-53 kDa. This size is in the range of that reported for algal Rubisco LS (Plumley et al. 1986; Newman et al. 1989).

**Fig. 1.** Immunoblot characterization of antisera. Pre-stained molecular mass standards (in kDa) are shown in blot a, lane 1. About 5  $\mu$ g total protein was loaded into each sample well. **a.** Immunoblot showing reactivity of anti-PRK from *Chlorogloeopsis fritschii* with soluble protein extracts from *Chlamydomonas reinhardtii* (Lane 2) and *Porphyridium cruentum* (Lane 3). There was no reaction observed with the *Chlamydomonas* extract whereas a major band of ~16 kDa was stained in the extract from *Porphyridium*. The immunoreactive polypeptide migrated to a position slightly below that of the  $\beta$  subunit of phycoerythrin whose pink-coloured chromophore was transferred from the gel to nitrocellulose during Western blotting. **b.** A single band of ~40 kDa from the *Chlamydomonas* extract (Lane 1) was stained by anti-PRK from *C. reinhardtii*. There were no immunoreactive polypeptides evident in the extract from *Porphyridium* (Lane 2). **c.** Single polypeptides from both *C. reinhardtii* (Lane 1) and *P. cruentum* (Lane 2) extracts were stained by anti-Rubisco LS. The immunoreactive polypeptides co-migrated on the gel and each possessed an apparent mass of ~52-53 kDa.

1 2 3 1 2 1 2

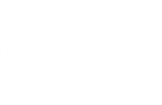
80.0-

49.5-

32.5-

27.5-

18.5-



a b c

-β

### 3.2. Immunoelectron Microscopy

Immunogold labelling of *P. cruentum* demonstrates that there exists a different subcellular localization of the Calvin cycle enzymes PRK and Rubisco. Figure 2 shows a cell which has been immunolabelled by anti-PRK. Gold particles, are abundant throughout the thylakoid-containing chloroplast stroma but are excluded from the pyrenoid. In contrast, the pyrenoid regions of *P. cruentum* are densely labelled by anti-Rubisco LS whereas the labelling over the remainder of the chloroplast is at background level (Fig. 3). Similarly, PRK appears to be excluded from the pyrenoid of the green alga *C. reinhardtii* (Fig. 4). Gold particles are found throughout the chloroplast stroma whereas the pyrenoid is mainly unlabelled. A morphometric analysis made of sections through 15 different cells of *C. reinhardtii* confirms our qualitative observations of immunolabelling by anti-PRK. Gold label over the chloroplast stroma (not including stromal inclusions of pyrenoids) was present at a density of  $17.4 \pm 1.0$  particles  $\cdot \mu\text{m}^{-2}$ . In contrast, label density over the pyrenoid was much lower ( $2.7 \pm 0.4$  particles  $\cdot \mu\text{m}^{-2}$ ) and similar to that observed over background nuclear ( $2.7 \pm 0.6$  particles  $\mu\text{m}^{-2}$ ) and cytoplasmic ( $1.4 \pm 0.2$  particles  $\cdot \mu\text{m}^{-2}$ ) compartments. When *Chlamydomonas* is immunolabelled by anti-Rubisco LS, however, labelling appears to be restricted to the pyrenoid, with only a few, scattered gold particles evident over the remainder of the cell (Fig. 5).

We believe the pyrenoid to be functional in  $\text{CO}_2$  fixation. It then becomes imperative that there exists a means by which metabolites can be transferred between pyrenoid and stroma. In red algae, starch is stored outside the chloroplast and a direct interface exists between

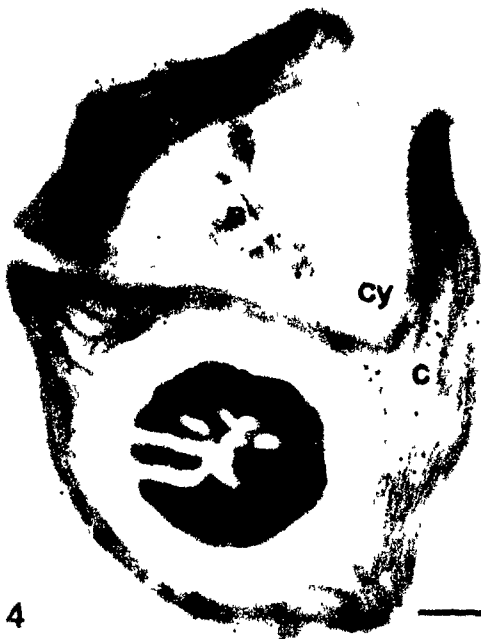
**Figs. 2-5.** Immunolocalization of PRK and Rubisco in logarithmic phase cells of *P. cruentum* and *C. reinhardtii*. Bars = 0.5  $\mu\text{m}$ . **Fig. 2.** Cell of *P. cruentum* immunolabelled by anti-PRK from *Chlorogloeopsis fritschii*. Gold particles are evident throughout the chloroplast (c) with the exception of the pyrenoid (py) regions. **Fig. 3.** Anti-Rubisco LS is predominantly localized in the pyrenoid regions of *P. cruentum*. Only a few, scattered gold particles are found elsewhere in the chloroplast. **Fig. 4.** Anti-PRK from *Chlamydomonas reinhardtii* labels the thylakoid-containing chloroplast stroma of this alga. The level of labelling over the pyrenoid is low and is similar to that encountered over background cytoplasmic (cy) and nuclear (n) compartments. **Fig. 5.** The pyrenoid of *C. reinhardtii* is heavily labelled by anti-Rubisco LS. The remainder of the chloroplast is largely devoid of gold particles. nucleus (n).



2



3



4



5

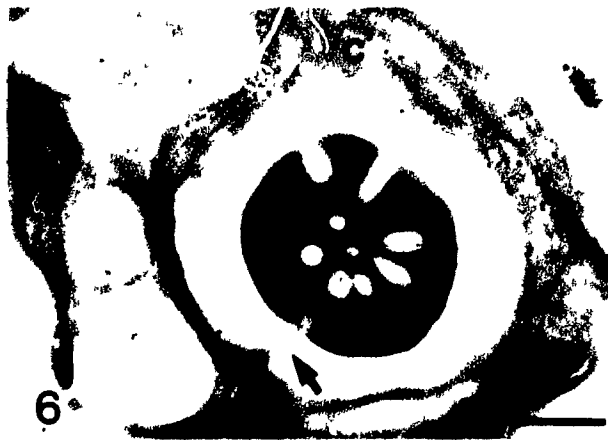
pyrenoid and stroma (Figs. 2,3) In contrast, green algae, like higher plants, store starch within the chloroplast. Furthermore, a portion of this starch is normally found associated with the pyrenoid, often appearing to surround the structure completely (Figs. 4-8). In *Chlamydomonas*, tubule-like elements are often seen to be continuous between the chloroplast stroma and the pyrenoid (Fig. 6). These structures, however, are not labelled by anti-PRK. Instead, novel inclusion regions are observed in the pyrenoid of *Chlamydomonas* (Figs. 7,8). These regions are heavily labelled by anti-PRK (Fig. 7), but are not labelled by anti-Rubisco LS (Fig. 8).

#### 4.0. Discussion

##### 4.1. Characterization of Antisera

Phosphoribulokinase isolated from different sources has been shown to exhibit fundamental differences in structure as well as in catalytic and regulatory properties. This is partially demonstrated in our attempts to characterize immunologically the two antibodies used in the present investigation. Our immunoblot results demonstrate that antiserum raised against PRK isolated from the cyanobacterium *Chlorogloeopsis fritschii* recognizes a polypeptide from a crude protein extract of the red alga *P. cruentum* but not from the chlorophyte *Chlamydomonas reinhardtii*, whereas the reciprocal is true when extracts are probed with antiserum raised against *Chlamydomonas* PRK (Fig.1). Although both cyanobacterial and green algal phosphoribulokinases seem to be regulated in the same light-

**Figs. 6-8.** Novel association of PRK with the pyrenoid of *Chlamydomonas reinhardtii*. Bars = 0.5  $\mu\text{m}$ . **Fig. 6.** The tubule-like structures of the *Chlamydomonas* pyrenoid (*py*) were frequently observed to be continuous between pyrenoid and chloroplast (*c*) stroma. These structures, however, are not labelled by anti-PRK (arrow) **Fig. 7.** Inclusions (arrowhead) were sometimes observed in the pyrenoid of *C. reinhardtii*. Such pyrenoid inclusions were always labelled by anti-PRK. **Fig. 8.** Pyrenoid inclusions (arrowhead) are not labelled by anti-Rubisco LS. Instead, Rubisco is restricted to the surrounding pyrenoid matrix



dependent manner (Duggan and Anderson 1975; Marsden and Codd 1984, Lazaro et al 1986, Serra et al. 1989), enzymes from the two sources are structurally distinct. The active form of the enzyme isolated from *Chlorogloeopsis fritschii* has been characterized as a hexamer consisting of identical 40 kDa subunits (Marsden and Codd 1984). In contrast, the active enzyme form isolated from green algal sources is reported to be a dimer, similar to that found in higher plants (e.g. Kagawa 1982), and consisting of identical subunits ranging from 38.5 kDa in *Chlamydomonas* (Roesler and Ogren 1990b) to 41-42 kDa in *Brvopsis maxima* (Sato et al 1985) and *Scenedesmus obliquus* (Lazaro et al 1986). In this context, the specific reaction observed between anti-PRK and the 16 kDa polypeptide in the *Porphyridium* extract is puzzling. It is possible that our result may be due to partial proteolysis of a larger mass PRK subunit normally present in this alga. Phosphoribulokinase, however, has yet to be characterized from red algal sources. It is perhaps relevant that Serra et al (1989) report that PRK from the cyanophyte *Anabaena variabilis* might consist of two nonidentical subunits having apparent molecular weights of 43 kDa and 26 kDa.

Unfortunately, there is no sequence information available with which to compare cyanobacterial PRK with that obtained from eukaryotic sources. To our knowledge, the only PRK sequence comparison made between prokaryotic and eukaryotic sources indicates only 30% homology between the amino-terminal amino acid sequences of spinach PRK and Form 1 PRK from the photosynthetic non-sulphur purple bacterium *Rhodospira rubra* (Hallenbeck and Kaplan 1987). In contrast, amino acid sequence comparisons made amongst the prokaryotic enzymes (Hallenbeck

and Kaplan 1987) or amongst the eukaryotic enzymes (Roesler and Ogren 1990) demonstrate much higher levels of homology.

#### 4.2 Subcellular Distribution of Phosphoribulokinase

Pyrenoids are conspicuous proteinaceous regions found in the chloroplasts of numerous algal and hornwort species. Increasingly, in recent years, their potential role in the functioning of the pathway of photosynthetic carbon reduction has been examined. Numerous immunocytochemical investigations have convincingly shown the Calvin cycle enzyme Rubisco to be predominantly pyrenoid-localized among diverse species of algae and hornworts (McKay and Gibbs 1991a; see also Chapter I). Moreover, the recent immunolocalization of Rubisco activase to the pyrenoids of the green algae *Chlamydomonas reinhardtii* and *Coleochaete scutata* (McKay et al. 1991a; see also Chapter III) and its presence also in the pyrenoids of various hornwort species (K. Vaughn, pers. comm.) support a catalytic role for pyrenoid-localized Rubisco.

In contrast to Rubisco, there has been relatively little information on the subcellular location of other Calvin cycle enzymes, including PRK, in microalgae. Phosphoribulokinase and Rubisco, however, occupy sequential positions in the Calvin cycle. Moreover, several recent investigations have provided evidence for the existence in higher plants, of a multi-enzyme complex possessing PRK, Rubisco and possibly other Calvin cycle enzyme activities (Sainis and Harris 1986; Gontero et al. 1988; Sainis et al. 1989). It is tempting, then, to speculate on a possible co-localization of PRK and Rubisco. Holdsworth (1971) provided some support for this hypothesis. His pyrenoid

preparations from the green alga *Eremosphaera viridis* possessed not only a high specific activity for Rubisco, but also showed ribose 5-phosphate isomerase and PRK activities. Moreover, Satoh et al. (1985) speculated that a 42 kDa polypeptide recovered from a *Brvopsis maxima* pyrenoid preparation might be a subunit of PRK. Their peptide map comparison of this protein with that of PRK purified from this same alga, however, showed the two polypeptides to be dissimilar. Other investigators have also found no evidence to support the presence in pyrenoids of additional Calvin cycle enzymes apart from Rubisco (Salisbury and Floyd 1978).

Instead of examining preparations of intact pyrenoids, we have employed in the present investigation, the complementary approach of immunoelectron microscopy to determine the subcellular distribution of PRK. Results from our immunolabelling study indicate that although PRK and Rubisco occupy sequential positions in the pathway of photosynthetic carbon reduction, there exists a difference in the intracellular location of these two enzymes. In both the red alga *P. cruentum* and the green alga *Chlamydomonas reinhardtii*, PRK is distributed throughout the chloroplast proper and appears to be excluded from the pyrenoid (Fig.2,4). In contrast, Rubisco is predominantly pyrenoid-localized in both of these algae (Fig.3,5). It is of interest to note that the observed intracellular partitioning of PRK and Rubisco in microalgae mimicks that reported for a number of prokaryotic organisms. All cyanobacteria thus far investigated and many chemolithoautotrophic bacteria possess distinct polyhedral-shaped inclusion bodies. These cellular inclusions have been named carboxysomes (Shively et al. 1973).

since, like pyrenoids, they contain much of the cell's complement of Rubisco. Cell fractionation experiments demonstrate that unlike Rubisco, PRK activity is predominantly associated with the soluble cell fraction rather than the carboxysome-containing pelletable fraction in the cyanobacterium *Chlorogloeopsis fritschii* (Lanaras and Codd 1981a; Marsden et al 1984) and in the cyanelles of the glaucophyte *Cyanophora paradoxa* (Mangenev et al 1987). Moreover, the isolation of intact carboxysomes from both *Chlorogloeopsis* (Lanaras and Codd 1981a) and the chemolithoautotrophic sulphur bacterium *Thiobacillus neapolitanus* (Cannon and Shively 1983, Holthuijzen et al 1986) provides no evidence for an association of PRK activity with these structures. Immunogold labelling studies of cell sections have provided similar results and demonstrate conclusively the exclusion of PRK from the carboxysomes of the cyanobacteria *C. fritschii* (Hawthornthwaite et al. 1985) and *Synechococcus* (Hawthornthwaite et al 1985; McKay et al. 1991c; see also Chapter V) as well as from carboxysomes of prochlorophytes (Codd 1988) and from the carboxysome-like regions in the cyanelles of *Cyanophora paradoxa* and *Glaucocystis nostochinearum* (Mangenev et al 1987).

Our immunolabelling results indicate that in pyrenoid-containing algae, PRK is preferentially localized in the chloroplast stroma whereas Rubisco is mainly pyrenoid-localized. Coupled with these observations, however, are special logistical problems in attempting to understand how the sequential Calvin cycle reactions catalyzed by PRK and Rubisco are linked. In the red alga *P. cruentum*, there exists a direct interface between pyrenoid and stroma (Fig. 2,3). As a result, RuBP could be readily directed to the site of CO<sub>2</sub> fixation in the pyrenoid. In

contrast, the pyrenoids of green algae cultured under air levels of CO<sub>2</sub> often appear to be completely demarcated by a sheath of starch (Miyachi et al. 1986; Kuchitsu et al. 1988b). This pyrenoid starch would appear to impose a barrier to the efficient shuttling of metabolites back and forth between pyrenoid and stroma. Frequently, pyrenoids are traversed by thylakoid lamellae or tubule-like structures (Griffiths 1970). In the hornworts, intrapyrenoid thylakoids may occur singly or in stacks and are accompanied by varying amounts of stromal material (Vaughn et al. 1990), an arrangement which contributes to the dissected or unit-like nature typical of many hornwort pyrenoids. These stromal regions are not labelled by antiserum to Rubisco (Vaughn et al. 1990) and presumably provide an additional interface between pyrenoid and stroma in these organisms. The strain of *Chlamydomonas reinhardtii* employed in the present investigation possesses a pyrenoid which is traversed by tubule-like elements. Often these tubules are observed to be continuous between pyrenoid and stroma; however, our immunolabelling results do not support an association of PRK with these structures (Fig. 6). Rather, we have observed unique inclusions in the pyrenoid of *Chlamydomonas*. These inclusions appear in micrographs as regions of lower electron density than the surrounding pyrenoid matrix. Furthermore, they are densely labelled by antiserum to PRK thereby identifying them as regions of chloroplast stroma (Fig. 7). Rubisco is excluded from such stromal inclusions (Fig. 8). In a three-dimensional arrangement, one can envision how the pyrenoid of *Chlamydomonas* might be penetrated by fingers of chloroplast stroma. We anticipate that this arrangement would provide *Chlamydomonas* with a direct interface between pyrenoid and

stroma and presumably facilitates an efficient exchange of metabolites between these two compartments. Stromal inclusions do not seem to be peculiar to *Chlamydomonas* pyrenoids, in a previous immunolabelling investigation from this lab, we observed regions in the pyrenoid of the green alga *Chlorella pyrenoidosa* from which Rubisco was also excluded (see Figure 1 in McKay and Gibbs 1989; see also Chapter II). Like *Chlamydomonas*, the pyrenoid of *Chlorella* also appears to be completely delimited by starch. The need for a mode of metabolite exchange between pyrenoid and stroma deems it likely that stromal inclusions will be identified in the pyrenoids of other green algae as well, and might, in fact, have been responsible for the measured ribose 5-phosphate isomerase and PRK activities reported from Holdsworth's (1971) *Eremosphaera* pyrenoid preparation.

#### **Acknowledgements**

We are grateful to those who provided the antisera employed in this study. Dr. G.A. Codd (Univ. of Dundee, UK) provided antibody against *Chlorogloeopsis* PRK and Drs. W.L. Ogren and K.R. Roesler (Univ. of Illinois, Urbana, USA) provided antiserum to PRK of *Chlamydomonas*. Dr. J. Fleck (CNRS, Strasbourg, France) kindly provided antibody to Rubisco LS. This research was supported by the Natural Sciences and Engineering Research Council of Canada (NSERC grant No. A-2921 to S.P. Gibbs). In addition, R.M.L. McKay acknowledges support through a NSERC postgraduate scholarship.

## CHAPTER V

Effect of dissolved inorganic carbon on mode of  
carbon transport, expression of carboxysomes  
and localization of Rubisco in cells of the  
cyanobacterium *Synechococcus* UTEX 625

## Preface

From the results of this thesis and from references contained herein, it is apparent that in air-grown cells of microalgae, Rubisco is mainly localized in the pyrenoid region of the chloroplast and that it is functional in this location. Why Rubisco is confined to a particular region of the plastid is unclear; however, it is possible that this arrangement is necessary to ensure efficient photosynthesis. It is well documented that microalgae, when grown under conditions of low dissolved inorganic carbon (DIC) in the growth medium (e.g. air levels of CO<sub>2</sub>), possess low K<sub>1/2</sub>(DIC) values for photosynthesis and low CO<sub>2</sub> compensation points (Aizawa and Miyachi 1986). Moreover, photorespiration is usually not apparent in these cells. Such photosynthetic characteristics are likely manifest in part through induction of a DIC concentrating mechanism and expression of high levels of carbonic anhydrase by cells cultured in this manner. It remains a possibility, however, that modifications in the morphological expression of pyrenoids and/or in the intracellular distribution of Rubisco may play a role in determining the efficiency with which a cell can utilize its inorganic carbon resources.

The effect of growth DIC on pyrenoid structure has been seldom investigated; the few studies made being limited to green algae. These studies indicate that under air levels of CO<sub>2</sub>, pyrenoids and pyrenoid starch are well developed in cells of *Dunaliella* (Tsuzuki et al. 1986), *Chlamydomonas* (Kuchitsu et al. 1988b), *Chlorella* and *Scenedesmus* (Miyachi et al. 1986). However, in all cases, pyrenoid starch is either dramatically reduced or absent when these cells are bubbled with higher

levels of CO<sub>2</sub> (1.5-4%). Moreover, it is apparent from the studies of Tsuzuki et al. (1986) and Miyachi et al. (1986) that the pyrenoid itself often becomes reduced in size or is completely absent from high CO<sub>2</sub>-grown cells.

Investigations conducted by the Candidate on the effect of varying growth DIC levels on the morphological expression of pyrenoids have been restricted to a collaborative effort conducted with Dr. Catherine Potvin of this department. As part of an investigation on the adaptation of *Chlamydomonas reinhardtii* to varying levels of CO<sub>2</sub>, cells were processed for electron microscopy. High CO<sub>2</sub> conditions in this experiment, however, were only 650 μl CO<sub>2</sub>·l<sup>-1</sup> (i.e. ~twice the amount found in air). Moreover, pyrenoids and pyrenoid starch were similarly well-developed in both high CO<sub>2</sub>-grown and air-grown cell types (data not shown).

Cyanobacteria possess intracellular structures called carboxysomes, that, like pyrenoids, contain much of the cell's complement of Rubisco. Furthermore, in view of the proposed evolutionary proximity between cyanobacteria and the chloroplasts of eukaryotic algae, the idea that pyrenoids are derived from carboxysomes is attractive. During the Candidate's tenure as a student at McGill, the opportunity arose to engage in a collaboration with Dr. George Espie, who during the course of 1988-1990, was a NSERC University Research Fellow at Concordia University in Montréal. Dr. Espie is well known for his research on DIC transport in cyanobacteria, particularly with the unicellular species *Synechococcus* UTEX 625. His laboratory was equipped to undertake a well controlled study of the effect of growth DIC on the expression of carboxysomes and the intracellular distribution of Rubisco

in this cyanobacterium. Cyanobacteria exhibit more plasticity in dealing with environmental perturbations than do eukaryotic microalgae, and in this context the results obtained from this study are not directly applicable to pyrenoids and Rubisco distribution in eukaryotes. Nevertheless, the collaboration provided an opportunity to investigate a related system in which Rubisco is likewise compartmentalized away from other reactions of the Calvin cycle.

## Summary

In the cyanobacterium *Synechococcus* UTEX 625, the extent of expression of carboxysomes appears dependent on the level of DIC in the growth medium. In cells grown under 5% CO<sub>2</sub> and in those bubbled with air, carboxysomes were present in low numbers (< 2·longitudinal section<sup>-1</sup>) and were distributed in a somewhat random manner throughout the centropiasm. In contrast, cells grown in standing culture and those bubbled with 30 μl CO<sub>2</sub>·l<sup>-1</sup> possessed many carboxysomes (> 8 long section<sup>-1</sup>). Moreover, carboxysomes in these cells were usually positioned near the cell periphery, aligned along the interface between the centropiasm and the photosynthetic thylakoids. Immunolocalization studies indicate that the Calvin cycle enzyme Rubisco is predominantly carboxysome-localized regardless of the [DIC] of the growth medium. It is postulated that such a peripheral arrangement of carboxysomes may provide for a more efficient use of the internal DIC pool in cells from cultures where carbon resources are limiting.

## 1.0. Introduction

Depending on the conditions under which they are grown, cyanobacteria may possess an array of intracellular inclusions (Allen 1984; Shively et al. 1988). Among the various inclusions, polyhedral bodies have attracted a great deal of attention in recent years, mainly as a result of biochemical and immunocytochemical evidence indicating the presence of the Calvin cycle enzyme ribulose 1,5-bisphosphate carboxylase/oxygenase (Rubisco; E.C. 4.1.1.39) in these structures. Rubisco catalyzes the fixation of CO<sub>2</sub> to ribulose 1,5-bisphosphate (RuBP) in the initial reaction of photosynthetic carbon reduction. In recognition of this potential function of polyhedral bodies, the term "carboxysome" was coined by Shively and colleagues (1973) to designate these unique prokaryotic inclusions.

Despite evidence linking Rubisco to carboxysomes, the role of these structures in cyanobacterial photosynthesis remains to be elucidated. Numerous investigations have shown a portion of the cell's complement of Rubisco to be soluble rather than carboxysome-associated (Cossar et al. 1985; Hawthornthwaite et al. 1985; references in Codd 1988) thereby fueling speculation that carboxysome-localized Rubisco may function as a photosynthetic reserve. Still, other investigators have suggested that carboxysomal Rubisco may be a general cellular nitrogen reserve (deVasconcelos and Fay 1974; Duke and Allen 1990). However, most studies detailing the effect of nitrogen-deprivation on cyanobacterial fine structure do not support this function (Peat and Whitton 1967; Stevens et al. 1981; Turpin et al. 1984; Wanner et al.

1986).

The possibility that carboxysomes are active sites of CO<sub>2</sub> fixation in vivo has been explored in a recent series of mathematical models (Reinhold et al. 1987; 1989). Cyanobacterial photosynthetic efficiency is regulated in part by a mechanism for the active transport of CO<sub>2</sub> and HCO<sub>3</sub><sup>-</sup> which acts to concentrate these species of inorganic carbon intracellularly to levels beyond those found in the external medium (Miller et al. 1990). The carboxysome models proposed by Reinhold and colleagues place the carboxysome as an integral component of this inorganic carbon concentrating mechanism, identifying it as the exclusive site where high levels of CO<sub>2</sub> are generated by carbonic anhydrase for use by Rubisco. Evidence in support of this hypothesis has recently been provided by Friedberg et al. (1989) and Pierce et al (1989) who demonstrated that structurally intact carboxysomes were important for the efficient operation of the inorganic carbon concentrating mechanism. Furthermore, Price and Badger (1989a) have shown that equilibration of the cytosolic pool of HCO<sub>3</sub><sup>-</sup> with CO<sub>2</sub> results in a dramatic increase in the efflux of CO<sub>2</sub> and an inability of the cells to accumulate DIC. Since the equilibration of cytosolic HCO<sub>3</sub><sup>-</sup> was brought about by the induction of plasmid borne human carbonic anhydrase, the clear implication of these experiments was that native carbonic anhydrase is normally absent from the cytosol but present in carboxysomes.

As with other cyanobacterial inclusion bodies, the morphological expression of carboxysomes is often dependent upon the nutrient status of the cell. Support for this comes from ultrastructural investigations

of cyanophytes undergoing various forms of nutrient-limitation. Investigators have commented on the expression of carboxysomes in cells of cultures limited in nitrogen (Peat and Whitton 1967; deVasconcelos and Fay 1974; Stevens et al 1981; Turpin et al 1984; Wanner et al. 1986), phosphorus (Turpin et al. 1984), sulphur (Wanner et al. 1986), iron (Sherman and Sherman 1983), and carbon (Miller and Holt 1977; Turpin et al 1984). Understandably, studies of the latter nature may be extremely valuable in elucidating a potential role for carboxysomes in cyanobacterial photosynthesis. In this report, we present a detailed analysis on the effect of varying levels of dissolved inorganic carbon (DIC) in the growth medium on the mode of carbon transport, the expression of carboxysomes and the subcellular localization of Rubisco in the unicellular cyanobacterium *Synechococcus* UTEX 625.

## 2.0. Materials and methods

### 2.1. Organism and growth conditions

*Synechococcus leopoliensis* (Raciborski) Komarék was obtained from the Culture Collection of Algae at the University of Texas at Austin (UTEX 625) and grown in batch culture in a modified Allen's medium (Espie and Canvin 1987). Cultures were grown at 29°C and continuous light was provided at a photon fluence rate of 50  $\mu\text{mol}\cdot\text{m}^{-2}\cdot\text{s}^{-1}$  for air-bubbled cells and 25  $\mu\text{mol}\cdot\text{m}^{-2}\cdot\text{s}^{-1}$  for standing culture cells. All cultures were inoculated to an initial chlorophyll (chl) concentration of 0.2  $\mu\text{g}\cdot\text{ml}^{-1}$  and were allowed to grow to the appropriate stage. Cells grown in

standing culture were used as inoculum. In the case of cultures bubbled with 5% CO<sub>2</sub>, cells were grown to late log phase and these in turn were used to start a second 5% CO<sub>2</sub>-grown culture which was subsequently used for analysis. Inorganic carbon was supplied by bubbling the cultures with air containing various concentrations of CO<sub>2</sub> (Table 1). The DIC concentration in the growth medium at harvest was determined by gas chromatography (Birmingham and Colman 1979). Chlorophyll *a* was determined spectrophotometrically at 665 nm following extraction in methanol (MacKinney 1941).

## 2.2. *Immunoelectron microscopy*

Cells were harvested by centrifugation and washed in ice-cold 100 mM sodium phosphate, pH 7.2. Cell pellets were fixed at 4°C for 2 h in a solution containing 1% glutaraldehyde in sodium phosphate buffer. The pellets were washed with cold buffer and the cells dehydrated through a graded ethanol series and embedded in L.R. White medium grade resin (J.B. EM Services, Montréal, P.Q., Canada) as described previously (Lichtle et al. 1991a).

For immunolabelling, pale gold-coloured sections were cut with a diamond knife and mounted on formvar-coated nickel grids. The grids were floated section-side down on drops of the following solutions: 1% bovine serum albumin (BSA; fraction V) in phosphate-buffered saline (PBS), 30 min; antiserum, 30 min; 1% BSA in PBS, 4 X 3 min; protein A-gold (15 nm; Intermedico, Markham, Ont., Canada) diluted 1:25 in 1% BSA in PBS, 25 min; PBS, 4 X 3 min; de-ionized water rinse. Rabbit antiserum raised against the large subunit (LS) of Rubisco isolated from

Table 1. Mode of carbon transport, morphological expression of carboxysomes, and Rubisco labelling density as dependant on culture growth parameters

Inflow Gas ( $\mu\text{l CO}_2 \text{ l}^{-1}$ )	Bubbling Rate <sup>a</sup> ( $\text{ml min}^{-1}$ )	[chl] ( $\mu\text{g chl g ml}^{-1}$ )	Culture pH	Culture [DIC] ( $\mu\text{M}$ )	Mode of DIC Transport <sup>b</sup>				Carboxysomes cell <sup>-1 c</sup>			Cell Volume <sup>c</sup> ( $\mu\text{m}^3$ )	Carboxysome Relative Volume <sup>d</sup> (%)	Carboxysome Volume ( $\mu\text{m}^3$ )	Label Density (gold particles $\mu\text{m}^{-2} \pm \text{SE}$ )		
					A	B	C	D	x-section	Long section					Carboxysome	Centrioplasm	Thylakoids
30	200	6.9	8.0	3	X	X	X		4.6 <sub>(90)</sub>	10.2 <sub>(24)</sub>	1.02 <sub>(16)</sub>	17.7	0.18	326.8 $\pm$ 10.4	9.0 $\pm$ 1.3	1.7 $\pm$ 0.2	
30	200	10.1	9.5	n.d. <sup>g</sup>	X	X	X		3.5 <sub>(106)</sub>	9.4 <sub>(21)</sub>	0.96 <sub>(17)</sub>	12.0	0.12	430.4 $\pm$ 12.1	5.9 $\pm$ 0.6	2.1 $\pm$ 0.3	
330	0 <sup>e</sup>	3.9	10.0	27	X	X	X		4.0 <sub>(79)</sub>	8.5 <sub>(30)</sub>	0.61 <sub>(29)</sub>	17.4	0.11	401.4 $\pm$ 13.4	6.9 $\pm$ 1.1	3.4 $\pm$ 0.6	
330	70	20.0	10.0	n.d.	X	X			0.7 <sub>(103)</sub>	1.5 <sub>(122)</sub>	0.83 <sub>(43)</sub>	2.5	0.02	491.9 $\pm$ 17.9	2.1 $\pm$ 0.3	0.7 $\pm$ 0.1	
330	70	8.0	10.0	n.d.	X	X			0.7 <sub>(176)</sub>	1.4 <sub>(48)</sub>	n.d.	n.d.	n.d.	n.d.	n.d.	n.d.	
330	70	3.4	10.0	68	X	X			0.9 <sub>(147)</sub>	1.9 <sub>(44)</sub>	0.77 <sub>(29)</sub>	2.9	0.02	515.5 $\pm$ 16.5	3.2 $\pm$ 0.5	2.6 $\pm$ 0.2	
330	540 <sup>f</sup>	4.7	8.8	743	X				0.8 <sub>(252)</sub>	1.9 <sub>(63)</sub>	0.78 <sub>(37)</sub>	2.0	0.02	496.3 $\pm$ 20.5	2.0 $\pm$ 0.1	0.7 $\pm$ 0.1	
5X10 <sup>d</sup>	140	11.5	7.5	>2000	X				0.6 <sub>(45)</sub>	0.8 <sub>(82)</sub>	1.72 <sub>(46)</sub>	2.8	0.05	368.8 $\pm$ 16.7	2.0 $\pm$ 0.3	1.6 $\pm$ 0.2	

<sup>a</sup>Cells grown in glass culture tubes (Espie and Calvin 1987) except where noted

<sup>b</sup>A= low affinity CO<sub>2</sub> transport

B= high affinity CO<sub>2</sub> transport

C= Na<sup>+</sup>-dependent HCO<sub>3</sub><sup>-</sup> transport

D= Na<sup>+</sup>-independent HCO<sub>3</sub><sup>-</sup> transport

<sup>c</sup>No. of cells examined in ( )

<sup>d</sup>Calculated as percentage of total cell area

<sup>e</sup>Cells grown in 125 ml Erlenmeyer flasks without supplementary aeration or stirring (Espie and Calvin 1987)

<sup>f</sup>Cells grown in large volume Roux flasks to accommodate high bubbling rate

<sup>g</sup>not determined

tobacco was kindly provided by Dr J Fleck (IBMC-CNRS, Strasbourg, France). Antiserum directed against phosphoribulokinase (PRK, E.C. 2.7.1.19) purified from the cyanobacterium *Chlorogloeopsis tritichii* was kindly provided by Dr. G.A. Codd (Univ of Dundee, Dundee, UK). Both antisera were diluted 1:500 in 1% BSA in PBS. Immunolabelled sections were post-stained with 2% aqueous uranyl acetate prior to viewing in a Philips EM 410 electron microscope at an operating voltage of 80 kV.

In control experiments, the antibody was replaced with rabbit non-immune immunoglobulin G, or with PBS alone, prior to protein A-gold incubation.

### 2.3. Quantitative evaluation

Cell volume was determined from measurements of individual cells on micrographs. Only longitudinal sections, through cells whose shape approximated that of a cylinder, were used for analysis.

The relative volume of carboxysomes was determined from measurements of surface areas of both carboxysomes and whole cells. That area measurements can be used to determine relative volumes has been shown previously (Gibbs 1968).

The density of labelling over various cell compartments was obtained by determining the number of gold particles per square micrometer of compartment sectioned. All area determinations were made using a Zeiss MOP-3 digital analyser.

### 2.4. Protein extraction and immunoblotting

Cells taken from a standing culture were harvested by centrifugation,

resuspended in 3.5 ml of 62.5 mM Tris-HCl, pH 7.0, containing 1 mM phenylmethylsulfonyl fluoride and then broken by passage (twice) through a chilled French pressure cell (Aminco, Urbana, IL) at 18,000 p s i. The resulting crude protein extract was clarified by centrifugation to remove unbroken cells and debris and polypeptides retained in the soluble fraction were separated by electrophoresis essentially as described by Laemmli (1970) on 12.5% sodium dodecyl sulfate-containing polyacrylamide mini-gels. Western blotting and immunodetection of Rubisco LS was performed as described previously (McKay and Gibbs 1991b; see also Chapter IV).

#### *2.5. Transport of inorganic carbon*

The active transport and intracellular accumulation of  $\text{CO}_2$  and/or  $\text{HCO}_3^-$  by *Synechococcus* results in a characteristic quenching of chl *a* fluorescence which can be used to indirectly monitor these transport events (Miller et al. 1991). The occurrence of active  $\text{CO}_2$  transport,  $\text{Na}^+$ -dependent and  $\text{Na}^+$ -independent  $\text{HCO}_3^-$  transport was assayed for in this way with subsamples of cells used in the immunolabelling studies. Fluorescence yield was measured at 30°C and  $100 \mu\text{mol} \cdot \text{m}^{-2} \cdot \text{s}^{-1}$  white light with a pulse amplitude modulation fluorometer (PAM 101, H. Walz, Effeltrich, Germany) as described by Espie et al. (1989) following addition of DIC to cells suspended in Bis-Tris Propane buffer, pH 8.0. The results of fluorescence assays were subsequently confirmed using the silicone fluid centrifugation method to provide a direct transport assay with either  $^{14}\text{CO}_2$  or  $\text{H}^{14}\text{CO}_3^-$  as substrate. Mass spectrometry was also used to directly monitor active  $\text{CO}_2$  uptake from the medium (data not

shown).

### 3.0. Results

#### 3.1. Antisera specificity

The Rubisco antiserum employed in the present study recognized a single polypeptide from a crude protein extract of *Synechococcus*, the stained band having an apparent mass of ~54 kilodaltons (Fig 1). The immunological recognition observed between higher plant Rubisco LS and its cyanobacterial counterpart was not unexpected. With the possible exception of Rubisco LS from red algae and from chromophyte algae (Newman and Cattolico 1990), the primary structure of this protein appears to be well conserved among evolutionarily-diverse species (Akazawa et al. 1984).

Immunoblotting was not performed for anti-PRK. The antiserum was raised against cyanobacterial PRK and its specificity for the cyanobacterial enzyme has been demonstrated (Marsden et al. 1984)

#### 3.2. Subcellular location of Rubisco

Our quantitative (Table 1) and qualitative (Figs. 2-10) analyses of immunolabelling by anti-Rubisco LS showed that Rubisco was predominantly localized in carboxysomes of *Synechococcus* regardless of the DIC content of the culture medium or the stage of growth at which cells were harvested. A high density of label was routinely measured over carboxysomes whereas label density over the DNA-containing centropiasm

**Fig. 1.** Immunoblot analysis of anti-Rubisco LS. Sizes of pre-stained molecular mass standards (in kDa) are shown at left. Anti-Rubisco LS was reacted with blotted soluble proteins (8  $\mu$ g total protein) from standing culture cells of *Synechococcus* UTEX 625. A polypeptide having a mass of ~54 kDa is stained

80.0-

49.5-

32.5-

and over the peripherally-located thylakoid region was very low (Table 1). The slightly higher values reported over the centropasm of cells cultured under low levels of growth DIC might be related to the increased numbers of carboxysomes present in these cells coupled with the resolution of the protein A-gold technique. A gold particle could lie up to 35 nm from the antigen labelled (15 nm antibody; 5 nm protein A; 15 nm gold particle). Thus, a gold particle located outside of, but near to a carboxysome might actually represent binding to a Rubisco epitope within the carboxysome. This, when taken together with the higher frequency of carboxysomes, might then explain the slight increase in label density found outside of the carboxysome in these cells.

When *Synechococcus* was immunolabelled by anti-PRK, gold label was restricted to the peripherally-located thylakoid region (Fig. 11). Carboxysomes and the centropasmic region were unlabelled. That PRK is excluded from carboxysomes has been demonstrated previously for the cyanobacterium *Chlorogloeopsis fritschii* (Hawthornthwaite et al. 1985). That PRK was similarly excluded from the centropasmic region of this cyanophyte, however, was not clear from their study.

When antiserum was replaced by rabbit non-immune immunoglobulin G, or by PBS alone, sections were mainly unlabelled. In Figure 12, a section incubated in non-immune serum is marked by only a couple of scattered gold particles.

### 3.3. Morphological expression of carboxysomes

The morphological expression of carboxysomes in cells of *Synechococcus* UTEX 625 was examined over a wide range of cellular growth conditions.

**Figs. 2,3.** Air-grown cells of *Synechococcus* UTEX 625 immunolabelled by anti-Rubisco LS. Bars = 0.25  $\mu\text{m}$ . 1. Cell from a culture harvested at low ( $3.4 \mu\text{g chl}a \cdot \text{ml}^{-1}$ ) cell density. Gold particles are concentrated over the carboxysome. Neither the centrioplasm (*ce*) nor the thylakoids (*t*) are labelled. 2. Longitudinal-section through a cell from a culture of high ( $20 \mu\text{g chl}a \cdot \text{ml}^{-1}$ ) cell density. The label is predominantly over a polyhedral-shaped carboxysome



2

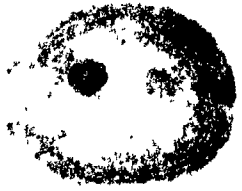


3



**Fig. 4.** Cells from a culture bubbled with air at a rate of 540 ml·min<sup>-1</sup>. Rubisco LS is concentrated over carboxysomes (top and bottom cell). The cells are mainly devoid of extra-carboxysomal label. Bar - 0.25 μm

**Figs. 5,6.** Cells from a culture bubbled with 5% CO<sub>2</sub>. In these cells, Rubisco LS is restricted to the carboxysomes. Bars=0.25 μm 5. Two carboxysomes are present in this cell. One is large and irregular in shape whereas the other has a more typical polyhedral shape (arrow) 6. A smaller carboxysome (arrowhead) appears to have aligned itself with a "giant" carboxysome



4

5

6

**Figs. 7,8.** Cells from a standing culture that have been immunolabelled by anti-Rubisco LS Bars = 0.25  $\mu\text{m}$  7. Rubisco is mainly restricted to carboxysomes in these cells. The carboxysomes are located at the cell periphery, positioned at the interface between the centropasm and the photosynthetic thylakoid membranes. 8. Similarly, in this longitudinal-section, carboxysomes are aligned at the cell periphery

**Figs. 9,10.** Cells from a culture bubbled with 30 p.p.m.  $\text{CO}_2$  and buffered at pH 8.0. Bars = 0.25  $\mu\text{m}$ . 9. Similar to standing culture cells, the carboxysomes, which are immunolabelled by anti-Rubisco LS, are positioned at the cell periphery. In the cell pictured at bottom, carboxysomes appear to ring the cell. 10. In this longitudinal-section, carboxysomes are found associated with the peripherally-located thylakoids. One of the carboxysomes is extended, shaped like a rod (arrow)

**Fig. 11.** This air-grown cell has been labelled by anti-PRK. Gold particles are located over the photosynthetic thylakoid membranes but are excluded from the centropasmic region and from a carboxysome (*cb*). Bar = 0.25  $\mu\text{m}$

**Fig. 12.** A control section incubated in non-immune serum. The cell is mainly devoid of label. Bar = 0.25  $\mu\text{m}$



7



8



9



10



11



12

Cultures of *Synechococcus* bubbled with air at a rate of  $70 \text{ ml} \cdot \text{min}^{-1}$  (air-grown cells) were examined at three different cell densities (3.4, 8 and  $20 \mu\text{g chl}a \cdot \text{ml}^{-1}$ ). Carboxysomes were present in low numbers in all air-grown cells regardless of the density at which the cells were harvested (Table 1). Carboxysomes observed in air-grown cells were mainly regular (polyhedral) in shape and were usually found in the centropasm and not in association with the thylakoids which were located around the cell periphery (Figs. 2,3).

Cells from cultures bubbled with air at a high ( $540 \text{ ml min}^{-1}$ ) bubbling rate were very similar to air-grown cells in terms of their carboxysomes. The carboxysomes were present in low numbers (Table 1), were quite regular in structure, and were found mainly in the centropasm and displayed no obvious association with the peripherally-located thylakoids (Fig. 4).

Cells from cultures bubbled with 5%  $\text{CO}_2$  (high DIC cells) frequently possessed aberrant carboxysomes (Figs 5,6). These structures were often large and irregular in shape. Of the total number of carboxysomes measured in these cells, over 52% had an area greater than  $4 \times 10^{-2} \mu\text{m}^2$ . Furthermore, 18% of the carboxysomes observed in these cells had an area greater than  $1 \times 10^{-1} \mu\text{m}^2$ . Carboxysomes of this size were only rarely observed in any other cells. For example, in air-grown cells of both high and low cell density, more than 96% of the total carboxysomes measured had an area of less than  $4 \times 10^{-2} \mu\text{m}^2$ . In addition to the "giant" carboxysomes observed in cells grown under 5%  $\text{CO}_2$ , regular, polyhedral shaped carboxysomes were also observed (Fig. 5, arrow). In Figure 6, a small, discrete carboxysome is adjoined to one

which is much larger. This association may provide insight into how the "giant" carboxysomes are made. Carboxysomes were always present in low numbers in high DIC cells ( $< 1$  carboxysome/cell section; Table 1), yet partial serial sectioning analysis indicated that each cell possessed at least one carboxysome (data not shown). In high DIC cells, carboxysomes appeared to be positioned in a random manner throughout the centropiasm. The direct association of a carboxysome with the thylakoids as observed in Figure 6 was not a common occurrence.

Carboxysomes were present in much higher numbers in cells grown in standing culture and in those cells bubbled with  $30 \mu\text{l CO}_2 \cdot \text{l}^{-1}$  (low DIC cells) (Table 1). Moreover, in these cell types, carboxysomes accounted for a far higher percentage of relative cell volume than was measured for air-grown and high DIC cells (Table 1). Carboxysomes in standing culture cells were mainly regular in shape (Figs. 7,8), although occasionally, longer rod-like structures were observed. Their positioning in the cell was unusual, in that they were rarely found in the middle of the centropiasm, but rather, they seemed to be aligned at the cell periphery, in association with the thylakoid membranes. Similar observations were made for the cells bubbled with  $30 \mu\text{l CO}_2 \cdot \text{l}^{-1}$  (Figs. 9,10). Although only cells from cultures maintained at pH 8.0 are illustrated, similar results were observed for the pH 9.5 cells. Carboxysomes were largely polyhedral in shape, however, a long rod-shaped structure is evident in Figure 10. Moreover, as in standing culture cells, carboxysomes were nearly always aligned at the cell periphery and at times appeared to completely ring the cell interior (bottom cell in Fig 9).

### 3.4. *Transport of inorganic carbon*

The increase in carboxysome number in cells grown under low DIC was paralleled by an increase in  $\text{HCO}_3^-$  transport capability (Table 1) and an increase in the apparent photosynthetic affinity of the cells for DIC. In contrast, cells grown at all levels of DIC were capable of active  $\text{CO}_2$  transport although the apparent affinity of the transport system for  $\text{CO}_2$  was somewhat lower in cells bubbled with 5%  $\text{CO}_2$  (data not shown). Cells which contained high numbers of carboxysomes were capable of both  $\text{Na}^+$ -dependent and  $\text{Na}^+$ -independent  $\text{HCO}_3^-$  transport (Table 1) and are able to accumulate DIC in excess of 1000-fold the external [DIC] (Espie and Kandasamy 1991). The transition between high and low carboxysome number was characterized by a loss of  $\text{Na}^+$ -independent  $\text{HCO}_3^-$  transport capability. However, cells which possess  $\text{Na}^+$ -dependent  $\text{HCO}_3^-$  transport, in conjunction with active  $\text{CO}_2$  transport, are still capable of accumulating a large internal pool of DIC (Miller et al 1990). In contrast, cells lacking  $\text{HCO}_3^-$  transport capability (i.e. high DIC-grown cells) exhibit a low DIC accumulation ratio (Badger and Gallagher 1987).

## 4.0. Discussion

### 4.1. *Subcellular location of Rubisco*

It is well documented that in cyanobacteria, the Calvin cycle enzyme Rubisco is found associated with distinct polyhedral-shaped cellular inclusions (Codd and Marsden 1984; Codd 1988) named carboxysomes (Shively et al. 1973). However, numerous investigations have shown that

there may exist, in addition, a considerable extra-carboxysomal or "soluble" pool of the enzyme, an observation that calls into question the functional role of carboxysome-localized Rubisco. A number of these studies have employed cell fractionation techniques to ascertain the subcellular location of Rubisco in various cyanobacteria (Codd and Stewart 1976; Lanaras and Codd 1981a; 1982; Coleman et al. 1982; Marsden et al. 1984, Duke and Allen 1990). Results obtained from investigations of this nature, however, can be quite variable, readily altered by slight changes to the cell lysis protocol. For example, use of buffers of low ionic strength (Codd and Marsden 1984) or addition of millimolar amounts of  $Mg^{++}$  (Coleman et al. 1982) to the buffer during cell breakage favours recovery of carboxysomes. Additionally, results may be altered by the method chosen for cell lysis. Cell breakage by mechanical means (e.g. French pressure cell) is reported to result in a significant decrease in the amount of carboxysomal or "particulate" enzyme recovered (Coleman et al. 1982). In contrast, pretreatment of cells with lysozyme to produce sphaeroplasts followed by a gentle osmotically induced cell lysis resulted in recovery of nearly all Rubisco activity in the particulate fractions of 10 species of cyanobacteria (Coleman et al. 1982).

As a complementary approach to the investigation of Rubisco distribution in cyanobacteria, we have employed in the present study the technique of protein A-gold immunoelectron microscopy. This method provides not only fine structural detail, but also affords an accurate assessment of the subcellular location of Rubisco in situ. Moreover, both soluble and particulate Rubisco can be detected with a single

antibody since the two forms are immunochemically related (Lanaras and Codd 1981b). Using this technique, we have determined that under a wide variety of conditions, most of the cells Rubisco is carboxysome-localized in *Synechococcus* UTEX 625. Similar results have recently been reported for prochlorophytes (Swift and Leser 1989) and for the cyanelles of glaucophytes (Mangoney and Gibbs 1987), both of which are carboxysome-containing photoautotrophs. Our results, however, are in contrast to those obtained from earlier immunolabelling studies (Cossar et al. 1985; Hawthornthwaite et al. 1985). Using the filamentous cyanobacterium *Chlorogloeopsis fritschii*, Hawthornthwaite et al. (1985) observed only a slightly higher concentration of label over carboxysomes than over the centropiasm and thylakoid-containing regions. Cossar et al. (1985) investigated Rubisco partitioning in the filamentous N<sub>2</sub>-fixing cyanophyte *Anabaena cylindrica*. In this species, they observed a differential partitioning of the enzyme depending on the stage of growth at which cells were harvested. In stationary phase cells, Rubisco was mainly restricted to carboxysomes, whereas in more actively growing chemostat cultures, label was found not only over carboxysomes but also over the thylakoid-containing regions of the cell. These results are consistent with those reported by Lanaras and Codd (1982), whose cell fractionation experiments indicated that the subcellular location of Rubisco changes during photoautotrophic batch culture of *C. fritschii*. Our results with *Synechococcus* UTEX 625, however, do not support these findings. Rubisco was predominantly carboxysome-localized in air-grown cells harvested at both low ( $3.4 \mu\text{g chl}a \cdot \text{ml}^{-1}$ ) and high ( $20 \mu\text{g chl}a \cdot \text{ml}^{-1}$ ) cell densities (Table 1; Figs. 2,3). Furthermore, qualitative analysis

of cells harvested in mid-logarithmic phase ( $8 \mu\text{g chl}a \cdot \text{ml}^{-1}$ ) showed Rubisco to be restricted mainly to carboxysomes (data not shown). Labelling densities over centropasmic and thylakoid regions of air-grown cells were consistently low and there was no indication of a preferential association of Rubisco with thylakoids as was observed in *A. cylindrica* (Cossar et al 1985).

Likewise, the [DIC] of the growth medium did not affect the localization of Rubisco. This, however, was somewhat unexpected, especially when considering high DIC cells. Employing the same strain of *Synechococcus* as was used in the present study, Mayo et al. (1989) reported that Rubisco active site density was much higher for cells grown at high (1000-1800  $\mu\text{M}$ ) levels of DIC than for DIC-limited cells (10-20  $\mu\text{M}$ ). This, taken together with the finding that high DIC cells of *Synechococcus* UTEX 625 possess on average less than 1 carboxysome per cell section (Turpin et al. 1984; this study), had initially led us to believe that these cells would contain an increased soluble component of Rubisco. Instead, Rubisco was mainly carboxysome-localized in 5%  $\text{CO}_2$ -grown cells (Table 1, Figs. 5,6). It is noteworthy that in the sulphur-oxidizing bacterium *Thiobacillus neapolitanus*, the ratio of soluble:particulate Rubisco remained constant regardless of whether cells were grown under inorganic carbon limitation or whether they were grown under thiosulphate-limitation, but bubbled with 5%  $\text{CO}_2$  (Beudeker et al 1981). Moreover, in these cells, carboxysome content declined dramatically under the high DIC conditions.

In the present investigation, cells cultured under 5%  $\text{CO}_2$  frequently possessed large, irregular shaped carboxysomes. Carboxysome

volume in these high DIC cells, however, was still less than twice that measured for standing culture cells and for cells bubbled with  $30 \mu\text{l CO}_2 \cdot \text{l}^{-1}$  (Table 1). Thus, the presence of "giant" carboxysomes alone is not enough to resolve the discrepancy between a carboxysomal location for Rubisco, increased amounts of the enzyme and low numbers of carboxysomes per cell section. That cells grown under 5%  $\text{CO}_2$  did not produce increased amounts of Rubisco or that they only transiently increased amounts of the enzyme is possible; cellular Rubisco content was not measured in the present investigation. Cells cultured in this manner, however, exhibit higher rates of photosynthesis than do standing culture cells or those bubbled with  $30 \mu\text{l CO}_2 \cdot \text{l}^{-1}$ . It is likely that the high rates observed in 5%  $\text{CO}_2$ -grown cells are partially a result of increased levels of Rubisco.

The possibility that soluble Rubisco was present at a photosynthetically appreciable concentration in cells bubbled with 5%  $\text{CO}_2$  but that it was not detected by the protein A-gold technique should also be considered. This concern has been recently addressed with respect to the intracellular partitioning of Rubisco between chloroplast pyrenoid and stromal regions in eukaryotic algae and hornworts (McKay and Gibbs 1991a; see also Chapter I). It is our belief that if Rubisco is present in the chloroplast stroma of pyrenoid-containing organisms, it is present at very low concentrations; the soluble Rubisco of higher plants and of non-pyrenoid-containing algae and hornworts is readily detected by immunogold methodology. Moreover, our recent immunolabelling results with the cyanophyte *C. fritschii* indicate the presence of a soluble pool of Rubisco (data not shown). It seems likely

then that soluble Rubisco, if present in *Synechococcus* UTEX 625, would be measured by the protein A-gold technique

That Rubisco is present at a higher concentration in carboxysomes of 5% CO<sub>2</sub>-grown cells compared to cells grown under low DIC should also be considered. Although our quantitative analysis of Rubisco labelling density over carboxysomes does not support this possibility (Table 1), these values should not be directly compared. When an antigen is tightly packed within a compartment, as likely Rubisco is in carboxysomes, a single 15 nm gold particle probably indicates more than one antigenic site (Roth 1982). The exact number of reactive sites marked by the particle is unknown and this in turn makes absolute quantitation difficult to measure. In addition, effects of steric hindrance are possible when gold particles mark antigenic sites in close apposition

#### 4.2. *Is extra-carboxysomal label genuine?*

Although extra-carboxysomal labelling was low in the present study, it is difficult to determine whether that label measured over the centrioplasm and thylakoids is genuine. Often, conventional controls employed in immunocytochemical investigations are devoid of label (~ 1 gold particle· $\mu\text{m}^{-2}$ ; e.g. Fig 12) and are thus not always good indicators of true background labelling by a given antibody. A better indicator would be an intracellular compartment from which it is known that the protein of interest is excluded. In eukaryotic cells, this is readily provided by the various organelles. Rubisco LS, for example, is generally excluded from compartments other than the chloroplast. Label

measured over extra-plastidic compartments, therefore, can be considered background. In cyanobacteria, however, with the possible exception of inclusion bodies other than carboxysomes, there are no distinct intracellular compartments from which Rubisco is known to be excluded. Moreover, the conditions of growth were such in the current investigation that inclusion bodies apart from carboxysomes were not present. Although an intracellular control is lacking in unicellular forms, some  $N_2$ -fixing filamentous cyanobacteria possess a good internal control. Heterocysts are specialized cell types involved in nitrogen fixation. Rubisco is excluded from these cells (Codd and Stewart 1977). In the immunolabelling study performed by Cossar et al (1985), labelling by anti-Rubisco over a heterocyst of *A. cylindrica* is illustrated. Although background labelling is present over this structure, the labelling data were not quantified. Consequently, comparisons to label density over the vegetative cells cannot be made. In a more recent investigation, the subcellular distribution of Rubisco was quantitatively analyzed for  $N_2$ -fixing *Nostoc* symbionts in two species of lichen (Bergman and Rai 1989). Heterocysts were present in both *Nostoc* variants and anti-Rubisco label density over these structures was at the level of that found over the cytoplasm (centroplasm plus thylakoids) of carboxysome-containing vegetative cells. The low level of extra-carboxysomal label measured in vegetative cells of  $N_2$ -fixing *Nostoc* would then appear to be background. Still, the absence of a comparable internal control in the present study makes it difficult to comment on the validity of the extra-carboxysomal label observed in *Synechococcus* UTEX 625.

#### 4.3. Morphological expression of carboxysomes

The morphological expression of carboxysomes in *Synechococcus* UTEX 625 was not affected by the stage of growth at which cells were harvested. In air-grown cultures where cells were harvested and fixed for microscopy at three different chlorophyll concentrations, the carboxysome content on a cell section basis did not vary markedly (Table 1). This is in contrast to the results of Stewart (1977) who reported that carboxysome content was greatest in cells from lag and stationary phase cultures of *Anabaena cylindrica*. Cells from exponential phase cultures, he reported, possessed the fewest carboxysomes. It is possible, at least for his stationary phase cultures, that carbon limitation resulted in the observed increase in carboxysome number. In the present study, we noted a dramatic increase in the frequency of carboxysomes only when cells were grown at very low ( $< 30 \mu\text{M}$ ) concentrations of DIC (Table 1). This is consistent with the results of Turpin et al. (1984) using this same alga. In their chemostat cultures, the carboxysome content did not vary for cells grown under nitrogen or phosphorus limitation (i.e. carbon-replete cells). Only when cells were cultured under severe carbon limitation ( $4 \mu\text{M}$  DIC) did carboxysome numbers increase. Their value of  $3.4 \text{ carboxysomes} \cdot \text{cell section}^{-1}$  is very close to the values obtained in the present study from cross-sections of low ( $< 30 \mu\text{M}$ ) DIC-grown cells. Comparable results have been reported for *Anacystis nidulans* R2 (also known as *Synechococcus leopoliensis* PCC 7942) (Sherman and Sherman 1983). These workers investigated the effect of iron deficiency and its subsequent restoration on *A. nidulans* fine structure. In their controls, however,

Fe-replete cells were grown by either gentle shaking (125 rpm) on a gyratory shaker or by vigorous air-bubbling. Their results indicated that carboxysome numbers were considerably higher in cells from shaken cultures (8-14 carboxysomes·cell section<sup>-1</sup>) compared to cultures bubbled vigorously with air (5-7 carboxysomes·cell section<sup>-1</sup>). Moreover, these authors suggested that different levels of DIC that may have been present in the two cultures could have been responsible for the differential expression of carboxysomes.

In addition to the increased carboxysome content of cells from shaken compared to air-bubbled cultures, Sherman and Sherman (1983) also commented on a different intracellular distribution for carboxysomes between cultures. In air-bubbled cultures, carboxysomes were consistently observed throughout the nucleoplasm but rarely in contact with photosynthetic membranes. Carboxysomes are similarly distributed in cells of *Agmenellum quadruplicatum* (Nierzwicki-Bauer et al. 1983) and *Synechococcus lividus* (Edwards et al. 1968) bubbled with 3% and 5% CO<sub>2</sub>, respectively. In contrast, carboxysomes were nearly always aligned at the cell periphery and in contact with thylakoids in cells of *A. nidulans* from shaken cultures (Sherman and Sherman 1983). A similar DIC-dependent partitioning of carboxysomes was observed in the present investigation. In both air-bubbled cells and those cultured under 5% CO<sub>2</sub>, carboxysomes were more or less randomly distributed throughout the centropiasm (Figs. 2-6). There was no obvious association between carboxysomes and the photosynthetic membranes located at the cell periphery. Carboxysomes in cells grown under low DIC, however, were consistently located at the cell periphery, positioned along the

interface between the centrioplasm and thylakoids (Figs. 7-10). Codd (1988) has suggested that the presence of carboxysomes in an organism may serve as an ecological marker for autotrophy. Perhaps, at least for *Synechococcus*, the presence of large numbers of carboxysomes which are positioned at the cell periphery might serve as a marker not only for autotrophy, but also for growth in a low DIC environment.

#### 4.4. Carboxysome positioning: photosynthetic implications?

Results from the present study and those from previous investigations clearly establish that cyanobacterial carboxysomes contain Rubisco. Moreover, our results indicate that carboxysomal Rubisco must be functional *in vivo*, nearly all Rubisco was located in carboxysomes in cells of *Synechococcus* UTEX 625. For Rubisco to be catalytically competent, however, it must exist as an activated ternary complex in which activator CO<sub>2</sub> and Mg<sup>+2</sup> are bound to an essential lysine residue of the large subunit. Unfortunately, one is unable to distinguish between active and inactive enzyme forms using immunological techniques. For this reason, we are unable to comment on the activation state of carboxysomal Rubisco in the present investigation. Cannon et al. (1991), however, have recently provided direct evidence in support of an active role for Rubisco located in carboxysomes. Using chloroform-permeabilized cells of *T. neapolitanus*, they showed that radiolabelled activator CO<sub>2</sub> was trapped to carboxysomal Rubisco by 2-C-carboxy-D-arabinitol-1,5-bisphosphate, an analogue of the transition-state intermediate in the Rubisco-catalyzed carboxylation of RuBP. It appears then, that carboxysomal Rubisco can exist in an activated form *in vivo*.

This, taken together with our immunolabelling results leads us to believe that carboxysomal Rubisco in *Synechococcus* UTEX 625 is functional.

Since Rubisco appears to be functional in carboxysomes of *Synechococcus*, the expression and distribution of these structures within the cell might be important in determining photosynthetic efficiency. High DIC-requiring cyanobacterial mutants have been identified (Friedberg et al 1989, Pierce et al 1989, Price and Badger 1989b). Moreover, in these mutants, carboxysomes are either absent (Pierce et al. 1989) or are aberrant in shape (Friedberg et al. 1989; Price and Badger 1989b). In the present study, cells cultured under low levels of DIC ( $< 30 \mu\text{M}$ ) possessed many carboxysomes, most of which were found near the cell periphery along the interface between the centrioplasm and thylakoids (Figs. 7-10). In some instances, carboxysomes even appeared to ring the cell interior completely (Fig. 9). It is known that cells of *Synechococcus*, when grown under low DIC conditions, concentrate inorganic carbon species many-fold over that present in the external medium (Miller et al. 1990). The steep chemical gradient resulting from operation of this concentrating mechanism, however, inevitably leads to leakage of  $\text{CO}_2$  from the cell. Moreover, it is anticipated that leakage would occur regardless of the intracellular location of carbonic anhydrase. That is, even if carbonic anhydrase is restricted to carboxysomes as proposed by Reinhold and colleagues (1987, 1989) and Price and Badger (1989a), some  $\text{CO}_2$  would still be generated outside of these structures as a result of non-enzymatic dehydration of  $\text{HCO}_3^-$ . In order to optimize usage of the internal DIC pool, it is

possible that carboxysomes in low DIC-grown cells of *Synechococcus* provide a partial barrier to CO<sub>2</sub> efflux. The increased number of carboxysomes in these cells is paralleled by an effective increase in the "carboxylating" surface area. This coupled with their distribution along the cell periphery increases the probability that CO<sub>2</sub> generated in the centropiasm, must first encounter a carboxysome before it could leave the cell. Some CO<sub>2</sub>, of course, would be lost from the cells; carboxysomes are not omnipresent. However, a reduction in the amount of CO<sub>2</sub> leaked from the cell might be realized through this special carboxysome arrangement. A mechanism for scavenging leaked CO<sub>2</sub> is present in *Synechococcus* (Miller et al. 1990; Espie et al. 1991). However, if cells are truly DIC-limited, it would be advantageous to maximize retention of the intracellular DIC pool. This would be especially relevant to environments in which cells are competing with oneanother for scant carbon resources.

Being positioned at the interface between the centropiasm and the photosynthetic membranes also means that Rubisco is in closer proximity to incoming DIC as well as to its other substrate, RuBP. Our immunolabelling results demonstrate that PRK, the enzyme responsible for RuBP synthesis, is restricted to the peripherally-located thylakoid region in *Synechococcus* (Fig. 11). Although a more direct coupling between RuBP synthesis and its carboxylation would be anticipated when carboxysomes abut the thylakoids, it is not known how RuBP, or for that matter HCO<sub>3</sub><sup>-</sup>, is able to cross thylakoid membranes on route to the centropiasm without uncoupling photosynthetic electron transport.

A possible disadvantage associated with this structural

arrangement is the closer proximity between Rubisco and the reactions of photosynthetic oxygen evolution. Rubisco is a bifunctional enzyme, having in addition to its carboxylase capability, an oxygenase function. Oxidation of substrate RuBP leads to photorespiration, a process generally considered wasteful. Apparent photorespiration, however, is not measured in cells of *Synechococcus* or of other cyanophytes when cultured under low levels of growth DIC (Miller et al. 1990). The idea that carboxysomes are impermeable to oxygen has been forwarded. That carboxysomes are generally absent from the non-oxygenic photosynthetic bacteria (Codd and Marsden 1984) is consistent with this hypothesis. There is little other data to support this claim though. In fact, increasing the oxygen tension did not result in an increased carboxysomal component of Rubisco in *T. neapolitanus* as might have been expected if these structures act to "protect" Rubisco from oxygen (Beudeker et al. 1981).

Air-grown and high DIC cells of *Synechococcus* had low numbers of carboxysomes. Furthermore, carboxysomes in these cells were positioned more or less randomly throughout the centropalasmic region (Figs. 2-6). In these cells, DIC is not such a limiting resource and it is possible that a CO<sub>2</sub> scavenging mechanism could deal with any CO<sub>2</sub> that is leaked, thereby ensuring that a high internal DIC pool is maintained. Moreover, these cells are not faced with the need to synthesize large numbers of carboxysomes, a costly prospect since Rubisco must be packaged repeatedly and proteins that constitute the carboxysome shell must be produced. In contrast, the increased efficiency in utilizing the accumulated pool of DIC that may be realized by increasing carboxysome

numbers might be necessary to ensure the competitiveness of cells growing in environments where DIC levels are extremely low.

### **Acknowledgements**

We are grateful to Dr. J. Fleck (CNRS, Strasbourg, France) and to Dr. G.A. Codd (University of Dundee, Dundee, UK) for providing the antisera used in this study. We also thank Dr. B. Colman (York University, Toronto) who provided access to the gas chromatograph and Dr. C.E. Smith (McGill) for use of the MOP digital analyzer. The technical assistance of Ms. R. Kandasamy is kindly acknowledged. This research was supported by the Natural Sciences and Engineering Research Council of Canada. In addition, R.M.L. McKay acknowledges support through a NSERC postgraduate scholarship.

CHAPTER VI

Intrapyrenoid thylakoids: a paradox?

## 1.0. Introduction

Inconsistent with the proposal that the pyrenoid provides a microenvironment where the  $\text{CO}_2/\text{O}_2$  ratio is maintained at a high level is the observation that thylakoid membranes traverse the pyrenoids of a number of algal species (Griffiths 1970). Conceivably, it might be difficult to reconcile the maintenance of a high  $\text{CO}_2/\text{O}_2$  ratio in the pyrenoid in the presence of  $\text{O}_2$  evolution contributed by intrapyrenoid thylakoids. This apparent paradox can be addressed in several ways. Although thylakoid lamellae are often observed to dissect pyrenoids, overall, these thylakoids probably contribute little to chloroplast oxygen levels due to the fact that there are many fewer lamellae in the pyrenoid than in the chloroplast proper. Furthermore, intrapyrenoid thylakoids are often found to be structurally reduced. In a survey of the pyrenoids of different algal groups, Gibbs (1960, 1962a, 1962b) noted that intrapyrenoid lamellae often consisted of only one or two thylakoids. In contrast, thylakoids observed throughout the remainder of the chloroplast are often grouped as two, three or more per lamella. In addition, thylakoids in several green algal species were observed to be reduced to tubule-like structures within the pyrenoid (Gibbs 1962b, Griffiths 1970). In addressing the structural irregularity often observed with intrapyrenoid thylakoids, Gibbs (1962a) speculated that these thylakoids may be characterized as containing reduced amounts of chlorophyll. Moreover, she cites several studies where chlorophyll fluorescence originating from the pyrenoid region was found to be

markedly reduced or absent when compared to that originating from other chloroplast regions

Using cytochemical and immunocytochemical techniques, we have begun to characterize further intrapyrenoid thylakoids. Our main focus has been to elucidate the protein composition of these thylakoids, and, in addition, to assess qualitatively their photosynthetic activity. Photosystem I activity can be demonstrated at the electron microscope level by the photooxidation of 3,3'-diaminobenzidine (DAB) to an insoluble, osmiophilic polymer. Diaminobenzidine has proven to be a rather versatile reagent, having been employed routinely for the cytochemical localization of catalase activity in microbodies and cytochrome *c* activity in mitochondria (see Frederick 1987, for review). Its ability to stain higher plant thylakoid lamellae was first demonstrated by Nir and Seligman (1970). These investigators observed thylakoid staining in the presence of the PSII inhibitor 3-(3,4-dichlorophenyl)-1,1-dimethyl urea (DCMU), thereby suggesting that DAB photooxidation may be related to PSI activity. Further evidence relating the photooxidation of DAB to PSI was provided by Chua (1972) who demonstrated that in the presence of DCMU, electron flow from diaminobenzidine through PSI to the artificial electron acceptor methyl viologen was realized by a *Chlamydomonas* PSII mutant but not by a PSI mutant strain. Further evidence of the specificity of the reaction for PSI is outlined in a recent review by Vaughn (1987c)

Photosystem II can also be detected cytochemically at the electron microscope level. Activity is demonstrated by the photoreduction of one of several tetrazolium salts which yield osmiophilic diformazans upon

reduction (see Vaughn 1987c, for review) Staining of thylakoid lamellae is prevented by PSII inhibitors such as DCMU and atrazine thus indicating specificity for the PSII reactions.

### 1.1 *Light-harvesting and photosystem complexes*

Our renewed interest in intrapyrenoid thylakoids was initially generated from the observation that the thylakoid lamellae which traverse the pyrenoid of the red alga *Porphyridium cruentum* appear distinct from thylakoids of the chloroplast proper in that they seem to lack phycobilisomes. We speculated that phycobilisomes might actually be present in this region but were obscured in micrographs by the electron opacity of the pyrenoid matrix. Immunolabelling results, however, confirmed their absence (McKay and Gibbs 1990; see also Chapter VII). Moreover, cytochemical staining indicated the presence of PSI, but not PSII activity, associated with *Porphyridium* intrapyrenoid thylakoids. Lack of PSII activity and its associated O<sub>2</sub>-evolution might provide a means to reconcile maintenance of a high CO<sub>2</sub>/O<sub>2</sub> ratio in the pyrenoid in the presence of intrapyrenoid thylakoids.

The cryptomonad algae also possess phycobiliproteins. However, unlike cyanobacteria and red algae, cryptomonad biliproteins are not arranged into phycobilisomes. Rather, they appear to be localized in the thylakoid lumen with a fraction of the phycobiliproteins associated with the inner thylakoid membrane (Ludwig and Gibbs 1989; Spear-Bernstein and Miller 1989). Although all cryptomonad chloroplasts contain pyrenoids, in only two genera, *Hemiselmis* and *Chroomonas*, are thylakoid lamellae observed to traverse the pyrenoid (Santore 1984). In

contrast to results obtained with the red alga *P. cruentum*, cryptomonad intrapyrenoid thylakoids are immunolabelled by anti-phycocerythrin and by antiserum directed against a subunit of the light-harvesting chl *a/c* complex (McKav et al. 1991b). These results are discussed in greater detail in Chapter VIII.

We have further extended our investigation of intrapyrenoid thylakoids to the diatom *Phaeodactylum tricornutum*. The chloroplasts of diatoms and other chromophytes are characterized by lamellae made up of three thylakoids. However, only a single pair of thylakoids traverse the pyrenoid of *P. tricornutum* (Borowitzka and Volcani 1978). The diatoms have, as their major light-harvesting pigment-protein complex, a chl *a/c*-fucoxanthin complex (Owens 1988) and in *P. tricornutum*, this is composed of three polypeptides of 18, 19 and 19.5 kDa (Fawley and Grossman 1986). Antiserum raised against a mixture of the 19 and 19.5 kDa polypeptides immunoreacted with all thylakoid lamellae of *Phaeodactylum*, including the intrapyrenoid thylakoids (Appendix 4). In addition, the intrapyrenoid thylakoids of *Phaeodactylum* are immunolabelled by anti-PSI (Appendix 4).

The intrapyrenoid thylakoids of *Euglena gracilis* also possess light-harvesting pigments. Osafune et al. (1990a) have recently shown using the immunogold technique that antiserum raised against a 26.5 kDa polypeptide of the light-harvesting chl *a/b* complex isolated from *Euglena* labels all thylakoid lamellae including the thylakoid pairs observed to traverse the pyrenoids of this alga. Similar to *Phaeodactylum*, however, the intrapyrenoid thylakoids of *Euglena* are structurally reduced. The thylakoids of the chloroplast proper occur as

lamellae of three or more discs, whereas those that traverse the pyrenoid are present as pairs of thylakoids (Gibbs 1960).

Intrapirenoic thylakoids, when present, in green algae usually exhibit a reduced number of thylakoids per lamella or appear as tubule-like structures (Gibbs 1962a; Griffiths 1970; Dodge 1973). However, the thylakoid lamellae of the chloroplast proper can exhibit a stacking phenomenon similar to that observed in higher plants with membranes existing as both unstacked thylakoids or as part of small grana-like units. Moreover immunocytochemical results employing *Chlamydomonas reinhardtii* indicate that a lateral heterogeneity exists with respect to the distribution of photosystem-associated polypeptides among these thylakoids. In *Chlamydomonas*, PSII core polypeptides and polypeptides involved in oxygen evolution have been localized to stacked membrane regions (Vallon et al. 1986, de Vitry et al. 1989) whereas a PSI apoprotein and chloroplast ATPase coupling factor 1 appear to be restricted in their distribution to unstacked thylakoids (Vallon et al. 1986). Given the lateral heterogeneity with respect to photosystem distribution as observed in this alga, it follows that PSII components should be excluded from the pyrenoid as this region is generally devoid of membrane stacks. This is supported by immunolabelling results which demonstrate that antiserum raised against subunit 1 of the oxygen-evolving enhancer (OEE1) does not label the pyrenoid of *C. reinhardtii* (de Vitry et al. 1989). Furthermore, the pyrenoid of this alga was not specifically labelled by antiserum raised against several PSII intrinsic core polypeptides (D2, P5) (J. Olive, pers. comm.). Similarly, the single thylakoid lamellae which traverse the pyrenoid of the hornwort

species *Notothylas orbicularis* exhibit only PSI activity whereas in other hornwort species in which the pyrenoid is dissected by large regions of stroma containing both single lamellae and small grana stacks, both PSI and PSII activity are observed associated with the thylakoids (K Vaughn, pers. comm )

It appears then that through a reduction in number, or absence, of PSII activity, intrapyrenoid thylakoids probably contribute little to O<sub>2</sub> levels within the pyrenoid.

### 1.2. Polyphenol oxidase

Cytochemistry has also been employed to investigate the occurrence of polyphenol oxidase (PPO) activity in the chloroplasts of pyrenoid-containing organisms. Cytochemical detection of PPO activity involves the oxidation of dihydroxyphenylalanine (DOPA) to an electron-dense diquinone polymer (Vaughn 1987b). Although the physiological function(s) of PPO remain(s) unclear, it has been proposed that it may be involved in the dissipation of excess molecular oxygen during photosynthesis (Vaughn et al. 1988). Polyphenol oxidase has a low affinity for O<sub>2</sub>, however, during photosynthesis, the luminal oxygen concentration can reach 1 mM. Thus, at high levels of O<sub>2</sub>, PPO could function in the reduction of molecular oxygen. The species distribution of PPO, however, appears to correlate phylogenetically with the evolution of terrestrial plants (Sherman et al. 1989). Polyphenol oxidase was not detected in a variety of green algae (*Chlorella*, *Stigeoclonium*, *Microspora* and *Spirogyra*) or in the moss *Dicranium*. Enzyme activity was, however, readily detectable in liverworts,

hornworts and other lower and higher plants (Sherman et al 1989). Moreover, Vaughn and Owen (1989) report that in the hornwort *Phaeoceros laevis*, polyphenol oxidase activity is associated with all thylakoid lamellae except those which traverse the pyrenoid. These results have since been extended to two additional pyrenoid-containing hornworts (*Notothylas* and *Anthoceros*) and to *Coleochaete scutata*, a green alga belonging to the "bryophytan" line of evolution towards higher plants (K Vaughn, pers. comm.). Why PPO activity is absent from intrapyrenoid thylakoids is unclear. It is possible its absence may be a consequence of the cytochemical assay employed. The protocol involves tissue incubation in an oxygen-saturated solution of DOPA. Perhaps Rubisco, which exhibits a higher affinity for oxygen than does PPO, outcompetes PPO for the oxygen which enters the pyrenoid. As a result, PPO activity would not be detected associated with intrapyrenoid thylakoids. Alternatively, if, indeed, one function of PPO is to reduce excess molecular oxygen, its absence from the pyrenoid might reflect the maintenance of a low oxygen concentration in this region which in turn could be achieved by reduced rates of photosynthetic oxygen evolution associated with intrapyrenoid thylakoids as discussed previously. In this case, PPO would not be required in the pyrenoid.

I

CHAPTER VII

Phycoerythrin is absent from the pyrenoid of  
*Porphyridium cruentum*: photosynthetic implications

## Summary

The thylakoid lamellae which traverse the pyrenoid of the unicellular red alga *Porphyridium cruentum* (Agardh) Nageli appear to lack phycobilisomes. We have confirmed by immunoelectron microscopy that phycoerythrin (PE), an important structural component of the phycobilisomes of red algae, is absent from the pyrenoid. To characterize pyrenoid thylakoids further, EM cytochemical methods were employed to detect photosystem activity. Photosystem (PS) I activity was demonstrated in both stromal and pyrenoid thylakoids by the photooxidation of 3,3'-diaminobenzidine. In contrast, the localization of photoreduced distyryl nitroblue tetrazolium demonstrated that PSII activity was restricted to stromal thylakoids. The observed partitioning of PE and PSII activity within the plastid may be related to another observation, namely, the localization of nearly all ribulose-1,5-bisphosphate carboxylase/oxygenase (Rubisco; EC 4.1.1.39) within the pyrenoid of this alga. It is possible that the pyrenoid of *P. cruentum* functions as a specific metabolic compartment where CO<sub>2</sub> fixation is enhanced by the absence of photosynthetic O<sub>2</sub>-evolution.

## 1.0. Introduction

Photosynthetic accessory pigments function in the harvesting and transfer of excitation energy from absorbed solar radiation to the reaction center pigments of photosystems (PS) I and II through intermediary chlorophyll *a* molecules. Light-harvesting pigments may include chlorophylls, carotenes and xanthophylls, however, unique to the cyanobacteria, red algae and cryptomonads are the phycobiliproteins, a group of water-soluble, photosynthetic antenna pigments which absorb light of wavelengths that are poorly harvested by chlorophyll *a* (for a recent review, see MacColl and Guard-Friar 1987). In the cyanobacteria and red algae, phycobiliproteins are arranged into large pigment-protein complexes, named phycobilisomes, which are attached to the outer surface of the thylakoid membrane (Gantt 1980; Glazer 1982). Within these structures, the biliproteins are arranged in an energetically favourable pattern such that excitation energy can be transferred between molecules in a direction of decreasing energy levels, i.e. phycoerythrin → phycocyanin → allophycocyanin (Gantt et al 1976). From allophycocyanin, absorbed light energy is passed, probably by way of a 75-120 kDa "anchor" polypeptide (Gantt et al 1988), to the chlorophyll *a* molecules associated with PSII in the thylakoid membrane.

Morphological evidence for the close association between phycobilisomes and PSII has been obtained from both freeze-fracture microscopy and observations of isolated PSII-phycobilisome particles by transmission electron microscopy. Employing freeze-fracture techniques, Morschel and Muhlethaler (1983) and Giddings et al (1983) have shown

that rows of putative PSII core particles associated with the exoplasmic face (EF) of freeze-fractured thylakoid membranes are directly aligned with rows of phycobilisomes located on the outer membrane surface. Photosystem II-phycobilisome particles have been isolated from cyanobacteria and the red alga *Porphyridium cruentum*. In *P. cruentum*, the particles possess high rates of O<sub>2</sub> evolution and consist of several phycobilisomes attached to small membrane fragments (Clement-Metral et al 1985). These membrane fragments are enriched in PSII reaction-center polypeptides, deficient in PSI components, and contain no detectable chlorophyll P<sub>700</sub>.

The thylakoids of both cyanobacteria and red algae are unstacked and, as a general rule, when cells are growing in the light under unstressed conditions, phycobilisomes, if adequately preserved by the fixation procedure, are present on every thylakoid. An apparent exception to this observation are the thylakoids that traverse the pyrenoids of red algal chloroplasts. In published micrographs of the pyrenoids of *Porphyridium cruentum* (e.g. Gantt and Conti 1965), *P. aeruginosum* (Gantt et al 1968) and *Porphyra leucosticta* (Sheath et al., 1977), phycobilisomes appear to be restricted to thylakoids located within the chloroplast stroma and to be absent from thylakoids within the pyrenoid. However, in most algae, the pyrenoid matrix is very electron-dense and in electron micrographs appears darker than the adjacent chloroplast stroma. It is possible, therefore, that the dense matrix material of the pyrenoid obscures any phycobilisomes that might be present. The only authors who, to our knowledge, have commented on whether phycobilisomes are present in the pyrenoid report that

phycobilisomes are present, but not abundant, on the convoluted thylakoids of the pyrenoid of *Rhodella cvanea* (Billard and Fresnel 1986). Furthermore, the published micrographs of *Nemalion* (Sheath et al 1979; Brawley and Wetherbee 1981) indicate that phycobilisomes are also present on the pyrenoid thylakoids of this alga

To determine whether or not phycobiliproteins are present in the pyrenoids of red algae, we have studied the distribution of phycoerythrin in the plastid of *Porphyridium cruentum* by immunoelectron microscopy. We find that phycoerythrin is not present in the pyrenoid, and furthermore that the intrapyrenoid thylakoids display normal PSI activity but lack PSII activity. We discuss these findings with reference to another observation, namely the localization of nearly all the plastid's ribulose-1,5-bisphosphate carboxylase/oxygenase (Rubisco, EC 4.1.1.39) within the pyrenoid.

## **2.0. Materials and Methods**

### *2.1. Plant material*

*Porphyridium cruentum* (Agardh) Nageli was obtained from the Culture Collection of Algae at the University of Texas at Austin (UTEX 161) and grown in batch culture in an artificial seawater medium (Jones et al 1963). Cultures were maintained at 20°C and were continuously agitated by use of a rotary shaker. Light was provided by cool-white fluorescent lamps (Sylvania F72T12/CW/H0, Roy Marchand Ltd, Laval, P Q, Canada) at a fluence rate of 30  $\mu\text{mol} \cdot \text{m}^{-2} \cdot \text{s}^{-1}$  in 16 h light/ 8 h dark cycles

## 2.2 Immunoelectron microscopy

Logarithmic phase cells of *P. cruentum* were harvested at h 3 of the light period. Cell pellets were fixed at 4°C for 1 h in a solution containing 4% (v/v) paraformaldehyde and 0.8% (v/v) glutaraldehyde in phosphate-buffered saline (PBS), pH 7.1. The pellets were washed with cold buffer and the cells dehydrated through a graded ethanol series and embedded in Lowicryl K4M (J.B. EM Services, Montreal, P.Q., Canada) as described in Lacoste-Royal and Gibbs (1985). Gold-coloured sections were cut with a diamond knife and mounted on formvar-coated nickel grids (J.B. EM Services). For immunolabelling, grids were placed section-side down on drops of the following solutions: PBS, 15 min; 1% (w/v) bovine serum albumin (fraction V) (BSA) in PBS, 15 min; antiserum, 30 min; PBS rinse, 1% BSA in PBS, 15 min; protein A-gold diluted 1:10, 30 min; PBS rinse, de-ionized water rinse. Rabbit antiserum against PE 545 purified from the cryptomonad alga *Rhodomonas lens* was kindly provided by Robert MacColl (New York State Department of Health, Albany, NY, USA) and was used at a dilution of 1:5000. Antisera to sodium dodecyl sulfate dissociated large (LS) and small subunits of tobacco Rubisco were kindly provided by Jacqueline Fleck (Institut de biologie moleculaire et cellulaire, CNRS, Strasbourg, France) and were used at a dilution of 1:2000. Antisera and protein A-gold were diluted in 1% BSA in PBS. Colloidal gold was prepared according to the method of Frens (1973) and was conjugated to protein A (Pharmacia, Dorval, P.Q. Canada) as described previously (Roth et al. 1978). Immunolabelled sections were post-stained with 2% (w/v) aqueous uranyl acetate and viewed in a Philips (Eindhoven, The Netherlands) EM410 electron microscope at an

operating voltage of 80 kV

In control experiments, the antibody was replaced with rabbit non-immune immunoglobulin G, or with PBS alone, prior to protein A-gold incubation.

### 2.3 Quantitative evaluation

The density of labelling over various cell compartments was obtained by determining the number of gold particles per square micrometre of compartment sectioned. Area determinations were made using a Zeiss (New York, NY, USA) MOP-3 digital analyser.

### 2.4. Cytochemical detection of PS activity

Log phase cells of *P. cruentum* were harvested at hours 4 or 6 of the daily light period and treated to detect PS activity essentially as described in Vaughn and Outlaw (1983) and Vaughn (1987). Cell pellets were fixed in 2% (v/v) paraformaldehyde in 0.1 M sodium-phosphate buffer, pH 7.4, containing 0.2 M sucrose, for 20 min at 4°C in darkness (darkness and low temperature were maintained in all steps prior to resin infiltration except as noted). The pellets were washed in buffer through a decreasing sucrose gradient and then incubated with a reagent solution specific for each PS. Photosystem I activity was detected by the photooxidation of 3,3'-diaminobenzidine·4HCl (DAB) (Polysciences, Warrington, Penn., USA), whereas PSII activity was demonstrated by the photoreduction of distyryl nitroblue tetrazolium chloride (DS-NBT) (Analychem Corp., Markham, Ont., Canada). Both reagents were used at a concentration of 1 mg ml<sup>-1</sup> in 0.1 M sodium-phosphate buffer, pH 7.4.

The DS-NBT solution contained, in addition, 0.5% (v/v) dimethyl sulfoxide to aid in solubilization of the tetrazolium salt. For PS localization, cells suspended in freshly prepared reagent solution were incubated on a rotary shaker at 20°C under cool-white fluorescent lamps providing a fluence rate of 30  $\mu\text{mol m}^{-2}\cdot\text{s}^{-1}$  for either 1 h (DAB oxidation) or 45 min (DS-NBT reduction). Controls were performed by either incubating the cells in darkness at 20°C or, in the case of DS-NBT treatment, by pretreating and incubating with the PSII inhibitor atrazine (gift from Ciba-Geigy, Dorval, P.Q., Canada; provided under the commercial name Aatrex and used at a concentration of 5.4  $\mu\text{g}\cdot\text{ml}^{-1}$ , see Appendix 3). Following incubation, the pellets were washed with buffer and then postfixed in either 1% (v/v)  $\text{OsO}_4$  in 0.1 M sodium cacodylate, pH 7.4, for 70 min at 4°C (DAB-treated cells) or in cacodylate-buffered 2%  $\text{OsO}_4$  for 90 min at room temperature (DS-NBT-treated cells). The cell pellets were dehydrated through a graded ethanol series and then infiltrated and embedded in low viscosity epoxy resin (Spurr, 1969). Gold- and silver-coloured sections were mounted on formvar-coated copper grids and unstained sections were viewed in either a Philips EM200 or a Philips EM410 electron microscope at operating voltages of 60 and 80 kV, respectively.

### 3.0. Results

#### 3.1. Immunoelectron microscopy

The intracellular distribution of both the photosynthetic accessory

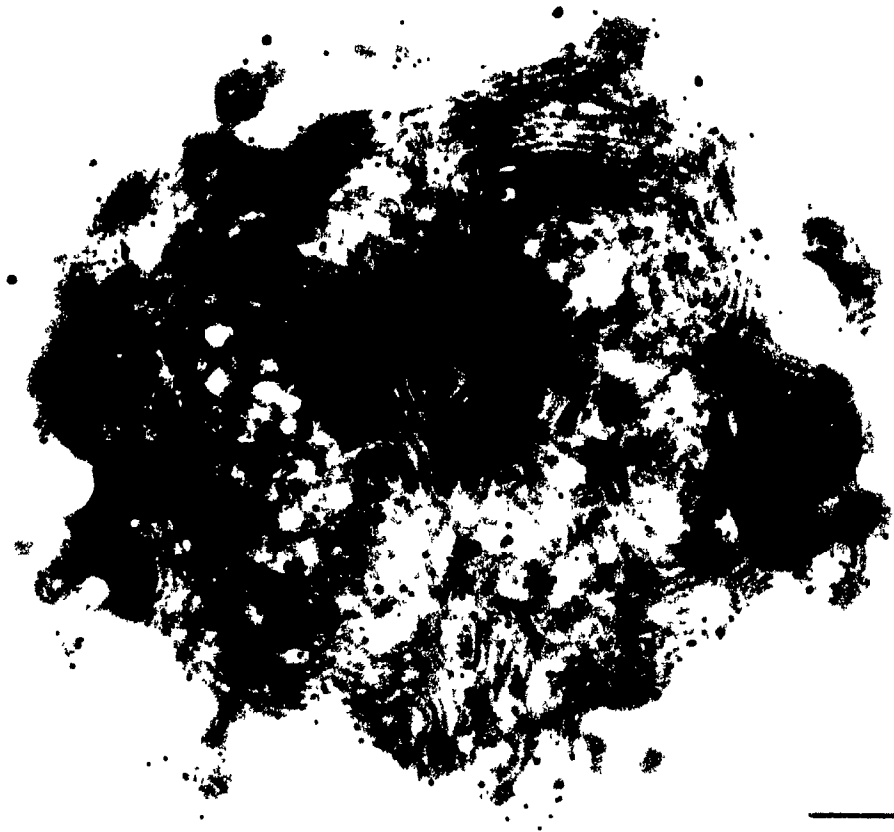
pigment PE and the Calvin-cycle enzyme Rubisco in cells of *Porphyridium cruentum* is shown in Figs. 1 and 2. Figure 1 shows a section through a log phase cell which has been labelled with anti-PE. Gold particles are abundant throughout the chloroplast stroma and are usually associated with the outer surfaces of the thylakoids. In contrast, the pyrenoid region is virtually label-free. Thus, PE, as visualized by protein A-gold labelling, does not appear to be associated with intrapyrenoid thylakoids.

Cell sections incubated with antiserum against the large subunit of Rubisco exhibit a different pattern of labelling (Fig. 2). Gold particles are highly concentrated over the pyrenoid region, whereas the remainder of the chloroplast shows only a few dispersed particles. Only a small amount of background labelling is present over the nucleus and cytoplasm. Sections labelled by antibody against the small subunit of Rubisco did not show the presence of any specific labelling (not shown), indicating that our antiserum against the small subunit, produced from a tobacco antigen, does not cross-react with the small subunit of Rubisco in *P. cruentum*.

A quantitative analysis of the density of labelling by each antibody over different cell and plastid compartments in *P. cruentum* showed that labelling by anti-PE was high over the chloroplast stroma ( $87.2 \pm 3.0$  particles  $\cdot \mu\text{m}^{-2}$ ) but over the pyrenoid region was not above background cytoplasmic labelling (Table 1). In contrast, the density of labelling by anti-Rubisco LS was very high over the pyrenoid matrix ( $196.6 \pm 7.2$  particles  $\cdot \mu\text{m}^{-2}$ ) but very low over the stroma ( $2.9 \pm 0.2$  particles  $\cdot \mu\text{m}^{-2}$ ). Stromal labelling, however, was significantly higher

Fig. 1. Log phase cell of *P. cruentum* labelled by anti-PE 545. Gold particles are abundant throughout the chloroplast stroma, usually associated with the outer surface of the thylakoids. The pyrenoid (py), which is traversed by numerous thylakoid lamellae, remains virtually label-free. Bar = 0.5  $\mu$ m.

B



—

B

**Fig. 2.** Log phase cell of *P. cruentum* labelled by anti-Rubisco LS  
Gold particles are highly concentrated over the pyrenoid (pv) whereas  
the chloroplast stroma displays a very low level of labelling, similar  
to that observed over the nucleus (n) and cytoplasm. A small, electron-  
dense region located at the chloroplast's periphery (arrowhead) is also  
moderately labelled and may represent a satellite pyrenoid  
mitochondrion (m) Bar = 0.5  $\mu$ m.



m

n



Table 1. Density of labelling over various cell compartments of *Porphyridium cruentum*.

	Chloroplast		Cytoplasm <sup>a</sup>	Nucleus <sup>b</sup>	$\gamma^c$
	Pyrenoid	Stromal region			
	gold particles $\mu\text{m}^{-2} \pm \text{SE}$				
Phycocerythrin					
Anti-PE 545	1.6 $\pm$ 0.3	87.2 $\pm$ 3.0	1.6 $\pm$ 0.2	1.1 $\pm$ 0.6 (9)	24
Rubisco					
Anti-LS	196.6 $\pm$ 7.2	2.9 $\pm$ 0.2	0.9 $\pm$ 0.2	2.0 $\pm$ 0.9 (4)	20
Controls					
Nonimmune IgG	0.3 $\pm$ 0.2	0.9 $\pm$ 0.2	0.8 $\pm$ 0.2	1.9 $\pm$ 0.9 (6)	14
Protein A-gold alone	0.8 $\pm$ 0.4	0.7 $\pm$ 0.1	0.3 $\pm$ 0.1	1.1 $\pm$ 0.7 (6)	14

<sup>a</sup> Includes mitochondria and starch

<sup>b</sup> No. of nuclei examined in ( )

<sup>c</sup> No. of cell sections analyzed

than background cytoplasmic labelling (one tailed paired *t*-test,  $P < 0.005$ )

Control experiments were performed by replacing the antiserum with either non-immune rabbit immunoglobulin G or phosphate-buffered saline alone, followed by protein A-gold (Table 1, see also Appendix 2). For each control, labelling densities were low over the thylakoid compartment analyzed. In addition, the specificity of the anti-Rubisco LS and anti-PE 545 used in this study, to their corresponding antigens, has been demonstrated by Mangenev and Gibbs (1987, see also Chapter 4) and Ludwig and Gibbs (1989).

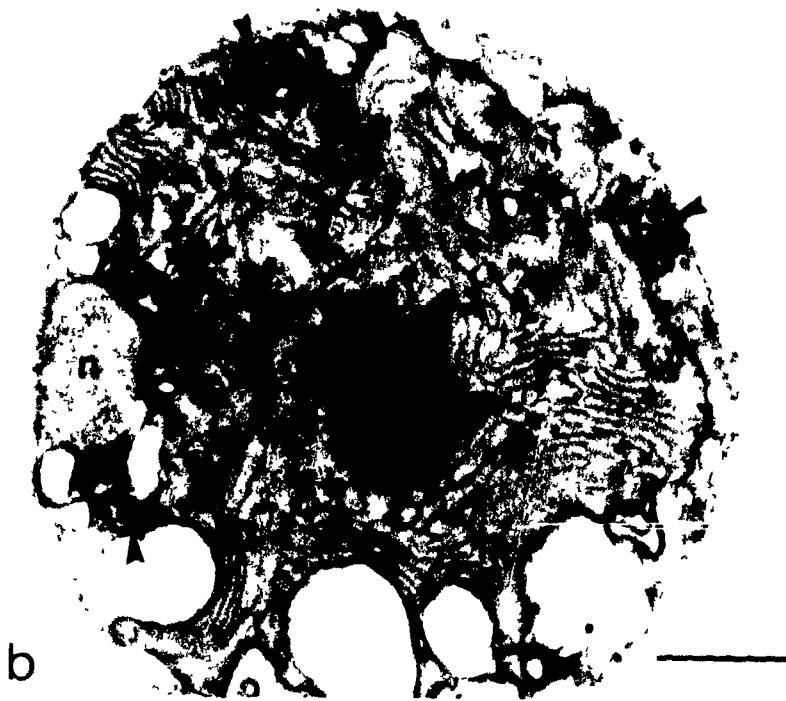
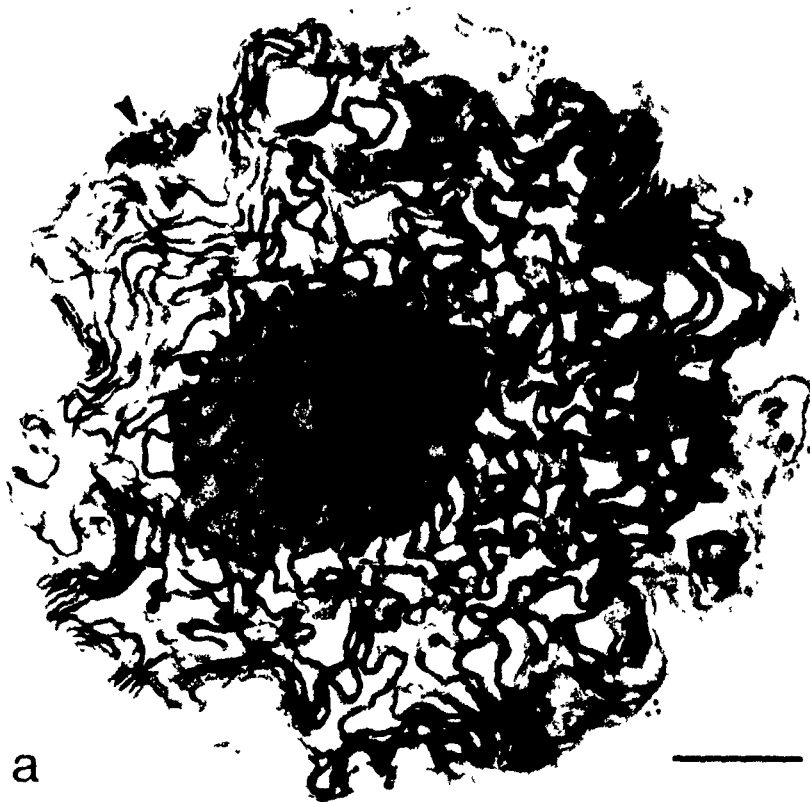
### 3.2 Cytochemical detection of PSI

Using photooxidation of DAB to demonstrate PSI activity within the chloroplast of *P. cruentum*, we found an electron-dense polymer to be associated with all of the thylakoids of the plastid, including those which traverse the pyrenoid (Fig. 3a). The dense material was deposited within the lumens of most thylakoids, however, where stromal thylakoids were swollen, the polymer appeared associated only with the membrane.

In addition to thylakoids, the mitochondrial cristae and envelope were often stained (Fig. 3a). This has been observed previously (Seligman et al. 1968, Marty 1977, Vaughn and Outlaw 1983) and is indicative of cytochrome-oxidase activity.

In control cells incubated in DAB in the dark, mitochondria retained the dense staining whereas chloroplast thylakoids were largely unstained (Fig. 3b). In the chloroplast, electron-dense deposits were restricted to small segments of only a few thylakoids.

**Figs. 3a,b.** Cytochemical localization of PSI activity in log phase cells of *P. cruentum*. Bars = 1  $\mu\text{m}$ . **a.** Cell incubated in DAB in the light. The electron-dense deposits produced by the photooxidation of DAB are associated with all chloroplast thylakoids including those which traverse the pyrenoid. Mitochondrial membranes are also stained (arrowhead). **b.** Control cell incubated in DAB in the dark. The chloroplast thylakoids are largely unstained whereas mitochondrial membranes retain their electron-dense deposits (arrowheads).



### 3.3 Cytochemical detection of PSII

Photosystem II activity was detected by the photoreduction of DS-NBT to diformazan. Reduction of the tetrazolium salt was visually monitored through a change in colour of the cell suspension from red to dark purple or black. This colour change is characteristic of the photoreduction of tetrazolium salts and was initiated within 1-2 min of incubation in the light. In cell sections, diformazan was localized in the lumens of stromal thylakoids but was absent from intrapyrenoid thylakoids (Fig. 4a). In thylakoids which extend from the chloroplast stroma into the pyrenoid region the luminal electron-dense deposits stopped abruptly at the pyrenoid border (Fig. 4a, arrowheads).

Cell suspensions incubated in the dark or in the presence of the PSII inhibitor atrazine did not change colour during incubation. In the atrazine-treated cell in Fig. 4b, the thylakoids do not possess electron-dense deposits. Darkly stained regions are limited mainly to areas of the chloroplast envelope (Fig. 4b, arrows). In addition, scattered osmiophilic globules are present in the plastid. These have been observed previously (Seligman et al. 1971) and are not considered to represent photoreduced DS-NBT.

## 4.0. Discussion

### 4.1. Absence of PE and PSII activity in the pyrenoid

We have demonstrated that the intrapyrenoid thylakoids of the red alga *Porphyridium cruentum* are not labelled by anti-PE although a high level

**Figs. 4a,b.** Cytochemical localization of PSII activity in log phase cells of *P. cruentum*. Bars = 0.5  $\mu$ m. **a.** Cell incubated in DS-NBT in the light. Electron-dense deposits resulting from photoreduction of DS-NBT are found in the lumens of most stromal thylakoids but not in the pyrenoid thylakoids. In thylakoids which extend from the chloroplast stroma into the pyrenoid, the luminal electron-dense deposits end abruptly at the pyrenoid border (arrowheads). **b.** Control cell incubated in DS-NBT in the light in the presence of atrazine. Dense product is not present in the thylakoids, many of which are greatly swollen. However, some regions of the chloroplast envelope are stained (arrows).



a



b

of labelling is associated with the thylakoid lamellae outside the pyrenoid. Phycocerythrin is the major component of the phycobilisomes of *P. cruentum*, accounting for more than 70% of their total protein (Gantt 1986). This pigment-protein complex occupies a peripheral position in the numerous rods which radiate out from the central allophycocyanin core of *P. cruentum* phycobilisomes (Gantt and Lipschultz 1977). Our data do not rule out the possibility of other phycobiliproteins being present in the pyrenoid of *P. cruentum*, however, since phycobilisomes of this species always contain PE, we conclude that there are no phycobilisomes attached to the thylakoids which traverse the pyrenoid of this alga. This confirms the visual impression given by the published micrographs of this species (e.g. Gantt and Conti 1965).

In addition, we observed that diformazan resulting from the photoreduction of DS-NBT was restricted to the stromal thylakoids. This indicates that PSII activity in the intrapyrenoid thylakoids is either markedly reduced or entirely absent. Lev and Butler (1977) have reported that upwards of 95% of the light excitation energy trapped by the phycobilisomes of *P. cruentum* is initially transferred to PSII. Thus, since phycobilisomes in the pyrenoid of *P. cruentum* are absent, the only energy that would be transferred to PSII complexes in the thylakoid membranes would be that trapped by the small number of chlorophyll *a* molecules associated with these reaction centers. Thus one would expect PSII activity in the pyrenoid to be much reduced.

A further contributing factor to the low PSII activity observed in the intrapyrenoid thylakoids might be a deficiency of PSII complexes associated with the EF faces of these thylakoids. In the cryptomonad

algae, where PE is attached to the lumenal surface of the thylakoid membrane (Lichtle et al. 1987; Ludwig and Gibbs 1989). Rhiel et al. (1985) and Lichtle et al. (1986) have shown that when the phycobiliprotein content of cells grown in high light is reduced by 90% or 50%, there is a corresponding reduction in the number of EF particles (the putative PSII complexes) located on the thylakoid membranes. In freeze-fracture studies of the chloroplast of *P. cruentum* (Neushul 1970; 1971), the EF face of the pyrenoid thylakoids is not identified. Clearly, additional freeze-fracture studies or, alternatively, immunocytochemical studies using antibodies against PSII polypeptides are needed in order to determine whether pyrenoid thylakoids are deficient in PSII complexes or whether the absence of PSII activity results solely from the lack of PSII light-harvesting antennae pigments.

#### 4.2. Photosystem I activity in the pyrenoid

Photosystem I activity was detected through the photooxidation of DAB. The resulting electron-dense reaction product was found associated with all thylakoid lamellae including those which traverse the pyrenoid. The staining of intrapyrenoid thylakoids is believed to be genuine. It seems unlikely that reaction products have secondarily migrated into the pyrenoid region since the oxidized polymer of DAB is highly insoluble and is assumed to remain close to the site of its formation (Frederick 1987). Oakley and Dodge (1974) have similarly observed DAB reaction product associated with the pyrenoid thylakoids in *P. cruentum*. These findings indicate that the pyrenoid thylakoids may be capable of cyclic photophosphorylation mediated by PSI. There would be little non-cyclic

photophosphorylation or  $O_2$  evolution associated with intrapyrenoid thylakoids. However

#### 4.3 Rubisco and pyrenoids

The apparent intracellular compartmentation of biliproteins and PSII activity observed in *P. cruentum* in the present study may be related to pyrenoid function. At present, the role of pyrenoids is not established; however, owing to their plastidic location, they are likely to be involved in photosynthesis. Evidence supporting this comes from biochemical and immunocytochemical reports all of which indicate that pyrenoids of various species of algae contain the bifunctional Calvin-cycle enzyme Rubisco (for references, see McKay and Gibbs 1989, see also Chapter I). In this study we have established that Rubisco is also present in the pyrenoid of *P. cruentum*. The large subunit of Rubisco was highly concentrated in the pyrenoid of this alga whereas stromal levels of the enzyme were only slightly, although significantly, above background cytoplasmic levels (Table 1).

Whether pyrenoid Rubisco is active in vivo is not known. Some studies indicate that the pyrenoid represents a storage pool of the enzyme (Lacoste-Royal and Gibbs 1987), whereas others indicate that the pyrenoid functions as a specific metabolic compartment where  $CO_2$  fixation is initiated (Miyachi et al. 1986, Kuchitsu et al. 1988; McKay and Gibbs 1989; see also Chapter I). The absence of phycobilisomes and PSII activity in the pyrenoid of *P. cruentum* indicates that there would be negligible  $O_2$  evolution within the pyrenoid. Although diffusion of  $O_2$  into the pyrenoid from the surrounding chloroplast stroma would

occur, conceivably the  $O_2$  tension in the pyrenoid might be lower than that in the adjacent stroma. In addition, cells of *P. cruentum* grown in low  $CO_2$  have been shown to take up and utilize dissolved inorganic carbon with high efficiency in photosynthesis (Colman and Gehl 1983). The cells possess an intracellular carbonic anhydrase (Dixon et al. 1987) which has been shown to be located mainly in the chloroplast stroma (Yagawa et al. 1987). Thus conceivably, the microenvironment of the pyrenoid would be one of high  $CO_2$  and low  $O_2$  and this in turn would favour the carboxylation reaction of Rubisco.

#### **Acknowledgments**

We thank Drs. Jacqueline Fleck (CNRS, Strasbourg) and Robert MacColl (New York State Department of Health, Albany) for providing us with the antibodies used in this study. We also thank Dr. C.E. Smith for use of the Zeiss MOP-3 digital analyser and Dr. Geneviève Bricheux for kindly providing Lowicryl-embedded samples of *P. cruentum*. Aatrex was kindly donated by Ciba-Geigy. This research was supported by the Natural Sciences and Engineering Research Council of Canada (grant No. A-2921).

#### **Notes Added**

Several papers published subsequent to this manuscript are relevant to the interpretation of our findings. We were unable to obtain a cross-

reaction on tissue sections of *P. cruentum* using antiserum raised against Rubisco SS isolated from tobacco (section 3.1.). In support of this, Newman and Cattolico (1990) report that red algal Rubisco SS polypeptides show only minimal similarity (20-40% identity from derived amino acid sequences) to the same polypeptides found in terrestrial plants, green algae and cyanobacteria. Red algal Rubisco SS, however, is highly related (structurally, immunologically, kinetically) to its counterpart found in chromophyte algae (Newman et al. 1989).

Of perhaps greater relevance to our results, two immunolabelling studies performed on *P. cruentum* support our finding that PSII, but not PSI, is excluded from the intrapyrenoid thylakoids of this alga. The two studies, both originating from Gantt's laboratory, show that *P. cruentum* intrapyrenoid thylakoids are immunolabelled by antiserum raised against a 60 kDa PSI core-associated chlorophyll binding protein (Mustardy et al. 1990; Cunningham et al. 1991). In contrast, intrapyrenoid thylakoids are not marked by antisera raised against two phycobilisome proteins (allophycocyanin and a 91 kDa phycobilisome-thylakoid linker polypeptide) nor are they labelled by antisera directed against PSII core-associated proteins (D2 and a 45 kDa PSII core-chlorophyll binding protein). These results indicate that the lack of PSII activity observed in our investigation is due not only to the absence of PSII-associated light-harvesting antennae pigments, but also reflects the exclusion of PSII core complexes from intrapyrenoid thylakoids of *P. cruentum*. These investigators also report that *P. cruentum* intrapyrenoid thylakoids are not labelled by antiserum raised against the  $\beta$  subunit of ATP synthase. This observation casts some

doubt on our speculation that these thylakoids possess the capacity for PSI-mediated cyclic photophosphorylation (section 4.2.). Also, in both studies, the pyrenoid of *P. cruentum* was heavily labelled by anti-Rubisco LS (source: spinach). Label over the chloroplast stroma, as reported in our investigation, was low and present at a similar level as background.

Finally, it has recently come to our attention that thylakoid lamellae themselves might represent a site for dehydration of  $\text{HCO}_3^-$  to provide a source of  $\text{CO}_2$  (Moroney and Mason 1991). That  $\text{HCO}_3^-$  can be transported into the thylakoid lumen has been proposed by Semenenko and colleagues (as reviewed in Moroney and Mason 1991). It is anticipated that the  $\Delta\text{pH}$  across the thylakoid membrane generated by electron transport could drive the dehydration of  $\text{HCO}_3^-$ ; the pH of the thylakoid lumen is ~5. In this way, intrapyrenoid thylakoids could supply Rubisco localized in the pyrenoid with substrate  $\text{CO}_2$ .

**CHAPTER VIII**

Immunocytochemical characterization of the intrapyrenoid  
thylakoids of cryptomonads

## Summary

Thylakoid lamellae extend into the pyrenoids of only two genera of cryptomonad algae, *Chroomonas* and *Hemiselmis*. In the present investigation, we used the technique of immunoelectron microscopy to assess the photosynthetic competency of cryptomonad intrapyrenoid thylakoids. Intrapyrenoid thylakoids were shown to possess phycobiliproteins and the chlorophyll *a/c*<sub>2</sub> light-harvesting complex, both of which are associated with photosystem II in a light-harvesting capacity. In addition, thylakoids that extend into the pyrenoid of *Hemiselmis brunnescens* were immunolabelled by anti-photosystem I. These results indicate that cryptomonad intrapyrenoid thylakoids likely function in a manner analogous to thylakoids of the chloroplast stroma. Moreover, our observation that the Calvin cycle enzyme Rubisco is pyrenoid-localized in these cryptophytes indicates that the processes of photosynthetic O<sub>2</sub>-evolution and RuBP carboxylation/oxidation are not spatially separated in these algae.

## 1.0. Introduction

Investigations of algal fine structure indicate that thylakoid lamellae, apart from being present in the chloroplast stroma, are frequently observed to extend into the pyrenoid regions of algal chloroplasts (Griffiths 1970). Moreover, there is evidence to indicate that a structural (Gibbs 1960; 1962a, 1962b) and perhaps functional (McKay and Gibbs 1990; Mustardy et al. 1990; see also Chapter VII) heterogeneity exists between lamellae found in the chloroplast stroma and those localized in the pyrenoid. Thylakoid lamellae that extend into the pyrenoid of the red alga *Porphyridium cruentum* appear to lack phycobilisomes (see Figure 1 in Gantt and Conti 1965). Employing the technique of immunoelectron microscopy, we determined that phycoerythrin (PE), the major component of the light-harvesting phycobilisomes of this alga, was excluded from the pyrenoid (McKay and Gibbs 1990; see also Chapter VII). Moreover, we demonstrated by cytochemical staining that *P. cruentum* intrapyrenoid thylakoids do not possess photosystem (PS) II activity.

Like red algae, cryptomonads also possess light-harvesting phycobiliproteins (MacColl and Guard-Friar 1987). Moreover, it is postulated that cryptomonads may have arisen by way of a eukaryote-eukaryote endosymbiosis involving a unicellular red alga and a non-photosynthetic flagellate (Gillott and Gibbs 1980). Much of the evidence supporting this hypothesis has come from studies of cryptomonad fine structure. Apart from demonstrating the requisite membranes involved in the acquisition of a eukaryotic endosymbiont, these studies

also demonstrate the presence of the nucleomorph, a structure postulated to be the vestigial nucleus of the endosymbiotic ancestral red alga (Gillott and Gibbs 1980). Further support for this hypothesis has come recently from a study by Douglas et al. (1991) who cloned and sequenced separate nuclear and nucleomorph genes encoding functional 18S rRNA from *Cryptomonas*  $\phi$ . Their phylogenetic analysis shows the nucleomorph sequence to be closely related to nuclear sequences encoding 18S rRNA reported from two red algae (Bird et al. 1990). In view of our previous findings concerning the intrapyrenoid thylakoids of *Porphyridium* and of the proposed evolutionary proximity between red algae and cryptomonads, we have characterized the intrapyrenoid thylakoids of two cryptophytes using the technique of immunoelectron microscopy.

## 2.0. Materials and Methods

### 2.1. Algal Culture

*Hemiselmis brunnescens* Butcher (CCAP 984/2) was obtained from the Culture Collection of Algae and Protozoa, Freshwater Biological Association, Ambleside, Cumbria, UK, and was grown in f/2 medium (McLachlan 1973). *Chroomonas* sp. was isolated in 1977 from Lake Memphramagog, Québec, and has since been maintained in unialgal culture at McGill University. During this investigation, it was cultured in S<sub>2</sub>T<sub>2</sub> medium (Lichtlé 1979). Both cryptomonads were maintained in batch culture at 20°C, and cultures were continuously agitated by use of a rotary shaker. Light was provided by cool-white fluorescent lamps

(Sylvania F72T12/CW/H0) at a photon fluence rate of  $40 \mu\text{mol}\cdot\text{m}^{-2}\cdot\text{s}^{-1}$  in 16 h light/8 h dark cycles.

## 2.2. Immunoelectron Microscopy

Logarithmic-phase cells were harvested at h 4 of the light period and cell pellets were fixed at  $4^{\circ}\text{C}$  for 1 h in a solution containing 1% (v/v) glutaraldehyde buffered with either 100 mM sodium phosphate, pH 7.1, for *Chroomonas* sp., or 100 mM sodium cacodylate, pH 7.5, for *H. brunnescens*. The pellets were washed with cold buffer and the cells dehydrated through a graded ethanol series followed by infiltration with propylene oxide and embedding in JEMBED 812 resin (Epon 812 equivalent; J.B. EM Services, Montréal, Canada). In addition, some *Hemiseimis* cells were embedded in Lowicryl K4M resin (J.B. EM Services). These cells were harvested at h 1.5 of the light period and were fixed at  $4^{\circ}\text{C}$  for 1 h in a solution containing 4% (v/v) paraformaldehyde, 0.2% (v/v) glutaraldehyde and 600 mM sucrose in 100 mM sodium cacodylate, pH 7.0. The cells were dehydrated through a graded ethanol series and embedded in Lowicryl K4M as described in Lacoste-Royal and Gibbs (1985).

For immunolabelling, pale gold-coloured sections were cut with a diamond knife and mounted on formvar-coated nickel grids. The grids were placed section-side down on drops of the following solutions: phosphate-buffered saline (PBS), 15 min; 1% (w/v) bovine serum albumin (fraction V) (BSA) in PBS, 15 min; antiserum, 30 min to 2.5 h; PBS, 4x5 min; 1% BSA in PBS, 15 min; protein A-gold solution (O.D.<sub>525</sub>=1.6), 30 min; PBS, 3x5 min; deionized water rinse. The antisera and dilutions used are described in Table 1. Colloidal gold was prepared according to the

Table 1. Antisera employed in the present investigation.

Antibody	Host	Source of Antigen	Dilution		Reference
			Immunoblots	Immunocytochemistry	
anti-PE ( $\beta$ subunit)	rabbit	<u>Rhodomonas lens</u> (Cryptophyceae)	1:10 <sup>4</sup>	1:500	Guard-Friar et al. 1986
anti-chl a/c <sub>2</sub> LHC (19 kDa subunit)	rabbit	<u>Cryptomonas rufescens</u> (Cryptophyceae)	-----	1:80	Lichtlé et al. 1991a
anti-PSI	rabbit	<u>Zea mays</u>	1:600	1:200	-----
anti-Rubisco (large subunit)	rabbit	<u>Olisthodiscus luteus</u> (Raphidophyceae)	1:10 <sup>3</sup>	1:500	Newman et al. 1989

method of Frens (1973) and was conjugated to protein A (Analychem Corp., Markham, Ontario, Canada) as described previously (Roth et al. 1978). Alternatively, in some labelling experiments, a commercially obtained preparation of protein A-gold was used (15 nm gold; Intermedico, Markham). Antisera and protein A-gold were diluted in 1% BSA in PBS. Immunolabelled sections were post-stained with 2% (w/v) aqueous uranyl acetate and viewed in a Philips EM 410 electron microscope at an operating voltage of 80 kV.

In control experiments, the antibody was replaced with rabbit pre-immune serum, or with PBS alone, prior to protein A-gold incubation. No specific labelling of cell sections was observed (see Appendix 2).

### 2.3. Protein Extraction and Immunoblotting

Soluble protein extracts of *Chroomonas* and *Hemiselmis* were obtained by sonicating (Sonifier Cell Disruptor, Heat Systems Ultrasonics Inc., Plainview, NY, U.S.A.) freshly harvested cells suspended in a small volume of ice-cold extraction buffer (Lichtle et al. 1987) containing phenylmethylsulfonyl fluoride (PMSF). The resulting crude protein extracts were clarified by centrifugation in a microcentrifuge (Fisher model 235C) for 10 min at 4°C and polypeptides retained within the supernatant were used to determine the specificity of antiserum raised against the large subunit (LS) of Rubisco and of antiserum directed against PE 545.

The specificity of antiserum raised against sucrose gradient purified PSI from maize was determined from immunoblots of detergent-solubilized thylakoid membrane proteins of *H. brunnescens*. Cells

suspended in a small volume of ice-cold buffer A (50 mM Tris-HCl, pH 7.9, 300 mM sucrose, 20 mM MgSO<sub>4</sub>·7H<sub>2</sub>O, 0.25% (w/v) BSA) containing 1 mM PMSF were broken by sonication after which the protein extract was clarified by centrifugation (30 min, 4°C, 40,000 x g, Ti 70 l rotor, Beckman L8-70 ultracentrifuge). The supernatant, containing PE and other soluble proteins, was discarded. The pellet, consisting of sedimented cell membranes and debris, was resuspended in 5 ml of ice-cold buffer B (50 mM Tris-HCl, pH 7.9, 300 mM sucrose, 20 mM MgSO<sub>4</sub>·7H<sub>2</sub>O, 1 mM Na-EDTA) and homogenized in a chilled glass tissue homogenizer. The homogenate was diluted to 10 ml and then centrifuged first at 750 x g for 7 min (4°C, SS-34 rotor, Sorvall RC2-B centrifuge) to remove unbroken cells and debris and then again at 40,000 x g for 30 min to sediment membranes. The thylakoids were washed again in buffer B and then twice in buffer C (50 mM Tricine-NaOH, pH 7.3) following which they were resuspended in buffer C at a chlorophyll concentration of 100 µg chl ml<sup>-1</sup>. Thylakoid membranes were solubilized by treatment with 1% (v/v) Triton X-100 for 30 min at room temperature with stirring and were then sedimented by centrifugation. The pellet was discarded and the clear green supernatant, containing solubilized protein, was layered on top of a continuous 10 to 40% (w/v) sucrose gradient (10 ml) containing 0.03% Triton X-100 and centrifuged (16 h, 4°C, 165,000 X g, SW 41 rotor, Beckman L8-70 ultracentrifuge). Following centrifugation, the green pigmented fractions were removed and used for immunoblotting.

Polypeptides were separated essentially as described by Laemmli (1970) on 12% or 15% sodium dodecyl sulfate-containing polyacrylamide mini-gels and were transferred electrophoretically to nitrocellulose

filters (0.45  $\mu$ m; Bio-Rad Laboratories Ltd., Mississauga, Ontario) in transfer buffer (25 mM Tris, 192 mM glycine, 20% (v/v) methanol) at room temperature for 2 h at 60 V. Filters containing the blotted polypeptides were washed in tris-buffered saline (TBS; 10 mM Tris-HCl, pH 8.0, 150mM NaCl) for 30 min and then were blocked overnight at 4°C with 1 to 2% BSA in TBS containing 0.05% (v/v) Tween-20 (TBST). After blocking, filters were incubated at room-temperature in the following solutions: primary antiserum, 30 min to 2 h; TBST, 3x10 min; 1:10<sup>3</sup> goat anti-rabbit IgG-horseradish peroxidase (heavy and light chains; BIO/CAN Scientific Inc., Toronto, Canada), 30 min; TBST, 3x10 min; TBS, 10 min. Immunoreactive bands were visualized by incubating blots in a solution containing the chromogen 4-chloro-1-naphthol in TBS/methanol plus H<sub>2</sub>O<sub>2</sub>. The reaction was stopped by washing with deionized water. All antisera were diluted in TBST containing 1% BSA.

Protein was determined with the Bio-Rad protein assay kit using BSA as a standard and following the instructions provided by the manufacturers. Chlorophyll concentrations were determined using the equations for chlorophyll (chl) *c*-containing algae as described in Jeffrey and Humphrey (1975).

### **3.0. Results and Discussion**

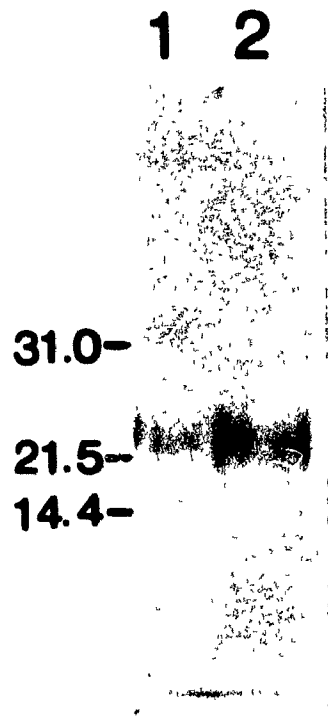
#### *3.1. Antisera Specificity*

Antisera raised against PE 545 and against Rubisco LS each cross-reacted with specific polypeptides in soluble protein extracts from *Chroomonas*

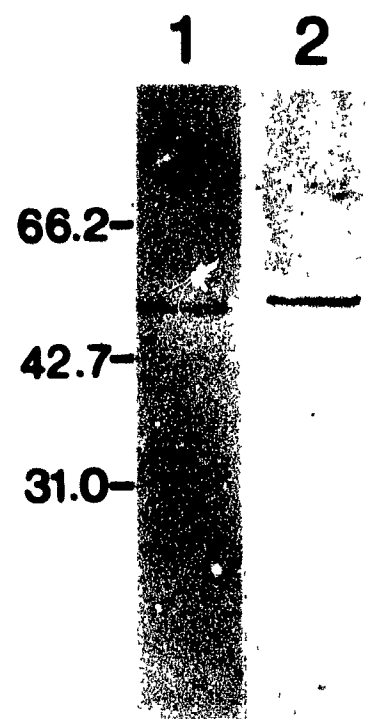
sp. and *Hemiselmis brunnescens* (Fig.1). Anti-PE 545 cross-reacted with a polypeptide having an apparent molecular mass of ~ 21 kDa in extracts from each cryptomonad (Fig. 1a); an observation of interest since *H. brunnescens* is a PE-containing alga (PE 555; Hill and Rowan 1989) whereas *Chroomonas* contains a phycocyanin (PC) as its biliprotein. Employing this same antiserum, Ludwig and Gibbs (1989) and Spear-Bernstein and Miller (1989) each reported antiserum recognition with a polypeptide of a similar size in extracts from the PE-containing cryptophyte *Rhodomonas lens* and concluded that the antibody specifically recognized the  $\beta$  subunit of PE. Our results with *Chroomonas*, however, extend this observation to include recognition between anti-PE 545 and the  $\beta$  subunit of PC. The immunorecognition between anti-PE 545 and PC was not unexpected. Unlike the biliproteins of cyanobacteria and red algae (Berns 1967), cryptomonad PE and PC are immunochemically related (Guard-Friar et al. 1986), the immunorecognition presumably being the result of a high amino acid identity between the  $\beta$  subunits of cryptomonad PE and PC ( Sidler et al. 1985). Antiserum raised against Rubisco LS cross-reacted with a polypeptide having an apparent molecular mass of ~52 kDa in extracts from each cryptomonad (Fig. 1b). The molecular size of the immunoreactive polypeptide is within the range of values reported previously for the LS of chromophyte Rubisco (Plumley et al 1986; Newman et al. 1989).

Polypeptide fractions obtained from sucrose gradient centrifugation of detergent solubilized thylakoid membrane proteins of *H. brunnescens* were used to determine the specificity of anti-PSI. Three chlorophyll-containing fractions were discernible following

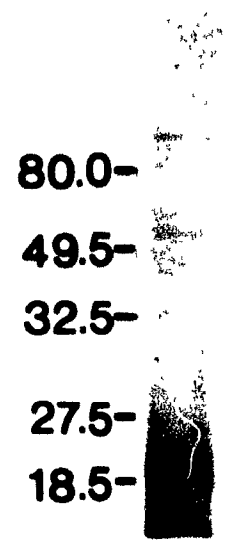
**Fig. 1.** Immunoblot characterization of antisera. Positions of molecular mass standards (in kDa) are shown. **a.** Soluble protein extracts of *Chroomonas* sp. (Lane 1) and *H. brunnescens* (Lane 2) incubated with anti-PE 545. In each lane, a single band having an apparent mass of ~21 kDa is stained. **b.** Anti-Rubisco LS recognizes a protein of ~52 kDa from soluble protein extracts of *Chroomonas* (Lane 1) and *Hemiselmis* (Lane 2). **c.** Detergent-solubilized membrane proteins derived from *H. brunnescens* were used to determine the specificity of anti-PSI. A diffuse staining band extending between 10 and 24 kDa likely represents several immunoreactive polypeptides. An immunoreactive band having an apparent mass of ~60 kDa is also prominent as are several bands of much higher mass.



a



b



c

centrifugation and were designated 1,2 and 3 depending on density, with fraction 3 being the most dense and fraction 1 the least dense. Anti-PSI recognized polypeptides from fraction 3. This is consistent with results from previous investigations using cryptomonads, all of which identify the most dense fraction from sucrose gradients as being enriched in PSI (Ingram and Hiller 1983; Lichtlé et al. 1987; Rhiel et al. 1987). The main reaction product was visible as a diffuse stained band, likely representing several polypeptides in the range of 10 to 24 kDa (Fig. 1c). Due to the conditions chosen for electrophoresis, these proteins were not well-resolved. A band in the range of 60 kDa was also stained. In addition, several bands of high molecular mass were stained and probably represent protein aggregates. From these results, it is likely that our polyclonal antiserum is directed against protein components of the PSI core complex. This complex includes two similar, but non-identical polypeptides of the PSI reaction centre in addition to a group of low mass polypeptides which in higher plants are designated subunits II-VII (Margulies 1989). The functions of these subunits have not yet been elucidated; however, they are required for electron transport through PSI.

Antiserum directed against the chl *a/c*<sub>2</sub> LHC was not characterized as part of the present investigation. It was raised against a 19 kDa apoprotein of the complex isolated from *Cryptomonas rufescens* and its specificity has been demonstrated previously (Lichtlé et al. 1991a).

### 3.2. Immunoelectron Microscopy

In cryptomonads, members of two genera possess intrapyrenoid thylakoids.

In *Hemiselmis*, the broadly-based, stalked pyrenoid is entered by a single pair of thylakoids (Santore 1982; 1984). In *Chroomonas*, several pairs of thylakoids may traverse the pyrenoid (Santore 1984; 1987; Hill 1991).

In order to assess the photosynthetic competency of cryptomonad intrapyrenoid thylakoids, we have employed in the present investigation, the technique of immunoelectron microscopy. Cryptomonads are unique among photosynthetic organisms in that they possess phycobiliproteins and chl  $c_2$ , both of which serve in a light-harvesting capacity, transferring excitation energy preferentially to PSII reaction centers (Lichtlé et al. 1980; Bruce et al. 1986; Biggins and Bruce 1989). Our results clearly demonstrate that in both the PE-containing *Hemiselmis brunnescens* and the PC-containing *Chroomonas* sp., phycobiliproteins (as shown by immunolabelling with anti-PE 545) are associated with all thylakoids, including those extending into the pyrenoid. In Figure 2, gold particles are clearly associated with thylakoids that cross the pyrenoid of *Chroomonas*. Similarly, an intrapyrenoid lamella of *H. brunnescens* is immunolabelled by anti-PE 545 (Fig 3). In both algae, thylakoids in the remainder of the chloroplast are also labelled. Previous studies have demonstrated that in cryptomonads, phycobiliproteins are localized within the thylakoid lumen (Gantt et al. 1971, Ludwig and Gibbs 1989, Spear-Bernstein and Miller 1989) and are not arranged into phycobilisomes as occurs in cyanobacteria and red algae.

Incubation of sections of Lowicryl-embedded *H. brunnescens* in anti-chl  $a/c_2$  LHC also confirms the association of this complex with the

**Figs. 2-7.** Sections through pyrenoids of *Chroomonas* sp. and *Hemiselmis brunnescens*. Bars = 0.25  $\mu$ m. **Figs. 2-3.** Epon-embedded cells immunolabelled by anti-PE 545. **Fig. 2.** Gold particles are found over thylakoids (arrowheads) extending into the pyrenoid (py) of *Chroomonas*. Thylakoids found in the remainder of the chloroplast are also labelled. **Fig. 3.** All thylakoids, including the single lamella that enters the pyrenoid of *H. brunnescens* are immunolabelled by anti-PE 545. **Figs. 4-5.** Lowicryl-embedded cells of *H. brunnescens*. **Fig. 4.** A single pair of thylakoids that traverse a small projecting pyrenoid are immunolabelled by anti-chl *a/c*<sub>2</sub> LHC. Thylakoids elsewhere in the chloroplast are also labelled. The nucleus (n) is unlabelled. **Fig. 5.** A grazing section over an intrapyrenoid lamella of *H. brunnescens*. The intrapyrenoid thylakoids are immunolabelled by anti-PSI. **Figs. 6-7.** Epon-embedded cells immunolabelled by anti-Rubisco LS. **Fig. 6.** In this cell section, three pairs of thylakoids traverse the pyrenoid of *Chroomonas*. Anti-Rubisco LS labels the pyrenoid matrix whereas only a few scattered gold particles are found elsewhere in the cell. **Fig. 7.** The pyrenoid of *H. brunnescens* is similarly immunolabelled by anti-Rubisco LS.



intrapyreoid thylakoids of this alga. In Figure 4, antiserum directed against a 19 kDa apoprotein of the complex labels the pair of thylakoids crossing the small projecting pyrenoid. In addition, thylakoids extending throughout the remainder of the chloroplast are also labelled, albeit sparsely. The chloroplast stroma is unlabelled. Specific thylakoid labelling using antiserum raised against apoproteins of the chl *a/c*<sub>2</sub> LHC has been demonstrated previously in cryptomonads (Rhiel et al. 1989, Lichtlé et al. 1991a). Thus, our results indicate that both peripheral light-harvesting pigment-protein complexes possessed by cryptophytes are present not only in the thylakoids of the chloroplast stroma, but are also associated with cryptomonad intrapyrenoid thylakoids. Although we have not performed a cytochemical activity stain for PSII, our results indicate that cryptomonad intrapyrenoid thylakoids likely function in a manner analagous to stromal thylakoids. This is further substantiated by our observation that the intrapyrenoid thylakoids of *Hemiselmis* are labelled by anti-PSI (Fig. 5)

Our observations for cryptomonads are in marked contrast to those reported for the red alga *Porphyridium cruentum* where peripheral phycobiliprotein (McKay and Gibbs 1990; Mustardy et al. 1990; see also Chapter VII) and PSII core light-harvesting complexes (Mustardy et al. 1990) are excluded from intrapyrenoid thylakoids. Moreover, these thylakoids are not labelled by antiserum raised against the PSII reaction center polypeptide D2 (Mustardy et al. 1990) nor do they stain for PSII activity (McKay and Gibbs 1990; see also Chapter VII). At the time, we speculated that the absence of PSII from intrapyrenoid thylakoids might be related to our observation that the bifunctional

Calvin cycle enzyme ribulose 1,5-bisphosphate carboxylase/oxygenase (Rubisco, E.C. 4.1.1.39) is mainly pyrenoid-localized in this alga (McKay and Gibbs 1990; see also Chapter VII). The resulting spatial separation between the process of photosynthetic O<sub>2</sub>-evolution and the reactions catalyzed by Rubisco, we argued, would promote Rubisco-catalyzed carboxylation, rather than oxygenation, of substrate ribulose 1,5-bisphosphate (RuBP). This, in turn, would promote photosynthetic carbon fixation rather than photorespiration.

Rubisco is similarly pyrenoid-localized in cryptophytes (Figs. 6,7), yet, our immunolabelling results indicate that cryptomonad intrapyrenoid thylakoids, unlike those of *Porphyridium*, possess a functional PSII complex. It appears, then, that spatial separation between the reactions of photosynthetic O<sub>2</sub>-evolution and RuBP carboxylation/oxygenation is not a feature possessed by all pyrenoid-containing algae. Rather, in many algal groups, the allocation of photosystem components to intrapyrenoid thylakoids appears to follow the pattern of distribution of these same proteins in thylakoids of the chloroplast stroma. In higher plants, there exists extreme lateral heterogeneity in the distribution of photosynthetic proteins among thylakoid membranes (Staehelin 1986). Those polypeptides associated with PSII are predominantly localized in the stacked grana regions whereas PSI-associated proteins are found mainly among unappressed thylakoid membranes. A similar partitioning of photosystem-related polypeptides has been reported for the green alga *Chlamydomonas reinhardtii* (Vallon et al. 1985; 1986; deVitry et al. 1989) and the hornwort *Phaeoceros laevis* (Vaughn and Owen 1989), both pyrenoid-

containing organisms. Moreover, in these organisms, intrapyrenoid thylakoids follow the same pattern of lateral heterogeneity in the distribution of photosystem components as established by the thylakoids of the chloroplast stroma. That is, PSII activity is present in the small grana stacks that often separate the pyrenoid subunits of *Phaeoceros* (Vaughn and Owen 1989) but is absent from the unstacked, single thylakoids that traverse the pyrenoid of the hornwort *Notothylas orbicularis* (K. Vaughn, pers. comm.). The single thylakoids that traverse the pyrenoid of *Notothylas*, however, stain for PSI activity (K. Vaughn, pers. comm.). Similarly, the unstacked thylakoid-like tubules that extend into the pyrenoid of *Chlamydomonas* are immunolabelled by neither intrinsic (J. Olive, pers. comm.) nor extrinsic (Vallon et al. 1985; deVitry et al. 1989) PSII core polypeptides.

The distribution of photosystem components, apart from phycobiliproteins, among the thylakoids of chromophyte algae has only recently been examined by immunocytochemical methods (Grevby et al. 1989; Rhiel et al. 1989; Lichtlé et al. 1991a; 1991b; Pyszniak and Gibbs 1991). Here, unlike higher plants and green algae, thylakoids are arranged in extended, loosely appressed bands of three thylakoids, or in the case of cryptomonads, in pairs of loosely appressed thylakoids. Distinct grana stacks are not evident. Moreover, immunolabelling results indicate that the marked asymmetry evident in the distribution of photosystem components among thylakoids of higher plants and green algae does not exist in cryptomonads (Rhiel et al. 1989; Lichtlé et al. 1991a), diatoms (Pyszniak and Gibbs 1991) or brown algae (Lichtlé et al. 1991b). That is, in chromophyte algae, PSI and PSII components are

located on both appressed and unappressed thylakoid membranes. In light of this, our observation that cryptomonad intrapyrenoid thylakoids possess both PSI and PSII complexes is not surprising. The single pair of thylakoids that traverse the pyrenoid of the diatom *Phaeodactylum tricornutum* is similarly immunolabelled by anti-PSI (Pyszniak and Gibbs 1991; McKay and Gibbs unpublished, see Appendix 4), stains for PSI activity (McKay and Gibbs 1991a) and is also labelled by antiserum raised against a peripheral light-harvesting complex for PSII (McKay and Gibbs 1991a; Pyszniak and Gibbs 1991; see also Appendix 4). Rubisco is also pyrenoid-localized in *Phaeodactylum* (McKay and Gibbs 1991a; see also Appendix 4).

Why PSII is excluded from the pyrenoid of *Porphyridium cruentum* is not known. Even among other pyrenoid-containing red algae this feature does not appear to be widely conserved. Although the published micrographs of *P. aeruginium* (Gantt et al. 1968) and *Porphyra leucosticta* (Sheath et al. 1977) indicate that intrapyrenoid thylakoids of these algae also lack light-harvesting phycobilisomes and presumably PSII activity, phycobilisomes are present on thylakoids found in the pyrenoids of *Rhodella cyanea* (Billard and Fresnel 1986) and *Nemalion* (e.g. Sheath et al. 1979). Our finding that PSII complexes are present in the pyrenoids of several chromophyte algae indicates that the absence of PSII from the pyrenoid of *Porphyridium* is not likely related to Rubisco functioning in algal pyrenoids. Nevertheless, it is probable that the microenvironment of the algal pyrenoid is one of high CO<sub>2</sub> and low O<sub>2</sub>. The frequency of thylakoids found in the pyrenoid is much reduced compared to that found in the chloroplast stroma. Moreover,

many algae, cryptophytes included (Suzuki and Ikawa 1985), possess effective concentrating mechanisms that act to concentrate inorganic carbon species intracellularly to high levels (for review, see Aizawa and Miyachi 1986). The mechanism is induced under levels of low inorganic carbon in the growth medium and results in the apparent suppression of photorespiration.

### **Acknowledgments**

We are grateful to those who supplied the antisera used in the present investigation. Dr. R. MacColl (New York State Department of Health, Albany) provided anti-PE 545. Dr. A. Barkan (Department of Botany, University of California, Berkeley) supplied anti-PSI and Dr. R.A. Cattolico (Botany Department, University of Washington, Seattle) provided anti-Rubisco LS. In addition, Dr. M.E. Goldstein provided us with the culture of *Chroomonas*. This research was supported by the Natural Sciences and Engineering Research Council (NSERC grant no. A-2921 to S.P. Gibbs) and in part by a Franco-Québec Exchange awarded to S.P. Gibbs and C. Lichtlé. In addition, R.M.L. McKay acknowledges support through a NSERC postgraduate scholarship.

## CONCLUDING REMARKS

The pyrenoids of evolutionarily diverse algae and hornworts contain the Calvin cycle enzyme Rubisco<sup>1</sup>. Moreover, through research presented in this thesis, it appears that pyrenoid-localized Rubisco is catalytically competent and that this Rubisco functions in the process of photosynthetic carbon reduction. In Chapter II, a study combining immunoelectron microscopy and photosynthetic physiology shows that in the green alga *Chlorella pyrenoidosa*, Rubisco remains pyrenoid-localized over a wide range of growth light fluence rates, including light that is saturating for photosynthesis. At all light levels tested, immunogold labelling over the remainder of the chloroplast was present at background levels. Since maximum Rubisco activity normalized to a per cell basis is only about 1.2-1.5 times higher than the maximum rate of photosynthesis (Tsuzuki et al. 1985), the rates observed cannot be accounted for solely by the low levels of Rubisco that may be present in the chloroplast stroma. Rubisco in the pyrenoid must be contributing to the observed rates of photosynthesis.

Results presented in Chapter III further support a functional role for pyrenoid-localized Rubisco. In higher plants, Rubisco activase catalyzes the activation and maintains the activated state of Rubisco in vivo. Recently it was demonstrated that Rubisco activase is also

<sup>1</sup> At present, we have no evidence to support a pyrenoid-location for enzymes of the Calvin cycle other than Rubisco; immunolocalization of phosphoribulokinase in a red and a green alga (Chapter IV) indicated that this enzyme is located predominantly in the chloroplast stroma.

present in the green alga *Chlamydomonas reinhardtii* (Roesler and Ogren 1990a). Moreover, immunolocalization studies reported in Chapter III indicate that in *Chlamydomonas*, activase is located mainly in the pyrenoid. A pyrenoid location for Rubisco activase would seem more likely if the Rubisco located in this structure were functional rather than a storage form.

In those organisms containing pyrenoids, why is Rubisco localized in this region, sequestered away from other reactions and processes occurring in the chloroplast? One possibility involves the observation that purified Rubisco irreversibly inhibits photophosphorylation in vitro. This inhibition appears to be a result of binding between Rubisco subunits and the  $\alpha$  and  $\beta$  subunits of  $H^+$ -ATP synthase (Suss 1990). In higher plants, it is postulated that two different pools of Rubisco exist; one form which catalyzes RuBP carboxylation/oxidation and another form which is complexed to receptors on the thylakoid membranes. Suss (1990) explains that this second pool of Rubisco prevents the former pool from complexing to ATP synthase and in this way, inhibition of photophosphorylation is avoided. Furthermore, he suggests that accumulating Rubisco in the pyrenoid region of algal chloroplasts may similarly provide a strategy for preserving ATP synthesis from inhibition by Rubisco.

It is possible that packaging of Rubisco in the pyrenoid may prevent the action of negative effectors. In Chapter III, it was shown that Rubisco activase is pyrenoid-localized in green algae. ATP is required by Rubisco activase. However, ADP has been shown to inhibit activase activity (Steusand and Portis 1987). Furthermore, Robinson et

al. (1988) have demonstrated that in the presence of ADP, Rubisco activase may also be modulated by other chloroplast metabolites. A number of the metabolites that act as negative effectors are also intermediates of the photosynthetic carbon reduction cycle. However, as a result of the compartmentalization of activase and Rubisco away from other reactions of the Calvin cycle, it would seem that in these organisms, activase is not subject to the same type of metabolite regulation as may occur in higher plants.

A novel explanation for the localization of Rubisco in pyrenoids might be provided by a model recently developed for cyanobacterial carboxysomes. Cyanobacterial Rubisco is very inefficient, possessing a value for  $K_m$  ( $\text{CO}_2$ ) of between 80 and 330  $\mu\text{M}$  (Badger 1980; Andrews and Abel 1981; Jordan and Ogren 1981; 1983). Immunoelectron microscopy and cell-fractionation investigations indicate that in cyanobacteria and other photosynthetic prokaryotes, Rubisco is predominantly localized in carboxysomes (see Codd 1988, for review; see also Chapter V). Recently, Reinhold et al. (1987; 1989) proposed, and Price and Badger (1989a) provided evidence supporting, a model identifying the carboxysome as an integral component of the inorganic carbon concentrating mechanism of cyanobacteria. Reinhold et al. (1987; 1989) speculated that the carboxysome might be a region of elevated  $\text{CO}_2$  concentration. This, they suggest, could be facilitated by excluding carbonic anhydrase (CA) from the thylakoid and centropasmic regions of the cell and instead, restrict its localization to the carboxysome. In their model, transport components of the inorganic carbon concentrating mechanism are localized at the cell membrane and  $\text{HCO}_3^-$  is the species of inorganic carbon

delivered to the cell interior, perhaps by way of a transporter possessing a CA-like moiety. With CA restricted to carboxysomes, dehydration of  $\text{HCO}_3^-$  in the centropasmic and thylakoid regions would proceed only at the uncatalyzed rate. It is anticipated that this would result in non-equilibrium ratios of  $\text{HCO}_3^-:\text{CO}_2$  in the cell interior, thereby preventing large scale leakage of  $\text{CO}_2$  from the cell.  $\text{HCO}_3^-$  entering carboxysomes would be dehydrated by the CA located in these structures and the  $\text{CO}_2$  generated by this reaction would be required to diffuse through Rubisco molecules confined to a small region. The resulting high  $\text{CO}_2$  microenvironment would ensure  $\text{CO}_2$  saturation of Rubisco, thereby offsetting the low affinity this enzyme naturally displays for  $\text{CO}_2$ .

Before the carboxysome model can be extended to include pyrenoids, one must examine existing biochemical and morphological data concerning them. In accordance with the model, the subcellular distribution of Rubisco in pyrenoid-containing algae and hornworts is mainly restricted to the pyrenoid. However, there is little evidence to support the restrictions imposed on the localization of CA (see Chapter I, section 5.0.) as required by the model. On the contrary, available evidence indicates that in microalgae, CA is localized throughout the chloroplast stroma. The localization of a portion of CA outside the pyrenoid is not predicted by the carboxysome model of Reinhold et al. (1987; 1989) and since exclusion of CA from regions other than carboxysomes is a major premise of their model, it appears that the model should not be extended to include pyrenoids. Moreover, it is not entirely clear whether a pyrenoid-localized CA is absolutely necessary to generate the  $\text{CO}_2$ ,

required as a substrate by Rubisco. Two protons are generated as part of the carboxylation reaction catalyzed by Rubisco and the resulting acidification of the pyrenoid compartment would promote formation of  $\text{CO}_2$  from  $\text{HCC}_3^-$ . Furthermore, Rubisco enzymes from diverse groups of eukaryotic algae appear to be more efficient than their cyanobacterial counterparts. Reported  $K_m(\text{CO}_2)$  values for Rubisco from pyrenoid-containing algae range from about 20  $\mu\text{M}$  for the cryptomonad alga *Chroomonas* sp. (Suzuki and Ikawa 1985) to 70  $\mu\text{M}$  for the green alga *Ulva fasciata* (Beer et al. 1990). These values would place the algal enzyme at an intermediate level between the low affinity enzyme of cyanobacteria and the higher affinity enzyme of terrestrial  $\text{C}_3$ -type plants ( $K_m(\text{CO}_2) = 10\text{-}25 \mu\text{M}$ ; Jordan and Ogren 1981; 1983; Yeoh et al. 1981). Perhaps in pyrenoid-containing algae, operation of an inorganic carbon concentrating mechanism alone ensures  $\text{CO}_2$ -saturation of pyrenoid-localized Rubisco.

It might be suggested that pyrenoids represent an evolutionary intermediate between Rubisco being contained in carboxysomes and its being distributed throughout the chloroplast stroma. The cyanelles of some endocyanomes may represent an extant link between pyrenoids and carboxysomes. Cyanelles are blue-green-coloured prokaryotes which are obligate endosymbionts in some eukaryotic protists. Usually, they are observed to possess electron-dense, carboxysome-like structures (Kies 1984). In some host genera (e.g. *Paulinella*, *Gloeochaete*), the "carboxysomes" of cyanelles are delimited by a non-unit membrane (Kies 1984), a characteristic similar to that of cyanobacteria. However, in the genera *Cyanophora* and *Glaucocystis*, cyanelle "carboxysomes" are not

membrane-bound (Kies 1984) and thus more resemble pyrenoids.

Furthermore, employing immunogold cytochemistry, Mangeney and Gibbs (1987) demonstrated that "carboxysomes" of the cyanelles of *Cyanophora paradoxa* and *Glaucocystis nostochinearum* contain Rubisco.

Likewise, the hornworts may represent an extant link between organisms that possess pyrenoids and the condition where Rubisco is distributed throughout the chloroplast stroma. The hornworts are the only terrestrial plant group having members that possess pyrenoids. Moreover, among the genera that contain these structures, several variations in pyrenoid morphology exist. Members of *Notothylas*, a primitive hornwort genus, typically possess algal-like pyrenoids, globular in nature and traversed by only single thylakoids and a small amount of stroma. Other hornwort genera exhibit more dissected pyrenoids. Many members of the genera *Anthoceros*, *Dendroceros*, *Folioceros*, *Phaeoceros* and *Sphaerosporoceros* possess multiple pyrenoids where individual units are dissected by large regions of stroma containing both stacked and unstacked thylakoid lamellae (Vaughn et al. 1990). In contrast, members of the genus *Megaceros* possess multiplastidic cells which do not contain pyrenoids. Instead, in these hornworts, Rubisco is distributed throughout the chloroplast stroma (Vaughn et al. 1990). Vaughn and colleagues suggest that an even distribution of Rubisco in the stroma might better facilitate chloroplast division in multiplastidic cells. Perhaps the loss of pyrenoids is associated with the evolution of multiplastidic cells.

The presence of intrapyrenoid thylakoids in diverse species of algae remains an enigma. They are often structurally, and sometimes

functionally modified compared to lamellae found in the chloroplast stroma. Moreover, not all pyrenoid-containing organisms possess intrapyrenoid thylakoids. Our initial observation that the intrapyrenoid lamellae of *Porphyridium cruentum* lack photosystem (PS) II activity, and presumably photosynthetic O<sub>2</sub>-evolution, (Chapter VII) led us to speculate that the pyrenoid might provide a microenvironment having a high CO<sub>2</sub>:O<sub>2</sub> ratio. That cryptomonad intrapyrenoid thylakoids possess PSII light-harvesting complexes (Chapter VIII) indicates that the absence of PSII from intrapyrenoid lamellae as observed in *P. cruentum* is not an omnipresent feature of these thylakoids. As discussed in Chapter VII, however, a possible function of intrapyrenoid thylakoids might be in providing CO<sub>2</sub>, generated in the acidic lumen.

## LITERATURE CITED

- Aizawa, K., and Miyachi, S. 1986. Carbonic anhydrase and CO<sub>2</sub> concentrating mechanisms in microalgae and cyanobacteria. *FEMS Microbiol. Rev.* **39**: 215-233.
- Akazawa, T., Takabe, T., and Kobayashi, H. 1984. Molecular evolution of ribulose-1,5-bisphosphate carboxylase/oxygenase (RuBisCO). *Trends Biochem. Sci.* **9**: 380-383.
- Allen, M.M. 1984. Cyanobacterial cell inclusions. *Ann. Rev. Microbiol.* **38**: 1-25.
- Andrews, T.J., and Abel, K.M. 1981. Kinetics and subunit interactions of ribulose bisphosphate carboxylase-oxygenase from the cyanobacterium, *Synechococcus* sp. *J. Biol. Chem.* **256**: 8445-8451.
- Badger, M.R. 1980. Kinetic properties of ribulose 1,5-bisphosphate carboxylase/oxygenase from *Anabaena variabilis*. *Arch. Biochem. Biophys.* **201**: 247-254.
- Badger, M.R., and Gallagher, A. 1987. Adaptation of photosynthetic CO<sub>2</sub> and HCO<sub>3</sub><sup>-</sup> accumulation by the cyanobacterium *Synechococcus* PCC 6301 to growth at different inorganic carbon concentrations. *Aust. J. Plant Physiol.* **14**: 189-201.

- Badger, M.R., Kaplan, A., and Berry, J.A. 1978. A mechanism for concentrating CO<sub>2</sub> in *Chlamydomonas reinhardtii* and *Anabaena variabilis* and its role in photosynthetic CO<sub>2</sub> fixation. Carnegie Inst. Wash. Yearbook 77: 251-261.
- Beer, S., Israel, A., Drechsler, Z., and Cohen, Y. 1990. Photosynthesis in *Ulva fasciata*. V. Evidence for an inorganic carbon concentrating system and ribulose-1,5-bisphosphate carboxylase/oxygenase CO<sub>2</sub> kinetics. Plant Physiol. 94: 1542-1546.
- Beesley, J.E. 1989. Colloidal gold: a new perspective for cytochemical marking. Oxford Univ. Press, New York.
- Bendayan, M. 1987. Introduction of the protein G-gold complex for high resolution immunocytochemistry. J. Electron Microsc. Tech. 6: 7-13.
- Bergman, B., and Rai, A. 1989. The *Nostoc-Nephroma* symbiosis: localization, distribution pattern and levels of key proteins involved in nitrogen and carbon metabolism of the cyanobiont. Physiol. Plant. 77: 216-224.
- Berns, D.S. 1967. Immunochemistry of biliproteins. Plant Physiol. 42: 1569-1586.
- Beudeker, R.F., Codd, G.A., and Kuenen, J.G. 1981. Quantification and intracellular distribution of ribulose-1,5-bisphosphate carboxylase

- in *Thiobacillus neapolitanus*, as related to possible functions of carboxysomes. *Arch. Microbiol.* **129**: 361-367.
- Biggins, J., and Bruce, D. 1989. Regulation of excitation energy transfer in organisms containing phycobilins. *Photosynth. Res.* **20**: 1-34.
- Billard, C., and Fresnel, J. 1986. *Rhodella cyanea* nov. sp., une nouvelle Rhodophyceae unicellulaire. *C.R. Acad. Sci. (Paris)*, **302** III: 271-276.
- Bird, C.J., Rice, E.L., Murphy, C.A., Liu, Q.Y., and Ragan, M.A. 1990. Nucleotide sequences of 18S ribosomal RNA genes from the red algae *Gracilaria tikvahiae* McLachlan, *Gracilaria verrucosa* (Hudson) Papenfuss and *Gracilariopsis* sp. *Nucl. Acids Res.* **18**: 4023-4024.
- Birmingham, B.C., and Colman, B. 1979. Measurement of carbon dioxide compensation points of freshwater algae. *Plant Physiol.* **64**: 892-895.
- Blank, R.J., and Trench, R.K. 1988. Immunogold localization of ribulose-1,5-bisphosphate carboxylase-oxygenase in *Symbiodinium kawagutii* Trench et Blank, an endosymbiotic dinoflagellate. *Endocyt. Cell Res.* **5**: 75-82.

- Borowitzka, M.A., and Volcani, B.E. 1978. The polymorphic diatom *Phaeodactylum tricornerutum* : ultrastructure of its morphophytes. *J. Phycol.* **14**: 10-21.
- Brawley, S.H., and Wetherbee, R. 1981. Cytology and ultrastructure. In *The biology of seaweeds*. Edited by C.S. Lobban and M.J. Wynne. Blackwell Scient. Publ., Oxford. pp. 248-299.
- Caers, M., Verbelen, J.-P., Vendrig, J.C. 1987. Ribulose-1,5-bisphosphate carboxylase and photosystem II activities during chloroplast development in mesophyll and bundle sheath cells of *Zea mays*. *Physiol. Plant.* **70**: 68-72.
- Cannon, G.C., and Shively, J.M. 1983. Characterization of a homogenous preparation of carboxysomes from *Thiobacillus neapolitanus*. *Arch. Microbiol.* **134**: 52-59.
- Cannon, G.C., English, R.S., and Shively, J.M. 1991. In situ assay of ribulose-1, 5-bisphosphate carboxylase/oxygenase in *Thiobacillus neapolitanus*. *J. Bacteriol.* **173**: 1565-1568.
- Chua, N-H. 1972. Photooxidation of 3,3'-diaminobenzidine by blue-green algae and *Chlamydomonas reinhardtii*. *Biochim. Biophys. Acta* **267**: 179-189.
- Clement-Metral, J.D., Gantt, E., and Redlinger, T. 1985. A photosystem

- II - phycobilisome preparation from the red alga, *Porphyridium cruentum*: oxygen evolution, ultrastructure, and polypeptide resolution. Arch. Biochem. Biophys. 238: 10-17.
- Codd, G.A. 1988. Carboxysomes and ribulose bisphosphate carboxylase/oxygenase. In Advances in microbial physiology. Vol. 29. Edited by A.H. Rose and D.W. Tempest. Academic Press, London. pp. 115-164.
- Codd, G.A., and Marsden, W.J.N. 1984. The carboxysomes (polyhedral bodies) of autotrophic prokaryotes. Biol. Rev. 59: 389-422.
- Codd, G.A., and Stewart, W.D.P. 1976. Polyhedral bodies and ribulose 1,5-diphosphate carboxylase of the blue-green alga *Anabaena cylindrica*. Planta 130: 323-326.
- Codd, G.A., and Stewart, W.D.P. 1977. Ribulose-1,5-diphosphate carboxylase in heterocysts and vegetative cells of *Anabaena cylindrica*. FEMS Microbiol. Lett. 2: 247-249.
- Coleman, A.W. 1985. Diversity of plastid DNA configuration among classes of eukaryote algae. J. Phycol. 21: 1-16.
- Coleman, J.R., Seemann, J.R., and Berry, J.A. 1982. RuBP carboxylase in carboxysomes of blue-green algae. Carnegie Inst. Wash. Yearbook 81: 83-87.

- Colman, B., and Gehl, K.A. 1983. Physiological characteristics of photosynthesis in *Porphyridium cruentum*: evidence for bicarbonate transport in a unicellular red alga. *J. Phycol.* **19**: 216-219.
- Cossar, J.D., Rowell, P., Darling, A.J., Murray, S., Codd, G.A., and Stewart, W.D.P. 1985. Localization of ribulose 1,5-bisphosphate carboxylase/oxygenase in the N<sub>2</sub>-fixing cyanobacterium *Anabaena cylindrica*. *FEMS Microbiol. Lett.* **28**: 65-68.
- Cunningham, F.X., Jr., Mustardy, L., and Gantt, E. 1991. Irradiance effects on thylakoid membranes of the red alga *Porphyridium cruentum*. An immunocytochemical study. *Plant Cell Physiol.* **32**: 419-426.
- Dalling, M.J., Tolbert, N.E., and Hageman, R.H. 1972. Intracellular location of nitrate reductase and nitrite reductase. I. Spinach and tobacco leaves. *Biochim. Biophys. Acta*, **283**: 505-512.
- Delieu, T., and Walker, D.A. 1972. An improved cathode for the measurement of photosynthetic oxygen evolution by isolated chloroplasts. *New Phytol.* **71**: 201-225.
- Dixon, G.K., Patel, B.N., and Merrett, M.J. 1987. Role of intracellular carbonic anhydrase in inorganic-carbon assimilation by *Porphyridium purpureum*. *Planta* **172**: 508-513.

- Dodge, J.D. 1973. The fine structure of algal cells. Academic Press, New York.
- Douglas, S.E., Murphy, C.A., Spencer, D.F., and Gray, M.W. 1991. Cryptomonad algae are evolutionary chimaeras of two phylogenetically distinct unicellular eukaryotes. *Nature (Lond.)* 350: 148-151.
- Downton, W.J.S., Berry, J.A., and Tregunna, E.B. 1970. C<sub>4</sub>-photosynthesis: non-cyclic electron flow and grana development in bundle sheath chloroplasts. *Z. Pflanzenphysiol.* 63: 194-198.
- Duggan, J.X., and Anderson, L.E. 1975. Light-regulation of enzyme activity in *Anacystis nidulans* (Richt.). *Planta* 122: 293-297.
- Duke, C.S., and Allen, M.M. 1990. Effect of nitrogen starvation on polypeptide composition, ribulose-1,5-bisphosphate carboxylase/oxygenase, and thylakoid carotenoprotein content of *Synechocystis* sp. strain PCC 6308. *Plant Physiol.* 94: 752-759.
- Ekman, P., Lignell, Å, and Pedersén, M. 1989. Localization of ribulose-1,5-bisphosphate carboxylase/oxygenase in *Gracilaria secundata* (Rhodophyta) and its role as a nitrogen storage pool. *Bot. Mar.* 32: 527-534.
- Edwards, M.R., Berns, D.S., Ghiorse, W.C., and Holt, S.C. 1968. Ultrastructure of the thermophilic blue-green alga, *Synechococcus*

- lividus* Copeland. J. Phycol. 4: 283-298.
- Espie, G.S., and Calvin, D.T. 1987. Evidence for Na<sup>+</sup>-independent HCO<sub>3</sub><sup>-</sup> uptake by the cyanobacterium *Synechococcus leopoliensis*. Plant Physiol. 84: 125-130.
- Espie, G.S., and Kandasamy, R.A. 1991. Na<sup>+</sup>-independent HCO<sub>3</sub><sup>-</sup> transport and accumulation in the cyanobacterium *Synechococcus* UTEX 625. Submitted.
- Espie, G.S., Miller, A.G., and Calvin, D.T. 1989. Selective and reversible inhibition of active CO<sub>2</sub> transport by hydrogen sulfide in a cyanobacterium. Plant Physiol. 91: 387-394.
- Espie, G.S., Miller, A.G., and Calvin, D.T. 1991. High affinity transport of CO<sub>2</sub> in the cyanobacterium *Synechococcus* UTEX 625. Plant Physiol. In press.
- Fawley, M.W., and Grossman, A.R. 1986. Polypeptides of a light-harvesting complex of the diatom *Phaeodactylum tricorutum* are synthesized in the cytoplasm of the cell as precursors. Plant Physiol. 81: 149-155.
- Fischer, P., and Klein, U. 1988. Localization of nitrogen-assimilating enzymes in the chloroplast of *Chlamydomonas reinhardtii*. Plant Physiol. 88: 947-952.

- Frederick, S.E. 1987. DAB Procedures. In CRC handbook of plant cytochemistry. Vol. 1. Edited by K.C. Vaughn. CRC Press, Boca Raton, Fla., U.S.A. pp. 3-23.
- Frens, G. 1973. Controlled nucleation for the regulation of the particle size in monodisperse gold suspensions. Nature Phys. Sci. 241: 20-22.
- Friedberg, D., Kaplan, A., Ariel, R., Kessel, M., and Seijffers, J. 1989. The 5'-flanking region of the gene encoding the large subunit of ribulose-1,5-bisphosphate carboxylase/oxygenase is crucial for growth of the cyanobacterium *Synechococcus* sp. strain PCC 7942 at the level of CO<sub>2</sub> in air. J. Bacteriol. 171: 6069-6076.
- Gantt, E. 1980. Structure and function of phycobilisomes: light harvesting pigment complexes in red and blue-green algae. Int. Rev. Cytol. 66: 45-80.
- Gantt, E. 1986. Phycobilisomes. In Encyclopedia of plant physiology. Vol. XIX. Photosynthesis III-Photosynthetic membranes and light harvesting systems. Edited by L.A. Staehelin and C.J. Arntzen. Springer, New York. pp. 260-268.
- Gantt, E., and Conti, S.F. 1965. The ultrastructure of *Porphyridium cruentum*. J. Cell Biol. 26: 365-375.

- Gantt, E., and Lipschultz, C.A. 1977. Probing phycobilisome structure by immuno-electron microscopy. *J. Phycol.* 13: 185-192
- Gantt, E., Edwards, M.R., and Conti, S.F. 1968. Ultrastructure of *Porphyridium aerugineum*, a blue-green coloured rhodophyten. *J. Phycol.* 4: 65-71.
- Gantt, E., Edwards, M.R., and Provasoli, L. 1971. Chloroplast structure of the Cryptophyceae. Evidence for phycobiliproteins within intrathylakoidal spaces. *J. Cell Biol.* 48: 280-290.
- Gantt, E., Lipschultz, C.A., and Zilinskas, B. 1976. Further evidence for a phycobilisome model from selective dissociation, fluorescence emission, immunoprecipitation, and electron microscopy. *Biochim. Biophys. Acta* 430: 375-388.
- Gantt, E., Cunningham, F.X., Jr., Lipschultz, C.A., and Mimuro, M. 1988. N-terminus conservation in the terminal pigment of phycobilisomes from a prokaryotic and eukaryotic alga. *Plant Physiol.* 86: 996-998.
- Gibbs, S.P. 1960. The fine structure of *Euglena gracilis* with special reference to the chloroplasts and pyrenoids. *J. Ultrastruct. Res.* 4: 127-148.
- Gibbs, S.P. 1962a. The ultrastructure of the pyrenoids of algae,

- exclusive of the green algae. *J. Ultrastruct. Res.* 7: 247-261.
- Gibbs, S.P. 1962b. The ultrastructure of the pyrenoids of green algae. *J. Ultrastruct. Res.* 7: 262-272.
- Gibbs, S.P. 1968. Autoradiographic evidence for the *in situ* synthesis of chloroplast and mitochondrial RNA. *J. Cell Sci.* 3: 327-340.
- Giddings, T.H., Jr., Wasmann, C., and Staehelin, L.A. 1983. Structure of the thylakoids and envelope membranes of the cyanelles of *Cyanophora paradoxa*. *Plant Physiol.* 71: 409-419.
- Gillott, M.A., and Gibbs, S.P. 1980. The cryptomonad nucleomorph: its ultrastructure and evolutionary significance. *J. Phycol.* 16: 558-568.
- Glazer, A.N. 1982. Phycobilisomes: structure and dynamics. *Ann. Rev. Microbiol.* 36: 173-198.
- Gontero, B., Cárdenas, M.L., and Ricard, J. 1988. A functional five-enzyme complex of chloroplasts involved in the Calvin cycle. *Eur. J. Biochem.* 173: 437-443.
- Gowri, G., and Campbell, W.H. 1989. cDNA clones for corn leaf NADH: nitrate reductase and chloroplast NAD(P)<sup>+</sup>: glyceraldehyde-3-phosphate dehydrogenase. Characterization of the clones and

- analysis of the expression of the genes in leaves as influenced by nitrate in the light and dark. *Plant Physiol.* **90**: 792-798.
- Graham, L.E. 1985. The origin of the life cycle of land plants. *Am. Sci.* **73**: 178-186.
- Grevby, C., Axelsson, L., and Sundqvist, C. 1989. Light-independent plastid differentiation in the brown alga *Laminaria saccharina* (Phaeophyceae). *Phycologia* **28**: 375-384.
- Griffiths, D.J. 1970. The pyrenoid. *Bot. Rev.* **36**: 29-58.
- Guard-Friar, D., Eisenberg, B.L., Edwards, M.R., and MacColl, R. 1986. Immunochemistry on cryptomonad biliproteins. *Plant Physiol.* **80**: 38-42.
- Gunning, B.E.S., Steer, M.W., and Cochrane, M.P. 1968. Occurrence, molecular structure, and induced formation of the 'stromacentre' in plastids. *J. Cell Sci.* **3**: 455-456.
- Hallenbeck, P.L., and Kaplan, S. 1987. Cloning of the gene for phosphoribulokinase activity from *Rhodobacter sphaeroides* and its expression in *Escherichia coli*. *J. Bacteriol.* **169**: 3669-3678.
- Hansmann, P., Falk, H., Scheer, U., and Sitte, P. 1986. Ultrastructural localization of DNA in two *Cryptomonas* species by use of a

- monoclonal DNA antibody. *Eur. J. Cell Biol.* **42**: 152-160.
- Hawthornthwaite, A.M., Lanaras, T., and Codd, G.A. 1987.  
Immunoelectronmicroscopic localization of Calvin cycle enzymes in  
*Chlorogloeopsis fritschii*. *J. Gen. Microbiol.* **131**: 2497-2500.
- Heber, U., and Heldt, H.W. 1981. The chloroplast envelope: structure,  
function, and role in leaf metabolism. *Ann. Rev. Plant Physiol.*  
**32**: 139-168.
- Herman, E.M. 1988. Immunocytochemical localization of macromolecules  
with the electron microscope. *Ann. Rev. Plant Physiol. Plant Mol.*  
*Biol.* **39**: 139-155.
- Hill, D.R.A. 1991. *Chroomonas* and other blue-green cryptomonads.  
*J. Phycol.* **27**: 133-145.
- Hill, D.R.A., and Rowan, K.S. 1989. The biliproteins of the  
Cryptophyceae. *Phycologia* **28**: 455-463.
- Holdsworth, R.H. 1971. The isolation and partial characterization of  
the pyrenoid protein of *Eremosphaera viridis*. *J. Cell Biol.* **51**:  
499-513.
- Holthuijzen, Y.A., van Breemen, J.F.L., Keunen, J.G., and Konings,  
W.N. 1986. Protein composition of the carboxysomes of *Thiobacillus*

neapolitanus. Arch. Microbiol. 144: 398-404.

Husic, H.D., Kitayama, M., Togasaki, R.K., Moroney, J.V., Morris, K.L., and Tolbert, N.E. 1988. Identification of intracellular carbonic anhydrase in *Chlamydomonas reinhardtii* which is distinct from the periplasmic form of the enzyme. Plant Physiol. 89: 904-909.

Ingram, K., and Hiller, R.G. 1983. Isolation and characterization of major chlorophyll *a/c*<sub>2</sub> light-harvesting protein from a *Chroomonas* species (Cryptophyceae). Biochim. Biophys. Acta 722: 310-319.

Jeffrey, S.W., and Humphrey, G.F. 1975. New spectrophotometric equations for determining chlorophylls *a*, *b*, *c*<sub>1</sub>, and *c*<sub>2</sub> in higher plants, algae and natural phytoplankton. Biochem. Physiol. Pflanzen. 167: 191-194.

Jones, R.F., Speer, H.L., and Kury, W. 1963. Studies on the growth of the red alga *Porphyridium cruentum*. Physiol. Plant. 16: 636-643

Jordan, D.B., and Chollet, R. 1983. Inhibition of ribulose biphosphate carboxylase by substrate ribulose 1,5-biphosphate. J. Biol. Chem. 258: 13752-13758.

Jordan, D.B., and Ogren, W.L. 1981. Species variation in the specificity of ribulose biphosphate carboxylase/oxygenase. Nature

291: 513-515.

Jordan, D.B., and Ogren, W.L. 1983. Species variation in kinetic properties of ribulose 1,5-bisphosphate carboxylase/oxygenase. Arch. Biochem. Biophys. **227**: 425-433.

Kagawa, T. 1982. Isolation and purification of ribulose-5-phosphate kinase from *Nicotiana glutinosa*. In Methods in chloroplast molecular biology. Edited by M. Edelman, R.B. Hallick and N.-H. Chua. Elsevier, Amsterdam. pp. 695-705.

Kajikawa, H., Okada, M., Ishikawa, F., Okada, Y., and Nakayama, K. 1988. Immunochemical studies on ribulose 1,5-bisphosphate carboxylase/oxygenase in the chloroplasts of the marine alga *Bryopsis maxima*. Plant Cell Physiol. **29**: 549-556.

Kamachi, K., Amemiya, Y., Ogura, N., and Nakagawa, H. 1987. Immuno-gold localization of nitrate reductase in spinach (*Spinacia oleracea*) leaves. Plant Cell Physiol. **28**: 333-338.

Kerby, N.W., and Evans, L.V. 1978. Isolation and partial characterization of pyrenoids from the brown alga *Pilayella littoralis* (L.) Kjellm. Planta **142**: 91-95.

Kerby, N.W., and Evans, L.V. 1981. Pyrenoid protein from the brown alga *Pilayella littoralis*. Planta **151**: 469-475.

- Kies, L. 1984. Cytological aspects of blue-green algal endosymbiosis. In *Compartments in algal cells and their interaction*. Edited by W. Weissner, D. Robinson, and R.C. Starr. Springer, Berlin, Heidelberg. pp. 191-199.
- Kiss, J.Z., Vasconcelos, A.C., and Triemer, R.E. 1986. Paramylon synthesis and chloroplast structure associated with nutrient levels in *Euglena* (Euglenophyceae). *J. Phycol.* 22: 327-333.
- Knox, R.B. 1982. Methods for locating and identifying antigens in plant tissues. In *Techniques in immunocytochemistry*. Vol. 1. Edited by G.R. Bullock and P. Petrusz. Academic Press, London. pp. 205-238.
- Kuchitsu, K., Tsuzuki, M., and Miyachi, S. 1988a. Characterization of the pyrenoid isolated from unicellular green alga *Chlamydomonas reinhardtii*: particulate form of RuBisCO protein. *Protoplasma* 144: 17-24.
- Kuchitsu, K., Tsuzuki, M., and Miyachi, S. 1988b. Changes of starch localization within the chloroplast induced by changes in CO<sub>2</sub> concentration during growth of *Chlamydomonas reinhardtii*: independent regulation of pyrenoid starch and stroma starch. *Plant Cell Physiol.* 29: 1269-1278.
- Kuchitsu, K., Tsuzuki, M., and Miyachi, S. 1991. Polypeptide

composition and enzyme activities of the pyrenoid and its regulation by CO<sub>2</sub> concentration in unicellular green algae. *Can. J. Bot.* **69**: 1062-1069.

Lacoste-Royal, G., and Gibbs, S.P. 1985. *Ochromonas* mitochondria contain a specific chloroplast protein. *Proc. Natl. Acad. Sci. USA* **82**: 1456-1459.

Lacoste-Royal, G., and Gibbs, S.P. 1987. Immunocytochemical localization of ribulose-1,5-bisphosphate carboxylase in the pyrenoid and thylakoid region of the chloroplast of *Chlamydomonas reinhardtii*. *Plant Physiol.* **83**: 602-606.

Laemmli, U.K. 1970. Cleavage of structural proteins during the assembly of the head of bacteriophage T4. *Nature (Lond.)* **227**: 680-685.

Lanaras, T., and Codd, G.A. 1981a. Ribulose 1,5-bisphosphate carboxylase and polyhedral bodies of *Chlorogloeopsis fritschii*. *Planta* **153**: 279-285.

Lanaras, T., and Codd, G.A. 1981b. Structural and immunoelectrophoretic comparison of soluble and particulate ribulose bisphosphate carboxylases from the cyanobacterium *Chlorogloeopsis fritschii*. *Arch. Microbiol.* **130**: 213-217.

- Lanaras, T., and Codd, G.A. 1982. Variations in ribulose 1,5-bisphosphate carboxylase protein levels, activities and subcellular distribution during photoautotrophic batch culture of *Chlorogloeopsis fritschii*. *Planta* 154: 284-288.
- Lazaro, J.J., Sutton, C.W., Nicholson, S., and Pows, R. 1986. Characterisation of two forms of phosphoribulokinase isolated from the green alga, *Scenedesmus obliquus*. *Eur. J. Biochem.* 156: 423-429.
- Lett, M.C., Fleck, J., Fritsch, C., Durr, A., and Hirth, L. 1980. Suitable conditions for characterization, identification, and isolation of the mRNA of the small subunit of ribulose-1,5-bisphosphate carboxylase from *Nicotiana sylvestris*. *Planta* 148: 211-216.
- Ley, A.C., and Butler, W.L. 1977. The distribution of excitation energy between photosystem I and photosystem II in *Porphyridium cruentum*. In *Photosynthetic organelles*. Edited by S. Miyachi. Japanese Society of Plant Physiology, Tokyo. pp. 33-46.
- Lichtlé, C. 1979. Effects of nitrogen deficiency and light of high intensity on *Cryptomonas rufescens* (Cryptophyceae). I. Cell and photosynthetic apparatus transformations and encystment. *Protoplasma* 101: 283-299.

- Lichtlé, C., Jupin, H., and Duval, J.C. 1980. Energy transfers from photosystem II to photosystem I in *Cryptomonas rufescens* (Cryptophyceae). *Biochim. Biophys. Acta* 591: 104-112.
- Lichtlé, C., Duval, J.C., and Lemoine, Y. 1987. Comparative biochemical, functional and ultrastructural studies of photosystem particles from a Cryptophyceae: *Cryptomonas rufescens*; isolation of an active phycoerythrin particle. *Biochim. Biophys. Acta* 894: 76-90.
- Lichtlé, C., McKay, R.M.L., and Gibbs, S.P. 1991a. Immunogold localization of photosystem I and of photosystem II light-harvesting complexes in cryptomonad thylakoids. Submitted.
- Lichtlé, C., Spilar, A., and Duval, J.C. 1991b. Immunogold localization of light-harvesting and PSI complexes in the thylakoids of *Fucus serratus* (Phaeophyceae). *Protoplasma* In press.
- Lönnerholm, G. 1984. Histochemical localization of carbonic anhydrase in mammalian tissues. *Ann. N.Y. Acad. Sci.* 429: 369-381.
- Lopez-Ruiz, A., Roldan, J.M., Verbelen, J.-P., and Diez, J. 1985a. Nitrate reductase from *Monoraphidium braunii*. Immunocytochemical localization and immunological characterization. *Plant Physiol.* 78: 614-618.

- Lopez-Ruiz, A., Verbelen, J.-P., Roldan, J.M., and Diez, J. 1985b.  
Nitrate reductase of green algae is located in the pyrenoid. *Plant Physiol.* **79**: 1006-1010.
- Lopez-Ruiz, A., Verbelen, J.-P., Bocanegra, J.A., and Diez, J. 1991.  
Immunocytochemical localization of nitrite reductase in green algae.  
*Plant Physiol.* **96**: 699-704.
- Ludwig, M., and Gibbs, S.P. 1989. Localization of phycoerythrin at the lumenal surface of the thylakoid membrane in *Rhodomonas lens*. *J. Cell Biol.* **108**: 875-884.
- MacColl, R., and Guard-Friar, D. 1987. *Phycobiliproteins*. CRC Press, Boca Raton, Florida, 218 pp.
- MacKinney, G. 1941. Absorption of light by chlorophyll solutions. *J. Biol. Chem.* **140**: 315-322.
- Mangenev, E., and Gibbs, S.P. 1987. Immunocytochemical localization of ribulose-1,5-bisphosphate carboxylase/oxygenase in the cyanelles of *Cyanophora paradoxa* and *Glaucocystis nostochinearum*. *Eur. J. Cell Biol.* **43**: 65-70.
- Mangenev, E., Hawthornthwaite, A.M., Codd, G.A., and Gibbs, S.P. 1987. Immunocytochemical localization of phosphoribulose kinase in the cyanelles of *Cyanophora paradoxa* and *Glaucocystis nostochinearum*.

Plant Physiol. **84**: 1028-1032.

Margulies, M.M. 1989. Photosystem I core. Plant Sci. **64**: 1-13.

Marsden, W.J.N., and Codd, G.A. 1984. Purification and molecular and catalytic properties of phosphoribulokinase from the cyanobacterium *Chlorogloeopsis fritschii*. J. Gen. Microbiol. **130**: 999-1006.

Marsden, W.J.N., Lanaras, T., and Codd, G.A. 1984. Subcellular segregation of phosphoribulokinase and ribulose-1,5-bisphosphate carboxylase/oxygenase in the cyanobacterium *Chlorogloeopsis fritschii*. J. Gen. Microbiol. **130**: 2089-2093.

Marty, D. 1977. Localisation ultra-structurale des sites d'activité des photosystèmes I et II dans les chloroplastes in situ. C.R. Acad. Sci. (Paris) **285 D**: 27-30.

Mayo, W.P., Elrifi, I.R., and Turpin, D.H. 1989. The relationship between ribulose bisphosphate concentration, dissolved inorganic carbon (DIC) transport and DIC-limited photosynthesis in the cyanobacterium *Synechococcus leopoliensis* grown at different concentrations of inorganic carbon. Plant Physiol. **90**: 720-727.

- McKay, R.M.L., and Gibbs, S.P. 1989. Immunocytochemical localization of ribulose 1,5-bisphosphate carboxylase/oxygenase in light-limited and light-saturated cells of *Chlorella pyrenoidosa*. *Protoplasma* **149**: 31-37.
- McKay, R.M.L., and Gibbs, S.P. 1990. Phycoerythrin is absent from the pyrenoid of *Porphyridium cruentum*: photosynthetic implications. *Planta* **180**: 249-256.
- McKay, R.M.L., and Gibbs, S.P. 1991a. Composition and function of pyrenoids: cytochemical and immunocytochemical approaches. *Can. J. Bot.* **69**: 1040-1052.
- McKay, R.M.L., and Gibbs, S.P. 1991b. Immunocytochemical localization of phosphoribulokinase in microalgae. *Bot. Acta*. In press.
- McKay, R.M.L., Gibbs, S.P., and Vaughn, K.C. 1991a. Rubisco activase is present in the pyrenoid of green algae. *Protoplasma* **162**: 38-45.
- McKay, R.M.L., Lichtlé, C., and Gibbs, S.P. 1991b. Immunocytochemical characterization of the intrapyrenoid thylakoids of cryptomonads. Submitted.
- McKay, R.M.L., Gibbs, S.P., and Espie, G.S. 1991c. Effect of dissolved inorganic carbon on mode of carbon transport, expression of carboxysomes and localization of Rubisco in cells of the

1  
cyanobacterium *Synechococcus* UTEX 625. Submitted.

- McLachlan, J. 1973. Growth media - marine. In Handbook of Phycological Methods. Culture Methods and Growth Measurements. Edited by J.R.Stein. Cambridge, New York, pp. 25-51.
- Michaels, A., Kriho, V., and Solomonson, L.P. 1986. Electron microscope localization of nitrate reductase in *Chlorella*. J. Cell Biol. 103: 427a.
- Miller, A.G., Espie, G.S., and Calvin, D.T. 1990. Physiological aspects of CO<sub>2</sub> and HCO<sub>3</sub><sup>-</sup> transport by cyanobacteria: a review. Can. J. Bot. 68: 1291-1302.
- Miller, A.G., Espie, G.S., and Calvin, D.T. 1991. The effects of inorganic carbon and oxygen upon fluorescence in the cyanobacterium *Synechococcus* UTEX 625. Can. J. Bot. 69: 1151-1160.
- Miller, L.S., and Holt, S.C. 1977. Effect of carbon dioxide on pigment and membrane content in *Synechococcus lividus*. Arch. Microbiol. 115: 185-198.
- Miyachi, S., Tsuzuki, M., Maruyama, I., Gantar, M., Miyachi, S., and Matsushima, H. 1986. Effects of CO<sub>2</sub> concentration during growth on the intracellular structure of *Chlorella* and *Scenedesmus* (Chlorophyta). J. Phycol. 22: 313-319.

- Miyamura, S., and Hori, T. 1991. DNA is present in the pyrenoid core of the siphonous green algae of the genus *Caulerpa* and yellow-green algae of the genus *Pseudodichotomosiphon*. *Protoplasma* **161**: 192-196.
- Miziorko, H.M., and Lorimer, G.H. 1983. Ribulose-1,5-bisphosphate carboxylase-oxygenase. *Ann. Rev. Biochem.* **52**: 507-535.
- Moroney, J.V., and Mason, C.B. 1991. The role of the chloroplast in inorganic carbon acquisition by *Chlamydomonas reinhardtii*. *Can. J. Bot.* **69**: 1017-1024.
- Mörschel, E., and Mühlethaler, K. 1983. On the linkage of exoplasmic freeze-fracture particles to phycobilisomes. *Planta* **158**: 451-457.
- Mustardy, L., Cunningham, F.X., Jr., and Gantt, E. 1990. Localization and quantitation of chloroplast enzymes and light-harvesting components using immunocytochemical methods. *Plant Physiol.* **94**: 334-340.
- Neushul, M. 1970. A freeze-etching study of the red alga *Porphyridium*. *Amer. J. Bot.* **57**: 1231-1239.
- Neushul, M. 1971. Uniformity of thylakoid structure in a red, a brown, and two blue-green algae. *J. Ultrastruct. Res.* **37**: 532-543.
- Newman, S.M., and Cattolico, R.A. 1990. Ribulose bisphosphate

carboxylase in algae: synthesis, enzymology and evolution.

Photosynth. Res. **26**: 69-85.

Newman, S.M., Derocher, J., and Cattolico, R.A. 1989. Analysis of chromophytic and rhodophytic ribulose-1,5-bisphosphate carboxylase indicates extensive structural and functional similarities among evolutionarily diverse algae. *Plant Physiol.* **91**: 939-946.

Nierzwicki-Bauer, S.A., Balkwill, D.L., and Stevens, S.E. Jr. 1983. Three-dimensional ultrastructure of a unicellular cyanobacterium. *J. Cell Biol.* **97**: 713-722.

Nir, I. and Seligman, A.M. 1970. Photooxidation of diaminobenzidine (DAB) by chloroplast lamellae. *J. Cell Biol.* **46**: 617-620.

Nisius, A. 1988. The stromacentre in *Avena* plastids: an aggregation of  $\beta$ -glucosidase responsible for the activation of oat-leaf saponins. *Planta* **173**: 474-481.

Nisius, A., and Ruppel, H.G. 1987. Immunocytological and chemical studies on the stromacentre-forming protein from *Avena* plastids. *Planta* **171**: 443-452.

Oakley, B.R., and Dodge, J.D. 1974. The ultrastructure and cytochemistry of microbodies in *Porphyridium*. *Protoplasma* **80**: 233-244.

- Okabe, Y., and Okada, M. 1988. Isolation of native pyrenoid core matrix having ribulose 1,5-bisphosphate carboxylase activity from the green alga *Bryopsis maxima*. *Plant Cell Physiol.* **29**: 89-96.
- Okabe, Y., and Okada, M. 1990. Nitrate reductase activity and nitrite in native pyrenoids purified from the green alga *Bryopsis maxima*. *Plant Cell Physiol.* **31**: 429-432.
- Osafune, T., Sumida, S., Ehara, T., and Hase, E. 1989. Three-dimensional distribution of ribulose-1,5-bisphosphate carboxylase/oxygenase in chloroplasts of actively photosynthesizing cell of *Euglena gracilis*. *J. Electron Microsc.* **38**: 399-402.
- Osafune, T., Schiff, J.A., and Hase, E. 1990a. Immunogold localization of LHCP II apoprotein in the golgi of *Euglena*. *Cell Struct. Funct.* **15**: 99-105.
- Osafune, T., Sumida, S., Ehara, T., Kodama, M., and Hase, E. 1990b. Immunoelectron microscopic evidence for the occurrence of ribulose-1,5-bisphosphate carboxylase/oxygenase in "propyrenoids" of *Euglena gracilis*. *J. Electron Microsc.* **39**: 101-104.
- Osafune, T., Yokota, A., Sumida, S., and Hase, E. 1990c. Immunogold localization of ribulose-1,5-bisphosphate carboxylase with reference to pyrenoid morphology in chloroplasts of synchronized *Euglena gracilis* cells. *Plant Physiol.* **92**: 802-808.

- Owens, T.G. 1988. Light-harvesting antenna systems in the chlorophyll *a/c*-containing algae. In Light-energy transduction in photosynthesis: higher plant and bacterial models. Edited by S.E. Stevens Jr. and D.A. Bryant. American Society of Plant Physiologists, Rockville, MD, USA. pp. 122-136.
- Peat, A., and Whitton, B.A. 1967. Environmental effects on the structure of the blue-green alga, *Chlorogloea fritschii*. Arch. Mikrobiol. 57: 155-180.
- Perchorowicz, J.T., Raynes, D.A., Jensen, R.G. 1981. Light limitation of photosynthesis and activation of ribulose bisphosphate carboxylase in wheat seedlings. Proc. Natl. Acad. Sci. USA 78: 2985-2989.
- Pervot-Rechenmann, C., and Gadal, P. 1986. Enzyme immunocytochemistry. In Immunology in plant science. Edited by T.L. Wang. Cambridge Univ. Press, New York, pp. 59-88.
- Pierce, J., Carlson, T.J., and Williams, J.G.K. 1989. A cyanobacterial mutant requiring the expression of ribulose bisphosphate carboxylase from a photosynthetic anaerobe. Proc. Natl. Acad. Sci. USA 86: 5753-5757.

- Plumley, F.G., Kirchman, D.L., Hodson, R.E., and Schmidt, G.W. 1986. Ribulose biphosphate carboxylase from three chlorophyll c-containing algae. Physica<sup>1</sup> and immunological characterizations. Plant Physiol. **80**: 665-691.
- Portis, A.R., Jr. 1990. Rubisco activase. Biochim. Biophys. Acta **1015**: 15-28.
- Portis, A.R., Jr., Salvucci, M.E., and Ogren, W.L. 1986. Activation of ribulose-bisphosphate carboxylase/oxygenase at physiological CO<sub>2</sub> and ribulosebisphosphate concentrations by rubisco activase. Plant Physiol. **82**: 967-971.
- Price, G.D., and Badger, M.R. 1989a. Expression of human carbonic anhydrase in the cyanobacterium *Synechococcus* PCC7942 creates a high CO<sub>2</sub>-requiring phenotype. Evidence for a central role for carboxysomes in the CO<sub>2</sub> concentrating mechanism. Plant Physiol. **91**: 505-513.
- Price, G.D., and Badger, M.R. 1989b. Isolation and characterization of high CO<sub>2</sub>-requiring-mutants of the cyanobacterium *Synechococcus* PCC 7942. Plant Physiol. **91**: 514-525.
- Pyszniak, A.M., and Gibbs, S.P. 1991. Immunocytochemical localization of photosystem I and the fucoxanthin-chlorophyll *a/c* light-harvesting complex in *Phaeodactylum tricornutum* (Bacillariophyceae).

J. Phycol. Submitted.

Reinhold, L., Zviman, M., and Kaplan, A. 1987. Inorganic carbon fluxes and photosynthesis in cyanobacteria - a quantitative model. In Progress in photosynthesis research Vol. IV. Edited by J. Biggins. Martinus Nijhoff, Dordrecht, The Netherlands, pp. 289-296.

Reinhold, L., Zviman, M., and Kaplan, A. 1989. A quantitative model for inorganic carbon fluxes and photosynthesis in cyanobacteria. Plant Physiol. Biochem. 27: 945-954.

Reynolds, E.S. 1963. The use of lead citrate at high pH as an electron-opaque stain in electron microscopy. J. Cell Biol. 17: 208-212.

Rhiel, E., Mörschel, E., and Wehrmeyer, W. 1985. Correlation of pigment deprivation and ultrastructural organization of thylakoid membranes in *Cryptomonas maculata* following nutrient deficiency. Protoplasma 129: 62-73.

Rhiel, E., Mörschel, E., and Wehrmeyer, W. 1987. Characterization and structural analysis of a chlorophyll *a/c* light harvesting complex and of photosystem I particles isolated from thylakoid membranes of *Cryptomonas maculata* (Cryptophyceae). Eur. J. Cell Biol. 43: 82-92.

- Rhiel, E., Kunz, J., and Wehrmeyer, W. 1989. Immunocytochemical localization of phycoerythrin-545 and of a chlorophyll *a/c* light harvesting complex in *Cryptomonas maculata* (Cryptophyceae). Bot. Acta 102: 46-53.
- Ridderstråle, Y. 1976. Intracellular localization of carbonic anhydrase in the frog nephron. Acta Physiol. Scand. 98: 465-469.
- Robinson, S.P., Streusand, V.J., Chatfield, J.M., and Portis, A.R., Jr. 1988. Purification and assay of Rubisco activase from leaves. Plant Physiol. 88: 1008-1014.
- Roesler, K.R., and Ogren, W.L. 1990a. Primary structure of *Chlamydomonas reinhardtii* rubisco activase and evidence for a single polypeptide. Plant Physiol. 94: 1837-1841.
- Roesler, K.R., and Ogren, W.L. 1990b. *Chlamydomonas reinhardtii* phosphoribulokinase. Sequence, purification, and kinetics. Plant Physiol. 93: 188-193.
- Rosowski, J.R., and Hoshaw, R.W. 1971. Results of an attempt to obtain pyrenoids of *Zygnema* by bulk-isolation methods. J. Phycol. 7: 312-316.
- Roth, J. 1982. The protein A-gold (pAg) technique - a qualitative and quantitative approach for antigen localization on thin sections. In

Techniques in immunocytochemistry. Vol. 1. Edited by G.R. Bullock and P. Petrusz. Academic Press, London. pp. 107-133.

Roth, J., Bendayan, M., and Orci, L. 1978. Ultrastructural localization of intracellular antigens by use of protein A-gold complex.

J. Histochem. Cytochem. **26**: 1074-81.

Rother, Th., Acker, G., and Scheibe, R. 1988. Immunogold localization of chloroplast proteins in spinach leaf mesophyll, epidermis, and guard cells. Bot. Acta **101**: 311-320.

Sainis, J.K., and Harris, G.C. 1986. The association of ribulose-1,5-bisphosphate carboxylase with phosphoriboisomerase and phosphoribulokinase. Biochem. Biophys. Res. Comm. **139**: 947-954.

Sainis, J.K., Merriam, K., and Harris, G.C. 1989. The association of D-ribulose-1,5-bisphosphate carboxylase/oxygenase with phosphoribulokinase. Plant Physiol. **89**: 368-374.

Salisbury, J.L., and Floyd, G.L. 1978. Molecular, enzymatic and ultrastructure characterization of the pyrenoid of the scaly green monad *Micromonas squamata*. J. Phycol. **14**: 362-368.

Salvucci, M.E. 1989. Regulation of rubisco activity in vivo. Physiol. Plant. **77**: 164-171.

- Salvucci, M.E., and Anderson, J.C. 1987. Factors affecting the activation state and the level of total activity of ribulose biphosphate carboxylase in tobacco protoplasts. *Plant Physiol.* **85**: 66-71.
- Salvucci, M.E., Portis, A.R. Jr., and Ogren, W.L. 1985. A soluble chloroplast protein catalyzes ribulose biphosphate carboxylase/oxygenase activation in vivo. *Photosynth Res.* **7**: 193-201.
- Salvucci, M.E., Portis, A.R. Jr., and Ogren, W.L. 1986. Light and CO<sub>2</sub> response of ribulose-1,5-biphosphate carboxylase/oxygenase activation in *Arabidopsis* leaves. *Plant Physiol.* **80**: 655-659.
- Salvucci, M.E., Werneke, J.M., Ogren, W.L., Portis, A.R., Jr. 1987. Purification and species distribution of rubisco activase. *Plant Physiol.* **84**: 930-936.
- Santore, U.J. 1982. The ultrastructure of *Hemiselmis brunnescens* and *Hemiselmis virescens* with additional observations on *Hemiselmis rufescens* and comments on the Hemiselmidaceae as a natural group of the Cryptophyceae. *Br. Phycol. J.* **17**: 81-99.
- Santore, U.J. 1984. Some aspects of taxonomy in the Cryptophyceae. *New Phytol.* **98**: 627-646.
- Santore, U.J. 1987. A cytological survey of the genus *Chroomonas* -

with comments on the taxonomy of this natural group of the Cryptophyceae. Arch. Protistenkd. 134: 83-114.

Satoh, H., Okada, M., Nakayama, K., and Miyaji, K. 1984. Purification and further characterization of pyrenoid proteins and ribulose-1, 5-bisphosphate carboxylase-oxygenase from the green alga *Bryopsis maxima*. Plant Cell Physiol. 25: 1205-1214.

Satoh, H., Okada, M., Nakayama, K., and Murata, T. 1985. Purification of ribulose 5-phosphate kinase and minor polypeptides of pyrenoid from the green alga *Bryopsis maxima*. Plant Cell Physiol. 26: 931-940.

Seligman, A.M., Karnovsky, M.J., Wasserkrug, H.L., and Hanker, J.S. 1968. Nondroplet ultrastructural demonstration of cytochrome oxidase activity with a polymerizing osmiophilic reagent, diaminobenzidine (DAB). J. Cell Biol. 38: 1-14.

Seligman, A.M., Nir, I., and Plapinger, R.E. 1971. An osmiophilic distyryl ditetrazolium salt (DS-NBT) for ultrastructural dehydrogenase activity. J. Histochem. Cytochem. 19: 273-285.

Serra, J.L., Llana, M.J., Rowell, P., and Stewart, W.D.P. 1989. Purification and characterization of phosphoribulokinase from the N<sub>2</sub>-fixing cyanobacterium *Anabaena cylindrica*. Plant Science 59: 1-9.

- Sheath, R.G., Hellebust, J.A., and Sawa, T. 1977. Changes in plastid structure, pigmentation and photosynthesis of the conchocelis stage of *Porphyra leucosticta* (Rhodophyta, Bangiophyceae) in response to low light and darkness. *Phycologia* 16: 265-276.
- Sheath, R.G., Hellebust, J.A., and Sawa, T. 1979. Effects of low light and darkness on structural transformations in plastids of the Rhodophyta. *Phycologia* 18. 1-12.
- Sherman, D.M., and Sherman, L.A. 1983. Effect of iron deficiency and iron restoration on ultrastructure of *Anacystis nidulans*. *J. Bacteriol.* 156: 393-401.
- Sherman, T.D., Vaughn, K.C., and Duke, S.O. 1989. Phylogenetic distribution of polyphenol oxidase and its physiological implications. *Plant Physiol.* 89s: 127.
- Shively, J.M., Ball, F., Brown, D.H., and Saunders, R.E. 1973. Functional organelles in prokaryotes: polyhedral inclusions (carboxysomes) of *Thiobacillus neapolitanus*. *Science* 182: 584-586.
- Shively, J.M., Bryant, D.A., Fuller, R.C., Konopka, A.E., Stevens, S.E. Jr, and Strohl, W.R. 1988. Functional inclusions in prokaryotic cells. *Int. Rev. Cytol.* 113: 35-100.
- Shojima, S., Nishizawa, N.K., and Mori, S. 1987. Do intrathylakoid

inclusions really contain RuBPCase? *Protoplasma* **140**: 187-189.

Sidler, W., Kumpf, B., Suter, F., Morisset, W., Wehrmeyer, W.,  
and Zuber, H. 1985. Structural studies on cryptomonad  
biliprotein subunits. Two different  $\alpha$ -subunits in *Chroomonas*  
phycoerythrin-645 and *Cryptomonas* phycoerythrin-545. *Biol.*  
*Chem. Hoppe-Seyler* **366**: 233-244.

Solomonson, L.P., and Barber, M.J. 1990. Assimilatory nitrate  
reductase: functional properties and regulation. *Ann. Rev. Plant*  
*Physiol. Plant Mol. Biol.* **41**: 225-253.

Spear-Bernstein, L., and Miller, K.R. 1989. Unique location of the  
phycobiliprotein light-harvesting pigment in the cryptophyceae. *J.*  
*Phycol.* **25**: 412-419.

Spurr, A.R. 1969. A low-viscosity epoxy resin embedding medium for  
electron microscopy. *J. Ultrastruct. Res.* **26**: 31-43.

Staehelin, L.A. 1986. Chloroplast structure and supramolecular  
organization of photosynthetic membranes. In *Encyclopedia*  
*of Plant Physiology*, Vol. 19. Photosynthesis III. Photosynthetic  
Membranes and Light Harvesting Systems. Edited by L.A.  
Staehelin and C.J. Arntzen. Springer, Berlin, pp. 1-84.

Stevens, S.E. Jr., Paone, D.A.M., and Balkwill, D.L. 1981. Accumulation

- of cyanophycin granules as a result of phosphate limitation in *Agmenellum quadriplicatum*. *Plant Physiol.* **67**: 716-719.
- Stewart, W.D.P. 1977. A botanical ramble among the blue-green algae. *Br. Phycol. J.* **12**: 89-115.
- Streusand, V.J., and Portis, A.R., Jr. 1987. Rubisco activase mediates ATP-dependent activation of ribulose bisphosphate carboxylase. *Plant Physiol.* **82**: 967-971.
- Suss, K.-H. 1990. Ribulose-1,5-bisphosphate carboxylase-binding chloroplast thylakoid membrane proteins. *In vitro* evidence that H<sup>+</sup>-ATP synthase may serve as a membrane receptor. *Z. Naturforsch.* **45 c**: 633-637.
- Suzuki, K., and Ikawa, T. 1985. Effect of oxygen on photosynthetic <sup>14</sup>C<sub>2</sub> fixation in *Chroomonas* sp. (Cryptophyta) III. Effect of oxygen on photosynthetic carbon metabolism. *Plant Cell. Physiol.* **26**: 1003-1010.
- Swift, H., and Leser, G.P. 1989. Cytochemical studies on prochlorophytes: localization of DNA and ribulose 1,5-bisphosphate carboxylase-oxygenase. *J. Phycol.* **25**: 751-761.
- Tabita, F.R. 1988. Molecular and cellular regulation of autotrophic carbon dioxide fixation in microorganisms. *Microbiol. Rev.* **52**:

155-189.

Taylor, S.E., Terry, N., and Bassham, J.A. 1986. Changes in steady-state photosynthetic  $^{14}\text{C}$ -incorporation into cellular metabolites of *Chlorella pyrenoidosa* during transitions from high to low irradiance. *Plant Cell Physiol.* **27**: 1169-1175.

Tsuzuki, M., Miyachi, S., and Berry, J.A. 1985. Intracellular accumulation of inorganic carbon and its active species taken up by *Chlorella vulgaris* 11h. In Inorganic carbon uptake by aquatic photosynthetic organisms. Edited by W.J. Lucas and J.A. Berry. American Society of Plant Physiologists. Rockville, MD. pp. 53-66.

Tsuzuki, M., Gantar, M., Aizawa, K., and Miyachi, S. 1986. Ultrastructure of *Dunaliella tertiolecta* cells grown under low and high  $\text{CO}_2$  concentrations. *Plant Cell Physiol.* **27**: 737-739.

Turpin, D.H., Miller, A.G., and Calvin, D.T. 1984. Carboxysome content of *Synechococcus leopoliensis* (Cyanophyta) in response to inorganic carbon. *J. Phycol.* **20**: 249-253.

Vallon, O., Wollman, F.A., and Olive, J. 1985. Distribution of intrinsic and extrinsic subunits of the PSII protein complex between appressed and non-appressed regions of the thylakoid membrane: an immunocytochemical study. *FEBS Lett.* **183**: 245-50.

- Vallon, O., Wollman, F.A., and Olive, J. 1986. Lateral distribution of the main protein complexes of the photosynthetic apparatus in *Chlamydomonas reinhardtii* and in spinach: an immunocytochemical study using intact thylakoid membranes and a PSII enriched membrane preparation. *Photobiochem. Photobiophys.* **12**: 203-220.
- deVasconcelos, L., and Fay, P. 1974. Nitrogen metabolism and ultrastructure in *Anabaena cylindrica*. I. The effect of nitrogen starvation. *Arch. Microbiol.* **96**: 271-279.
- Vaughn, K.C. 1987a. Two immunological approaches to the detection of ribulose-1,5-bisphosphate carboxylase in guard cell chloroplasts. *Plant Physiol.* **84**: 188-196.
- Vaughn, K.C. 1987b. Polyphenol oxidase. In *CRC handbook of plant cytochemistry*. Vol. 1. Edited by K.C. Vaughn. CRC Press, Boca Raton, Fla., U.S.A. pp. 159-162.
- Vaughn, K.C. 1987c. Photosynthetic partial reactions. In *CRC handbook of plant cytochemistry*. Vol. 2. Edited by K.C. Vaughn. CRC Press, Boca Raton, Fla., U.S.A. pp. 37-43.
- Vaughn, K.C., and Campbell, W.H. 1988. Immunogold localization of nitrate reductase in maize leaves. *Plant Physiol.* **88**: 1354-1357.
- Vaughn, K.C., and Duke, S.O. 1981. Histochemical localization of

- nitrate reductase. *Histochemistry*, **72**: 191-198.
- Vaughn, K.C., and Outlaw, W.H. 1983. Cytochemical and cytofluorometric evidence for guard cell photosystems. *Plant Physiol.* **71**: 420-424.
- Vaughn, K.C., and Owen, H.A. 1989. Organization of the hornwort (Anthocerotae) chloroplast. *Plant Physiol.* **89s**: 83
- Vaughn, K.C., Lax, A.R., and Duke, S.O. 1988. Polyphenol oxidase: The chloroplast oxidase with no established function. *Physiol. Plant.* **72**: 659-665.
- Vaughn, K.C., Campbell, E.O., Hasegawa, J., Owen, H.A., and Renzaglia, K.S. 1990. The pyrenoid is the site of ribulose 1,5-bisphosphate carboxylase/oxygenase accumulation in the hornwort (Bryophyta: Anthocerotae) chloroplast. *Protoplasma* **156**: 117-129.
- Veierskov, B., and Ferguson, I.B. 1991. Conjugation of ubiquitin to proteins from green plant tissues. *Plant Physiol.* **96**: 4-9.
- de Vitry, C., Olive, J., Drapier, D., Recouvreur, M., and Wollman, F.A. 1989. Posttranslational events leading to the assembly of photosystem II protein complex: a study using photosynthesis mutants from *Chlamydomonas reinhardtii*. *J. Cell Biol.* **109**: 991-1006.

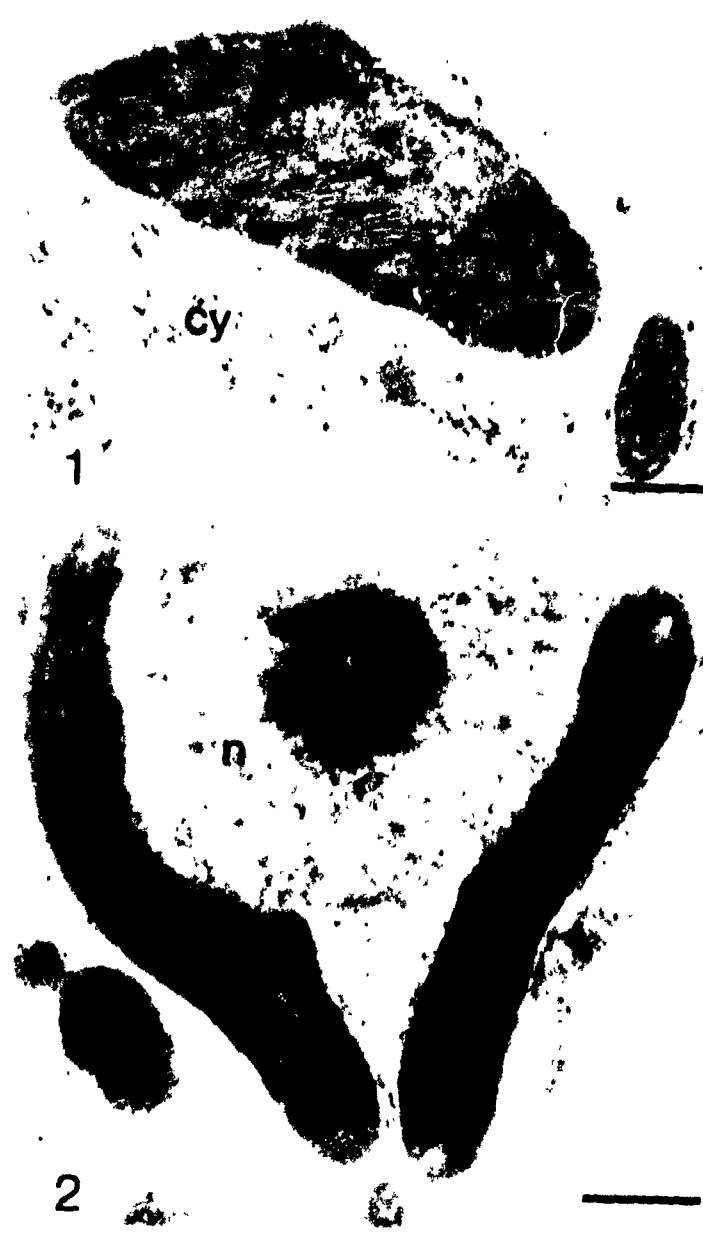
- Vladimirova, M.G., Markelova, A.G., and Semenenko, V.E. 1982. Use of the cytoimmunofluorescent method to clarify localization of ribulose biphosphate carboxylase in pyrenoids of unicellular algae. *Fiziol. Rast.* **29**: 941-950. (English translation: *Soviet Plant Physiol.* **30**: 725-734).
- Wanner, G., Henkelmann, G., Schmidt, A., and Kost H.-P. 1986. Nitrogen and sulfur starvation of the cyanobacterium *Synechococcus* 6301. An ultrastructural, morphometrical, and biochemical comparison. *Z. Naturforsch* **41**: 741-750.
- Werneke, J.M., Chatfield, J.M., Ogren, W.L. 1988a. Catalysis of ribulosebiphosphate carboxylase/oxygenase activation by the product of a rubisco activase cDNA clone expressed in *Escherichia coli*. *Plant Physiol.* **87**: 917-920.
- Werneke, J.M., Zielinski, R.E., Ogren, W.L. 1988b. Structure and expression of spinach leaf cDNA encoding ribulosebiphosphate carboxylase/oxygenase activase. *Proc. Natl. Acad. Sci. USA* **85**: 787-791
- Werneke, J.M., Chatfield, J.M., Ogren, W.L. 1989. Alternative mRNA splicing generates the two ribulosebiphosphate carboxylase/oxygenase activase polypeptides in spinach and *Arabidopsis*. *Plant Cell* **1**: 815-825.

- Wettern, M., Parag, H.A., Pollmann, L., Ohad, I., and Kulka, R.G.  
1990. Ubiquitin in *Chlamydomonas reinhardtii*. Distribution in the cell and effect of heat shock and photoinhibition on its conjugate pattern. *Eur. J. Biochem.* **191**: 571-576.
- Yagawa, Y., Muto, S., and Miyachi, S. 1987. Carbonic anhydrase of a unicellular red alga *Porphyridium cruentum* R-1. II. Distribution and role in photosynthesis. *Plant Cell Physiol.* **28**: 1509-1516.
- Yeoh, H.-H., Badger, M.R., and Watson, L. 1981. Variations in kinetic properties of ribulose-1,5-bisphosphate carboxylases among plants. *Plant Physiol.* **67**: 1151-1155.
- Yokota, A., and Calvin, D.T. 1986. Changes of ribulose bisphosphate carboxylase/oxygenase content, ribulose bisphosphate concentration, and photosynthetic activity during adaptation of high-CO<sub>2</sub> grown cells to low-CO<sub>2</sub> conditions in *Chlorella pyrenoidosa*. *Plant Physiol.* **80**: 341-345.
- Zielinski, R.E., Werneke, J.M., and Jenkins, M.E. 1989. Coordinate expression of rubisco activase and rubisco during barley leaf cell development. *Plant Physiol.* **90**: 516-521.

**APPENDIX 1**

**Fig. 1.** Immunolocalization of Rubisco LS in the leaf of a C<sub>3</sub>-type higher plant. A section through a mesophyll cell from a leaf of *Pisum sativa*. Rubisco LS is restricted to the chloroplast (c) and is located mainly in the stromal region. Thylakoid grana stacks are unlabelled. The cytoplasm (cy) and a mitochondrion (m) are free of label. Bar = 0.5  $\mu$ m.

**Fig. 2.** Immunolocalization of Rubisco LS in the non-pyrenoid-containing alga *Ochromonas danica*. Two profiles of chloroplast are labelled; the gold particles seemingly distributed throughout each plastid. The nucleus (n) is mainly unlabelled. Bar = 0.5  $\mu$ m.



**APPENDIX 2**

**Figs. 1-3.** Controls for immunolabelling studies. Bars = 0.5  $\mu$ m. **1.** Section through *Chlorella pyrenoidosa* incubated with rabbit non-immune IgG. Very few gold particles are evident over the pyrenoid (py) or the remainder of the chloroplast (c). A similar low level of labelling is observed over other cellular compartments. **2.** Section through *Chlamydomonas reinhardtii* incubated with rabbit pre-immune serum. The various cellular compartments are mainly unlabelled. nucleus (n). **3.** Section through *Phaeodactylum tricornutum* in which the primary antiserum was replaced by PBS alone. The cell is free of label.



1



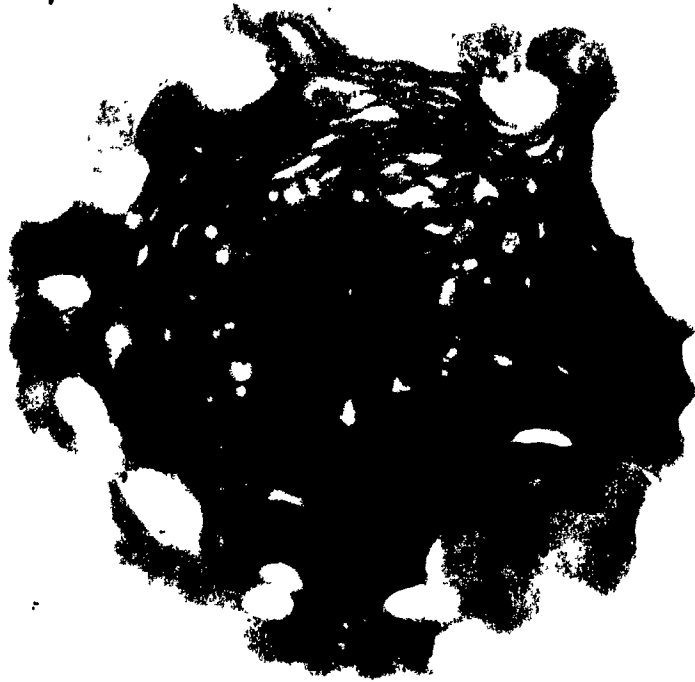
2



3

**Figs. 4,5.** Controls for immunolabelling studies. Bars = 0.5  $\mu\text{m}$ . 4. Section through *Porphyridium cruentum* incubated with rabbit non-immune IgG. Only a few scattered gold particles are evident over the pyrenoid (p) and chloroplast (c). The remainder of the cell is likewise, mainly free of label. nucleus (n). 5. Section through *Hemiselmis brunnescens* incubated with rabbit pre-immune IgG. Only a few gold particles are found scattered over each cellular compartment.

4

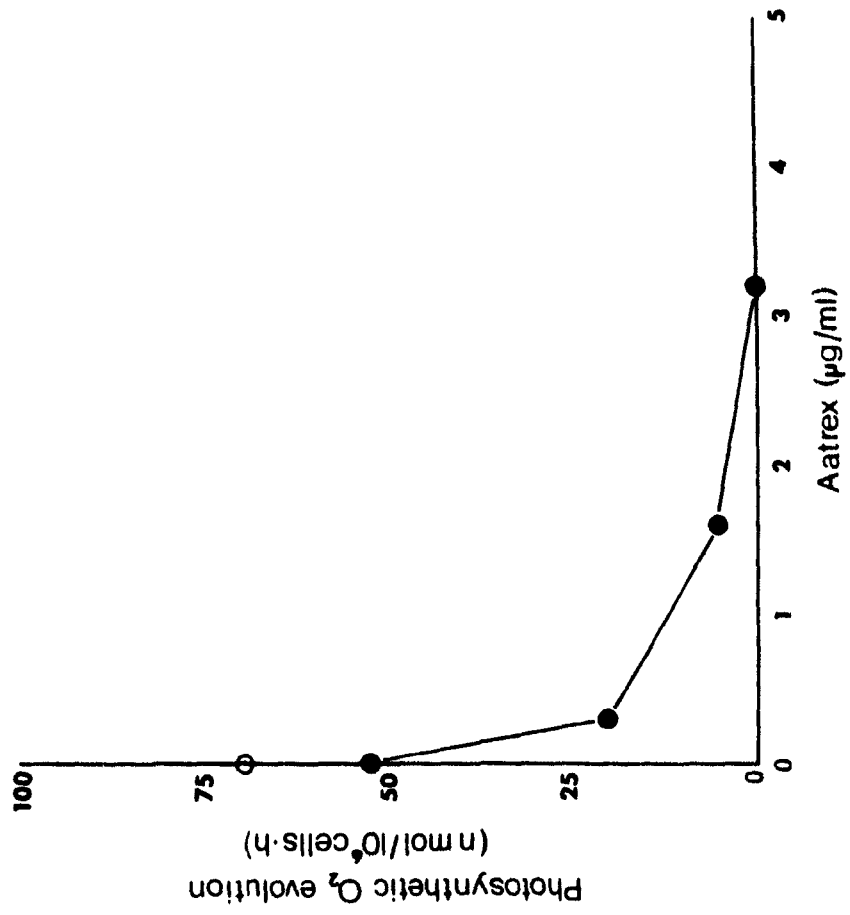


5



**APPENDIX 3**

**Fig. 1.** Dosage effect of Aatrex on photosynthetic O<sub>2</sub>-evolution in *Porphyridium cruentum*. Oxygen evolution was measured in a Clark-type electrode (see Chapter II, section 2.2.) at 23°C. Cells were concentrated to a density of  $\sim 3 \times 10^7$  cells·ml<sup>-1</sup> and light was provided at a near saturating fluence rate (160 μmol·m<sup>-2</sup>·s<sup>-1</sup>) Results are the average of two trials. ● Effect of Aatrex on photosynthetic O<sub>2</sub>-evolution. Aatrex was dissolved in methanol; the final concentration of methanol in the cell suspension used for assay being no greater than 1.5% (v/v). ⊙ Control. Rate obtained when no methanol was added to the cell suspension. This indicates that addition of methanol to the cells has a slight inhibitory effect on photosynthetic O<sub>2</sub>-evolution.



**APPENDIX 4**

**Fig. 1.** Two cells of the diatom *Phaeodactylum tricornutum* having recently completed division. These cells are embedded in Epon resin and immunolabelled by antiserum raised against a mixture of polypeptides of the fucoxanthin-chl *a/c* LHC isolated from this alga (antiserum was kindly provided by Dr. A. Grossman) Gold particles are abundant throughout the chloroplast, usually associated with thylakoid lamellae. In addition, a single pair of thylakoids (arrow) which traverse the pyrenoid in each cell are clearly labelled. Other cell compartments are mainly unlabelled. Golgi (*g*), nucleus (*n*). Bar = 0.5  $\mu$ m.

**Figs. 2,3.** Log phase cells of *P. tricornutum* processed for electron microscopy by rapid freezing followed by molecular distillation drying and embedding in L.R. White resin. Bars = 0.5  $\mu$ m. 2. Cell immunolabelled by anti-PSI. Gold particles are abundant throughout the chloroplast, usually associated with thylakoids. Intrapyrenoid thylakoids (arrow) are clearly marked by gold. 3. Immunolocalization of Rubisco LS in *P. tricornutum*. Gold particles are concentrated over the pyrenoid (arrowhead) whereas the remainder of the chloroplast is only lightly labelled. The nucleus (*n*) and other cell compartments are mainly unlabelled.

